Evaluation of Mechanical Properties of Recycled Polyamide-Cellulose Fiber Composite

by

Jiaxin Xu

A thesis

presented to the University of Waterloo

in fulfillment of the

thesis requirement for the degree of

Master of Applied Science

in

Chemical Engineering

Waterloo, Ontario, Canada, 2016

Author's Declaration

I hereby declare that I am the sole author of this thesis. This is a true copy of the thesis, including any required final revisions, as accepted by my examiners.

I understand that my thesis may be made electronically available to the public.

Abstract

Natural fiber as an alternative for glass fiber to reinforce thermoplastic in the automotive industry has already attracted many manufacturers' interest because of its many benefits. Natural fiber is biodegradable, has high modulus, low density, low cost and can be obtained from many natural resources. Thermoplastic composites of polyamide 6 (PA6) and cellulose from wood fiber can improve the modulus of PA6 and reduce the weight of an automotive component when compared to glass fiber. However, there is a challenge associated with the thermal stability of cellulose. Therefore one research challenge to processing PA6 with natural fibers is thermal degradation. High processing temperature, mechanical forces and oxygen environment can cause PA6 thermal-oxidation as well. Since the lifetime of automotive parts are closely related to the oxidation behavior of PA6, it is necessary to understand the oxidation mechanism and to find suitable antioxidants for PA6/cellulose composite.

The objective of this thesis is to evaluate appropriate levels of primary antioxidant Irganox 1010 and secondary antioxidant Irgafox 168 for such composites. Mechanical properties, thermal characteristics, crystallinity and morphology were measured to correlate with the antioxidant effectiveness. The effect of cellulose added to the composite was also evaluated. It was observed that 500 ppm of Irganox 1010 may be the best amount needed due to its increase of tensile modulus by 21.99% and its increase of flexural modulus by 8.75%. While the addition of Irgafox 168 combined with Irganox 1010 did not add improvement among different formulations.

The oxidation induction time (OIT) test is considered a good method to detect the antioxidant performance and help to find appropriate antioxidant for other polymers (such as polyethylene). However, the OIT procedure was not well established for PA6 as the test showed its ineffectiveness to evaluate thermal stability of polyamide. Alternative methodologies to evaluate thermal stability have

shown to be more suitable than OIT. Thermal gravimetric analysis was successfully used to measure thermal stability at constant (isothermal) temperatures.

Acknowledgements

I would like to gratefully acknowledge various people who have been helped me a lot in the past one year as I worked on this project and the thesis. Firstly, I would like to express the deepest gratitude to my supervisor, Leonardo Simon, for giving me the opportunity to continue my research work, the guidance and the encouragement. Thank you so much. Secondly, I would like to thank my group members: Charles Dal Castel, Azam Nasr, Chong Meng, Ahmad Raza Ashraf, Mariana Beauvalet, Douglas Casetta and Injula Khan, who encouraged me a lot when I was writing the thesis. Also I would like to express special thanks to Ford Motor Company and Suzano Papel e Celulose for partially funding this research , and Dr. Alper Kiziltas (Ford) for help molding the samples and Eng. Talyta Torrezan (Suzano) for help selecting the cellulose fiber . Finally, I would like to thank Professor Ali Elkamel and Professor Boxin Zhao for being my thesis readers and defense committee members.

Table of Contents

List of Figures

List of Tables

Chapter 1 - Introduction And Motivation

It is now important to understand our harmonious coexistence with the environment, since the rise of industry has lead to severe consequences such as global warming and loss of wildlife habitat. Our reliance on fossil fuels and non-renewable energy resources has established a need for more environmentally friendly alternatives. Natural fiber is an appropriate alternative that meets these conditions: it is renewable, widely available, has high mechanical performance, and can be used in a variety of applications. Thermoplastic composites of polymer and natural fiber have been widely studied in the last 40 years[1]. Polyamide 6 (PA6) is one of the most commonly used engineering thermoplastics matrix composite filled with glass fiber and it is applied in a variety of sectors, such as automotive, tools and appliances, carpet and textiles, food packaging, and medical applications.

Natural fiber as reinforcement for polymer shows many advantages over traditional fillers (glass fibers and mineral fibers). It presents high specific mechanical properties (strength and modulus), low abrasiveness to equipment, low density, low cost, friendly to the workforce during processing, renewability, recyclability and has a large number of sources [2]. However, some of the challenges associated with the addition of natural fibers to thermoplastics are surface compatibility and low thermal stability [3].

In the case of polyethylene and polypropylene, the major challenge with the addition of natural fibers is surface compatibility. These two polymers have a processing temperature that often does not exceed 220 ^{o}C. In the case of polyamide 6 (PA6), the major challenge is the relatively high processing temperature of the polymer, which in this case often exceeds 250 ^{o}C. The thermal stability of natural fibers depends greatly on their chemical composition. Removal of lignin increases the thermal stability of natural fibers.

Previous research in our group conducted by Amintowlieh has shown that polyamide 6 can be reinforced by wheat straw fiber with the addition of plasticizer and salt. It was found that adding salt to the formulation decreased the melting point of the polyamide and therefore decreas the processing temperature. Adding plasticizer to the formulation of the composite reduced the viscosity by providing a lubricating effect to the polymer matrix. These two additives decreased the degradation of the straw fibers in the composite and resulted in improved mechanical properties [4].

Other researchers found that surface modified jute fiber composite with polybutylene succinate improved mechanical properties of the composite and reached optimal values when the fiber content was 20%. This effect was attributed to the surface modification of jute decreasing the water absorption, increasing the compatibility between filler and matrix, and eliminating non-cellulose part in the jute, which leads to a better interfacial bonding in the composite [5].

Additives are necessary for the formulation of polyamide 6 (PA6) to minimize thermal decomposition during processing. The weakness of the carbon-hydrogen bond of the methylene group directly near the nitrogen from amide group may result in a series of oxidation reaction during the thermal processing (extrusion and molding), which will lead to a decrease of mechanical properties. Normally, the processing method of polyamide 6 and natural fiber may undergo a series of thermal and mechanical stresses common in extrusion and injection molding in an aerobic environment (all components are exposed to air) that may meet these thermal oxidation conditions: heat and oxygen [6]. Therefore, antioxidants are commonly used in this formulation. Another important reason for using antioxidant is to extend the lifetime of the end product.

There are many research achievements on polymer-natural fibers composite. The

Addition of only 0.1 phr Nocrac MB antioxidant to crosslinking polyethylene decreased the thermal oxidation detected by the tensile test, but did not affect any radiation aging [6]. Yang combined biphenol monoacrylate with traditional antioxidant system effectively to inhibit the formation of carboxyl groups and amine end groups in the PA6. This strategy also minimized the discoloration of PA6 and improved its mechanical properties [6].

Most applications for polyamide in the automotive industry are exposed to oxygen at relatively high temperatures under stresses (also called forces). The degradation or oxidation process will lead to undesired mechanical properties resulting in a short lifetime of the product. Therefore, antioxidants are necessary to inhibit thermal oxidation of the polymer.

1.2 Objectives

The objectives of this research are:
(1) To investigate the effect of primary antioxidant on recycled polyamide 6 and its cellulose composites as observed by the improvement of mechanical properties.
(2) To investigate the effect of a combination of primary antioxidant and secondary antioxidant on the improvement of mechanical properties.
(3) To evaluate the effect of different fiber loading on nylon 610 composite mechanical properties.
(4) To evaluate the effect of crystallinity on mechanical properties.
(5) To study the suitability of the method known as oxidation induction time (OIT) to evaluate the effect of antioxidants in recycled polyamide and its composites with natural fiber.

1.3 Outline of the thesis

The first part of this thesis introduces physical and mechanical characteristics of recycled polyamide 6 (PA6) and cellulose fiber. The advantages and limitations of these characteristics are associated with their chemical structure and physical properties. The major objective of this thesis is to first evaluate the effect of antioxidants on the properties of the composite materials, to evaluate the effect of the amount of fiber, and then compare recycled PA6 with PA6-10. The natural fiber selected for this study is cellulose fiber produced by wood pulping (Kraft process), it was supplied by Suzano Papel e Celulose. The rationale for selecting this type of cellulose fiber is its expected high thermal stability because of the absence of lignin and it expected low cost. This company uses feedstock from Eucalyptus tree farms in Brazil. Under regular growing condition such trees can be harvest in approximately 7 years. This is considered a very short time to harvest when compared to 20-30 years commonly observed in North America.

Five different kinds of antioxidants and mechanisms are reviewed, also including the preparation of polyamide and attempts to achieve better mechanical performance of composite. The materials and method section includes information about materials, formulations, as well as processing characterization.

The results of mechanical properties and thermal characteristic of both the pure materials and composites are presented in the results and discussion sections. The processability of the material was evaluated with Melting Flow Index (MFI). Differential Scanning Calorimetry (DSC) and Thermal Gravimetric Analysis (TGA) were used to measure thermal properties such as the melting point, crystallization temperature, and percentage of weight loss of different samples. Crystallinity was also obtained by integration of the second melting peak in DSC graph. X-Ray Diffraction (XRD) was used to investigate the crystalline type of the polyamide 6 and cellulose. The mechanical properties of the polyamide 6/cellulose fiber composites were evaluated by measuring impact strength, tensile and flexural properties according to ASTM standards, while the polyamide 6-10/cellulose fiber composite was molded according to ISO standards. Impact strength was evaluated by notched

Izod (pendulum hitting on the bar) impact test and by Gardner (dart drop hitting on disk) impact test. Scanning Electron Microscopy (SEM) was used to investigate the dispersion of cellulose fiber in polyamide 6-10 and to better understand the mechanism of failure by observation of the interface of 6-10 and cellulose fiber. The evaluation of the oxidation induction time (OIT) did not reveal clear trends, that was surprising because of the successful application of this methodology to other polymers (like polyethylene), so further research is needed to find the right OIT methodology for polyamide.

Finally, the discussion section addresses how to correlate the mechanical properties to the antioxidant level and its working mechanism as well as the crystallinity of the composite. The thesis layout presents in **Figure 1-** 1.

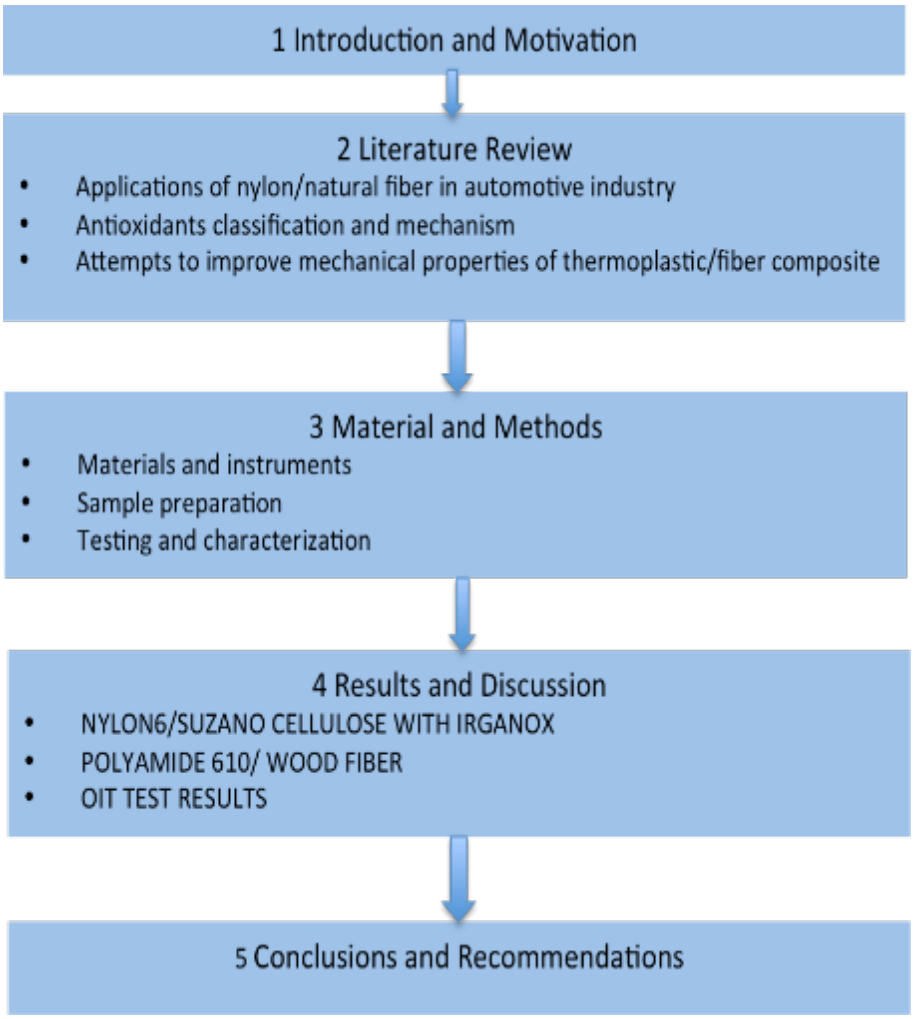

Figure 1- 1 Thesis layout

Chapter 2 Literature Review

2.1 Applications Of Nylon And Natural Fiber In Automotive

Natural fiber has already attracted attention from different industries especially the automotive industry, since they realize the importance of our harmonious coexistence with the environment [7]. Natural fiber has abundant renewable resources and is biodegradable, eco-friendly, low weight, low density, low cost compared with glass fiber; and at the same time it has high specific mechanical properties such as high strength and modulus that make it suitable for different automotive parts. The most attractive part is that it is recyclable or can be burnt out without any residues for energy recovery, which is a necessity for a product which needs to be disposed after end usage [7].

Recently, about half of the automotive interiors are made of polymer materials. As found by American Plastics Council, in developed countries nearly 120 kg of plastic was used in one vehicle and about 105 kg of plastic was used all over the world, which takes up almost 10 to 12 percent of one car's total weight [8]. Reducing the weight and noise, and improving the assurance factor are part of the main focus of automotive manufacturers [9]. According to the Corporate Average Fuel Economy (CAFE), fuel usage can be reduced by 6 to 8 percent if the car's weight is cut by 10% percent [10].

Many automotive manufactures are now focusing on using natural fiber to reinforce thermoplastics. For example, Toyota is investigating the performance of spare tire and floor mats that are made from sugar cane or corn reinforced plastics. DaimlerChrysler is investigating the use of flax, coconut and abaca in vehicles parts. In addition, Ford is investigating the use of biomaterials such as soy foam used for seats in the vehicles [7]. Using low weight natural fiber to reinforce thermoplastic may also lower the CO_2 emission and the improvement of fuel efficiency. Reducing CO_2 emission by 5g/km can be achieved by reducing 50 kg weight of the vehicle,

which can also increase 2% of fuel efficiency. Our research group has collaborated with researchers from Ford Motors, A. Schulman and Omtec Inc to support research and development of wheat straw fibers. This collaboration led to the successful commercialization of polypropylene filled with straw fiber and implementation of this new material in the manufacturing of interior parts in 2010 for the Ford Flex vehicle (assembled in Oakville, ON).

Lightweight vehicles are more effective fuel savers. Producing these vehicles could save refined gasoline up to 350 million liters and could save crude oil up to 3.4 million barrels [11]. Therefore, using lightweight natural fiber to glass fiber or other mineral fillers could potentially be cost saving and environmentally sustainable.

Currently, engineering thermoplastic especially polyamides including PA6, PA66, PA11, and PA12 are commonly used in different sectors of the automotive industries such as the engine covers, cooling system, transmission system, and fuel systems. These materials used in these parts need to have the high thermal stability to meet the high working temperature [12].

2.1.1 Nylon In Automotive Parts

In automotive industries, there are several important requirements that need to be met. These may include materials that have low density, high resistance to mechanical and physical abrasion, high mechanical properties, high thermal stability, large amount and easily accessible of the resources. From this point of view, different kinds of polyamides (also known as nylons) are just case because of their good thermal stability and excellent mechanical performance. But the high melting point of polyamides (often above 250 $^{\circ}C$) is much above the degradation temperature of natural fiber, which will lead to a decrease in the mechanical properties. So solve the contradictory between the high melting and processing temperatures of polyamides and the low degradation temperature of natural fiber is a challenging research task [4].

Polyamide (nylon) was used in different fields since its discovery in 1939. Until 1960, every car used about 0.4 lbs of polyamide. Since 1995, the average amount of polyamide used for one vehicle was 8.8 lbs in "under the hood" parts, which consumed over 100 million pounds in total. Since polyamide was discovered, it has been mostly used in gears, switch covers, and bearings. Radiators and fuel systems are the first components that employ nylons in "under the hood" applications. PA6-6 has shown excellent performance such as resistance to high temperatures and chemical abrasion and also has high mechanical properties [13].

Polyamide 6-6 (Nylon 6-6) was introduced in the automotive components nearly 50 years ago. PA 6-6reinforced by glass fiber was used in mechanical and electrical control systems by DuPont in 1968 and further used in air pollution control systems. In 1972, the air intake manifold in the fuel injection system was the first accepted reinforce nylon 66 used in Porsche vehicles. **Figure 2-** 1 shows the resonator. Because of the high resistance to different chemical corrosion and high temperatures, the exhaust emission system, sealing lids and hooks was the first accepted heat-stabilized nylon 66 used in 1976 by the Ford. In 1978, Chevrolet Vega adopted nylon 66 to be used as flex fan due to its energy saving achieved by less resistance of nylon blades. The first automotive major company to adopt nylon reinforced by glass fiber in brake cylinder reservoirs was Chrysler. These were used due to its excellent performance under high working temperature in "under the hood" parts in 1979.

Figure 2- 1 (a) Air intake manifolds (b) Resonator[14]

The Peugeot 505 adopted vibration welded nylon 66 as the air manifold at the same year. The K-series engine from Rover invented high volume throttle body by nylon 66. Luxury automotive Porsche 911 also adopted nylon 66 for the valve cover beginning in 1994 [14].

Molded PA11 and PA12 have more effective dimensional stability and have greater resistance to high temperature and chemical abrasion than PA6 and PA66 which were apply in high working temperature such as the case of the fuel system in vehicles [15]. PA10-12 is a competitive alternative for fuel system in vehicles because it is processing friendly, which could be extruded, injection molded, or sprayed and also has excellent mechanical properties and can be resistant to high working temperature applied in the line of natural gas, pipeline of oil, coating of optical cable.

Due to good mechanical properties and outstanding processing ability, PA6-12 is used as the raw material of extruded thermoplastic tube, which can be molded into complex 3D shape tubing for fuel system in vehicles. Akron Polymer was the first

option for automotive manufactures to provide injection molded rubber tube for gas emission application in vehicles, as it reduceed about 35% weight or similar components in the car [16]. It is widely used in Aston martin, Changfeng, Chery, DAEWOO, Dongfeng and Jeep. Figure 2- 2 (a) shows the OBVR fuel emission tube for the automotive industry and (b) shows the extruded thermoplastic tube made from PA6-12.

Figure 2- 2 (a) OBVR fuel emission tube (b) The extruded thermoplastic tube[16]

2.1.2 Natural Fiber In Automotive Industry

Composite materials were first used centuries ago, and all the first generation of composite materials is related with natural fiber. For instance, Ancient Egyptians reinforced clay by wheat straw for construction purpose 3000 years ago. However, its use declined due to the availability of more durable materials such as mineral materials. Recently, the use of natural fiber became more commonly used due to its cost-saving and low weight density [17]. Due to the environmental concerns associated with our dependence of non-renewable petroleum, natural fiber was a more environmental-friendly alternative sources as it is biodegradable. During the 1960s, natural fiber was used in vehicles. For example, its car seats were made from

coconut fiber, car interiors were made from polypropylene (PP)/wood fiber composite and polyethylene (PE) composite with natural fiber were applied in the deck board. Due to many advantages of natural fiber, automotive manufacturers used different kinds of natural fibers in the car such as flax, coconut, abaca fibers was applied in Mercedes Benz, soy-based foam applied in Ford vehicle as seat, and nowadays wood fiber is applied to produce door panels and window frames [18].

Nylon 6 is reinforced by Curaua fiber by extrusion and followed by injection molding. This was used in sun visors and related frame parts in the car. Figure 2- 3 shows the sun visor and related frame parts in the vehicle that are made from 20% Curaua reinforced PA6. The molded product presents perfect mechanical properties under 70 ℃ injection molding and 55 bars processing pressure [18].

Figure 2- 3 The sun visor and related frame pars in the vehicle made from 20% Curaua reinforced nylon 6 [18]

In the textile manufacturing industry, three main forms of textiles are used: woven fabric, nonwoven fabric and knitted fabric. The woven fabric is formed from weaving by yarn, while the nonwoven fabric is directly formed from long fibers by chemical, mechanical or thermal bonded together, which is made from recycled materials. Knitted fabric is another kind of textile form made by knitting, which is more flexible than woven fabric and more durable than nonwoven fabric [19],[20]. The corporation FlexForm

Techenologies used hemp fiber combined with polymer adhesives to produce a high performance nonwoven composite mat. This nonwoven mat can be composite with other components to form interior and door panel in automobiles by injection molding. Figure 2- 4 shows a general procedure of produced finished door panel by hemp fiber [21]. The UFP Technologies can provide a series of woven and nonwoven fabrics products that are used in the automotive industry, which can meet different requirement such as interior aesthetics, noise insulation and specific mechanical properties [22].

Figure 2- 4: The general procedure of producing finished door panel by hemp fiber [21]

In February 2016, the wood-based carbon fiber was first used in roof and battery systems in vehicles by Swedish researchers. The material is the lignin in wood fiber, and we all know that the lignin is the major component of plant cell wall, so that have a large amount of resource all over the world. The lignin battery system can be made from recycled materials from the paper pulp production, which is a very cost-effective process. The KTH Royal Institute of Technology has shown that the lightness

of the lignin-based battery system improved the efficiency of the electrical car or hybrid electrical vehicle [23].

The wood fiber can also be used to produce high quality car tires, which was found by an Oregon State University researcher. For instance, Li from the OSU College of Forestry found that microcrystalline cellulose is a competitive alternative for filling the rubber tire instead of silica, since it can save more energy to produce it and also has a higher fuel efficiency in hot weather compared to carbon black and silica filled traditional tires [24].

2.2 Cellulose

2.2.1 Introduction

Cellulose is the major content in the cell walls of plants, and it is a kind of macromolecule polysaccharose, which consists of glucose. Also it is not found as a pure substance in nature, as it is associated with hemicellulose and lignin present in the wood or plants. The land plants and algae in the oceans fix the carbon dioxide by photosynthetic organism produced by hundreds of million tons cellulose in nature, and suspected to be the most abundant organic compound in the earth [33]. Because of its excellent performance in tensile strength and durability combined with abundant natural resources, the cellulose was separated from the wood and used in variety of industries such as additives, food, paper, and construction field since middle nineteenth century [25].

Cellulose is a macromolecule, non-branched polysaccharide consisting of 1-4 linked β-D-glucopyranose [26]. Its chemical constitution and repeating units are shown in Figure 2-5.

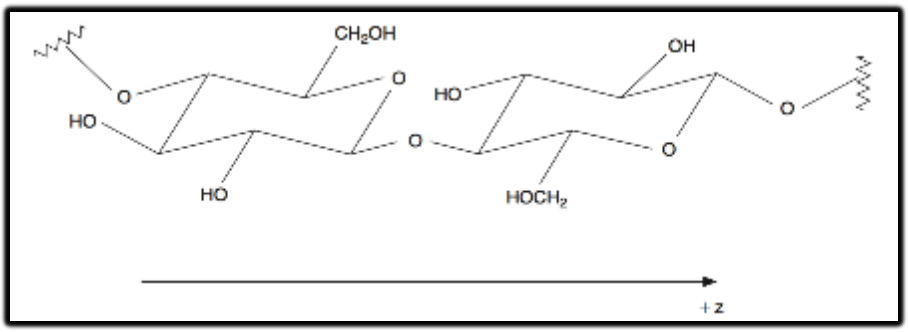

Figure 2- 5 The repeating unit of cellulose chain [26,27]

The conformation structure represents free hydroxyl groups in carbon 2,3, and 6 in the long cellulose chains form variety of hydrogen bonds among or between molecules, and it will lead to an increase of crystallinity of the material [25]. It is well known that the crystallinity and crystalline type are closely related to the mechanical properties of the material. So it is necessary to understand the structure and characteristics of different crystalline forms. It has revealed that there are four major crystalline forms in cellulose: Cellulose I, Cellulose II, Cellulose III, and Cellulose IV. The most common one is Cellulose I, which is naturally formed and is also called native cellulose. The microstructure of Cellulose I is complex and still not completely understood, but it is shown that there are two sub-forms: Iα and Iβ. Cellulose I can transfer to more stable type Cellulose II through two irreversible ways: Regeneration and mercerization. Regeneration process consists of first dissolving Cellulose I in a solvent, which is followed by precipitation or recrystallization to form Cellulose II. Mercerization process is using concentrated alkaline to swelling native cellulose and then washing out the swelling agent and recrystallization. Cellulose III_I and Cellulose III_{II} are obtained from Cellulose I or Cellulose II respectively by treating them by liquid ammonia or other amines followed by evaporate extra ammonia. The last form Cellulose IV_I and Cellulose IV_{II} are obtained from Cellulose III_I and Cellulose III_{II} by heating in glycerol respectively [25][27]. The relationship between different crystalline forms of cellulose is shown in Figure 2- 6.

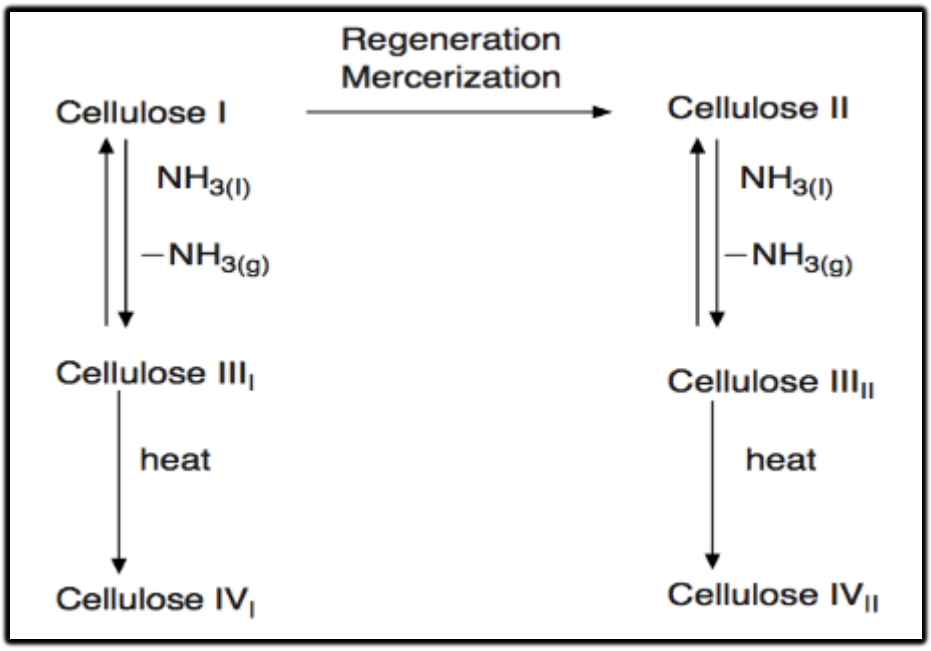

Figure 2- 6 Relationships among different cellulose allomorphs [27]

2.2.2 Different Crystalline Characteristics

2.2.2.1 Cellulose I (Iα, Iβ)

In 1988, Simon speculated that there are two types of crystalline form that exist in native cellulose; the crystalline form on the surface is different from that exist in the center of the crystals. Atalla and VanderHart confirmed these two sub-crystals by solid-state NMR spectrum and termed them Cellulose I α and Cellulose I β respectively. Different native cellulose based fiber contains different proportion of Cellulose Iα and Cellulose Iβ, and Cellulose Iα is produced more by organism while Cellulose Iβ exist more in plants. Cellulose Iα proved to be a triclinic symmetry with a detail dimension (a=7.784$\mathring{A}$, b=8.201 $\mathring{A}$, c=10.380 $\mathring{A}$, γ=96.5°). The Cellulose Iβ crystalline phase is shown to be a monoclinic unit cell with detail dimension (a=8.01$\mathring{A}$, b=5.93 $\mathring{A}$, c=10.36 $\mathring{A}$, α=117°, β=113°, γ=97.3°). One chain included in a triclinic unit cell in Cellulose Iα, while the two "parallel-up" chains in the monoclinic

unit cell in Cellulose Iβ [25]. The dimensional relationship between Cellulose Iα and Cellulose Iβ is shown in Figure 2- .

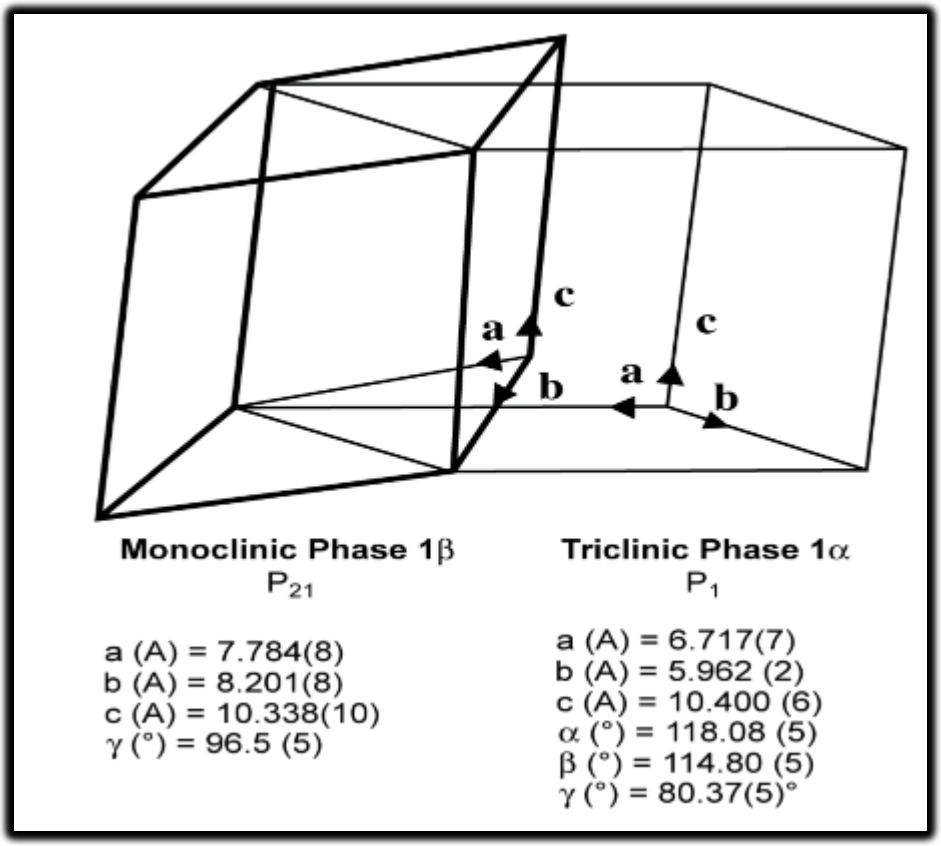

Figure 2- 7 The dimensional relationship between Cellulose Iα and Cellulose Iβ [25]

2.2.2.2 Cellulose Ii

Historically, Cellulose II was proposed with dimension (a=8.14$\mathring{A}$, b=14 $\mathring{A}$, c=10.3 $\mathring{A}$, α=117°, γ=62°), which included two cellulose chains. While another proposed dimension (a=15.92 $\mathring{A}$, b=18.22 $\mathring{A}$, c=18.22 $\mathring{A}$, α=117°, γ=117°) was introduced when using the neutron diffraction. However, this difference may due to the different preparation methods: mercerization and regeneration. The allomorph made by mercerization will obtain a lower value than from regeneration; while the allomorph made by regeneration obtained a lower value of angle γ than mercerization. Finally Cellulose II produced from Acetobacter xylinum was

investigated by XRD and molding method, which shown that it had a twofold symmetry crystalline form with a characteristic antiparallel structure of cellulose chains. Later the crystal structure of a mercerized Cellulose II after alkali treatment was proposed, and the dimension is: a=8.18 $Å$, b=9.04 $Å$, c=10.36 $Å$, γ=117. 1°. In addition, this method showed no difference of the antiparallel chain structure. Whether the difference of hydroxymethyl groups is due to the different level of hydroxymethyl disorder is not clearly understood [25].

2.2.2.3 Cellulose Iii

Cellulose III_I and Cellulose III_{II} are formed reversible from Cellulose I and Cellulose II, which means that the chain orientation is the same for allomorphs I and II. The chain structure is not a strict twofold symmetry model, and the dimension is as follows: a=10.25 $Å$, b=7.78 $Å$, c=10.34 $Å$, γ=122.4°. It was proposed that there is an intermediate cellulose complex I-EDA formed during the transformation between Cellulose I and Cellulose III. A decrease of lateral crystalline is shown when Cellulose I is transferred to Cellulose III_I based on a solid-state NMR test [25].

2.2.2.3 Cellulose Iv

Cellulose IV_I formed from Cellulose I and Cellulose IV_{II} formed from Cellulose II. However, this resulted in incomplete transformation and it is the reason for bad-quality X-ray diffraction results. The dimensions of these two crystalline forms are: IV_I (a=8.03 $Å$, b=8.13 $Å$, c=10.34 $Å$) and IV_{II} (a=7.99 $Å$, b=8.10 $Å$, c=10.34 $Å$) [25].

2.2.3 Cellulose Thermal Oxidation

Several materials in our environment do not burn directly, such as many wood products burn indirectly by the reaction between oxygen and gases released from the material. The thermal decomposition of cellulose and reaction among released gases are the basis for pyrolysis, which is then followed by ignition and combustion of wood [28].

According to different ambient conditions such as the temperature, oxygen concentration, relative humidity and pH value, the thermal decomposition of cellulose can be divided into two pathways: Tar forming pathway and char forming

pathway. The schematic graph of cellulose thermal decomposition is shown in Figure 2- 7. When the ambient temperature is around 300 ℃, the thermal decomposition behaved as tar forming pathway. The cellulose decompos and generates levoglucosan and continuously decomposes into flammable gases as the effect of heat. When the ambient temperature is around 200 ℃, the thermal decomposition behaves according to the char forming pathway. The cellulose firstly decomposes into active cellulose and continues decomposing into carbon dioxide, water, free radicals and carbonyl groups [28].

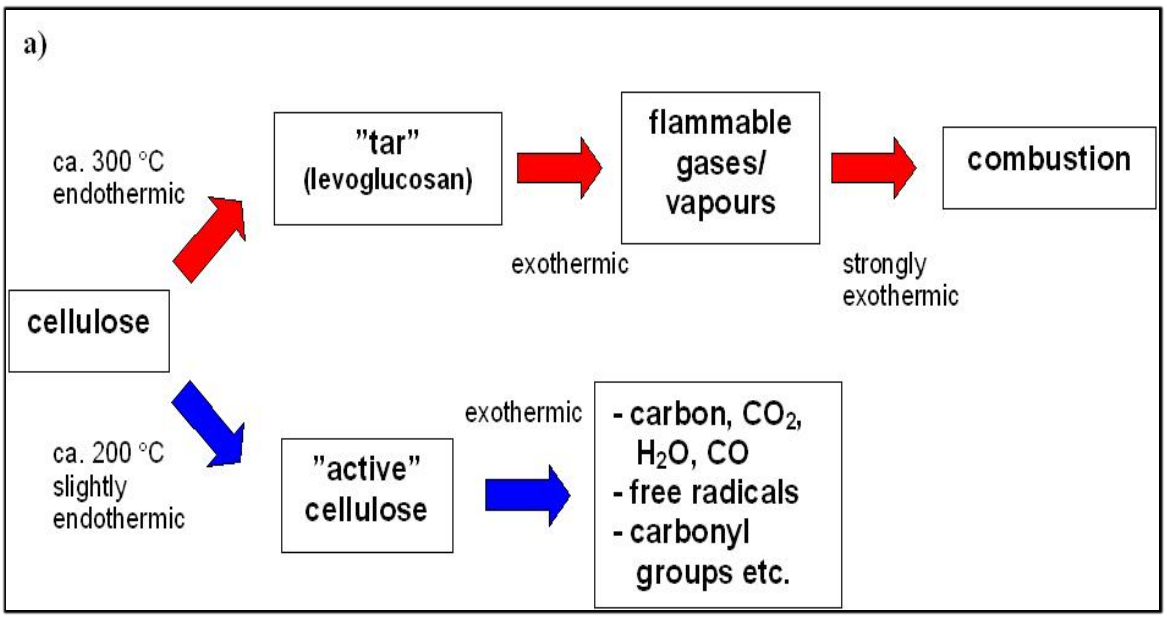

Figure 2- 7 The two main reaction pathway of thermal decomposition of cellulose [28]

2.3 Polyamide 6 Composition And Properties

Polyamide 6 is used in many types of applications as it can be manufactured as fiberes, films, molded parts or tubes (extrusion). Therefore, there are several types of stream of recycled polyamide 6 to be recovered in the market.

Recycled synthetic fibers (from carpets for example) include processing discarded synthetic fibers by melting or dissolution followed by reprocessing procedures that

may include depolymerization. The waste of polyamide 6 mainly consists of high caprolactam polymer and the residue of polyamide 6, which mainly consists of caprolactam oligomer. This may depolymerize to form caprolactam by acid process or alkaline process for reuse, however, the cost is high [29].

US Energy Laboratory developed a way to recycle carpet waste, which is known as selective pyrolysis specially used for processing nylon 6 carpets that may recycle almost one third of the used carpet all over the world. First, it cuts the used carpet into one inch square pieces and it is heated in a reactor together with a special catalyst. After the evaporation of the carpet, the extracted caprolactam flows into the second reactor. The burning process provides fuel for this procedure and the catalyst can be recycled during this step. The cost of this method is almost half the cost of production based on benzene and the energy consumption is one third of the latter procedure [29].

At the end of 1999, DSM Chemicals North America and Allied Signal set up a company called Evergreen Nylon Recycling LLC by joint –venture in Augusta. This company can recycle and process up to 9 million tons used nylon 6 carpet, which takes up 20% of total discarded nylon 6 carpet in America, occupied 2% of gross used carpet [29].

Polyamide 6 is one of the most widely used semi-crystalline polymorphic thermoplastic in different industries such as automotive industries, cover of equipment, carpet, textile, food packaging, and medical applications. Physical property of polyamide 6 is similar to polyamide 6-6, while it has a lower melting point and a broader temperature range for processing it. Compared with polyamide 6-6, polyamide 6 has higher impact strength, but it also has a higher water absorption that is an important factor in the plastic industry.

There are now three different ways to produce polyamide 6. Before that there is an introduction for methods to prepare the monomer caprolactam.

Phenol Method: Firstly, phenols react with hydrogen to generate cyclohexanol. Then cyclohexanol dehydrogenize to form cyclohexanone-oxime, which lead to inter conversion reaction within same amount of fuming sulphuric acid to generate caprolactam [30].

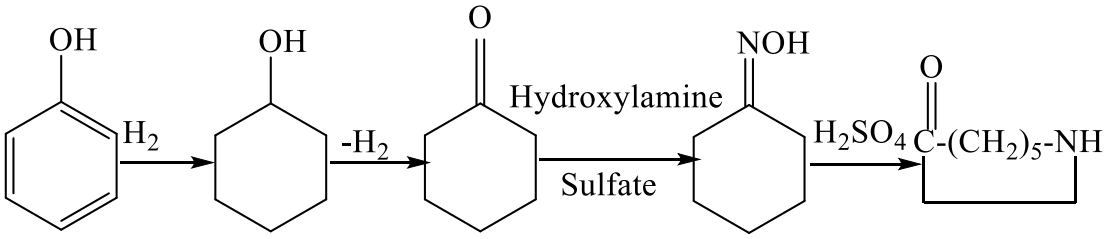

Figure 2- 8 The reaction schematic graph of phenol method [30]

Cyclohexane Oxidation Method: Cyclohexane through air oxidation produces cyclohexanol and cyclohexanone, and then after separation of cyclohexanone to form cyclohexanone-oxime. Lastly, it then goes through inter-conversion reaction with the same amount of fuming sulphuric acid to form caprolactam [30].

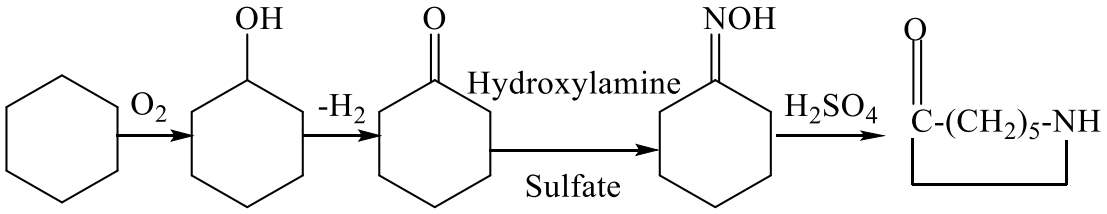

Figure 2- 9 The reaction schematic graph of cyclohexane oxidation method [30]

Illumination Nitrosation Process: Cyclohexane reacts with nitrosyl chloride (NOCl) under illumination (use of light) to produce cyclohexanone-oxime hydrochloride by nitrosylation, then through inter-conversion reaction with the same amount of fuming sulphuric acid generates caprolactam [30].

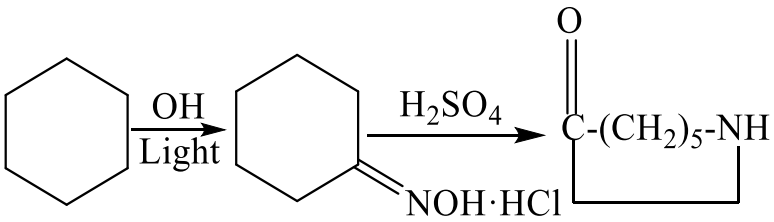

Figure 2- 10 The reaction schematic graph of illumination nitrosation process method [30]

Methylbenzene Method: Firstly, methylbenzene oxidizes to produce benzonic acid then hydrogenate to heptanaphthenic acid, then it reacts with nitrosyl sulfuric acid under fuming sulphuric acid condition to form caprolactam [30].

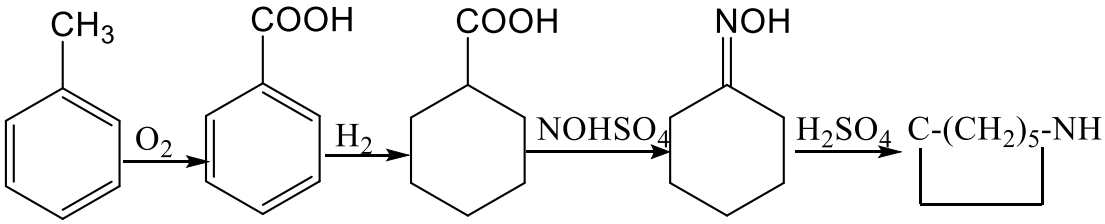

Figure 2- 11 Reaction schematic graph of methylbenzene method

The composition of monomer caprolactam is followed by the polymerization of polyamide 6. Hydrolyzation: Caprolactam hydrolyze under high temperature to produce aminocaproic acid.

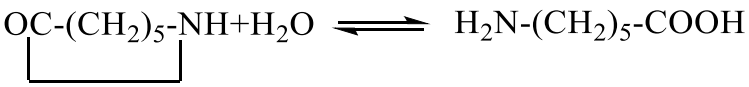

Figure 2- 12 Reaction of hydrolyzation [30]

Condensation:

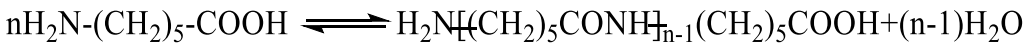

Figure 2- 13 Reaction of condensation [30]

Addition:

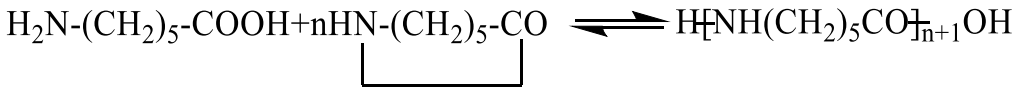

Figure 2- 14 Reaction of addition [30]

It is well known that the mechanical properties of polyamide 6 are closely related to the crystallinity and different crystalline forms. So it is necessary to consider the structure and character of different crystalline forms.

There are three types of crystalline forms in polyamide 6: Alpha structure, beta structure and gamma structure. Alpha structure is the most stable one, and it is a kind of multilayer planes that that consists of many antiparallel long chains [31]. The melting point of this monoclinic alpha crystalline is around 220 ℃, and it is usually generated from melting in a quiescent state and crystallized in a slow cooling rate, and the crystallization temperature is higher than 150 ℃ [32]. The alpha structure consists of zigzag conformation chains that antiparallel with adjacent chains, so that lead to an easy trend to form hydrogen bond between them [31]. The antiparallel alpha structure is shown in Figure 2- 15.

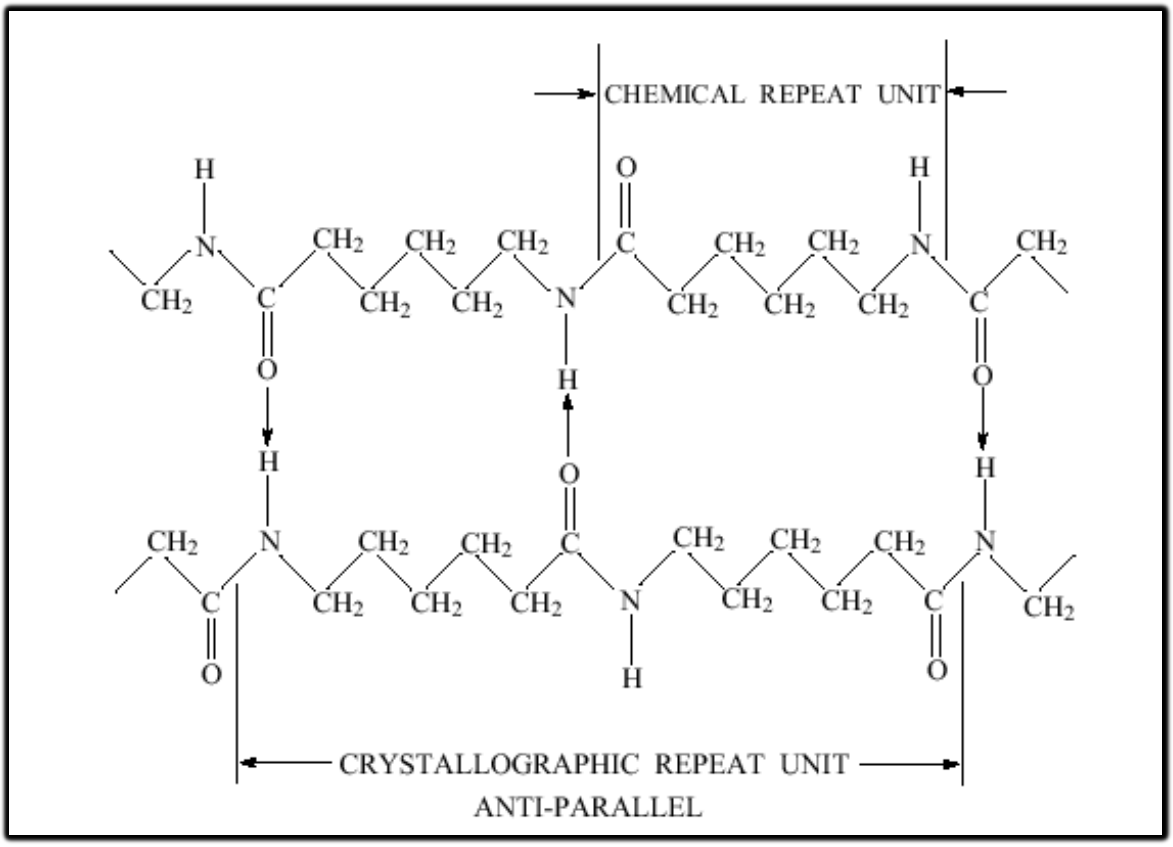

Figure 2- 15 Alpha structure of PA6 [31]

Another common crystalline form of polyamide 6 is gamma crystal. In contrast to alpha crystal, it is a kind of multilayer planes consist of many parallel long chains. The metastable gamma crystalline form is also generated from quiescent melt while the crystallization temperature is lower than 150 ℃. The gamma structure is unstable, which will experience cold crystallization at the normal room temperature and transfer to alpha structure if temperature is higher than 150℃ [33]. Also, the specific nucleating agent contributes to form this pseudo-hexagonal or monoclinic crystal. The melting point of gamma crystal is about 214 ℃. Another common way to obtain gamma crystal is by low spinning rate from fiber spinning; while this method will lead to gamma crystals shows early melting and results in a transfer to alpha structure under thermal processing [32]. Figure 2- shows the chain conformation of gamma structure and the amount of hydrogen bond in gamma crystals is as half as alpha crystals. To some extent this means lower stability and

mechanical properties because hydrogen bond will effect stiffness, flexibility, crystallinity, glass transition point and gas permeability[31].

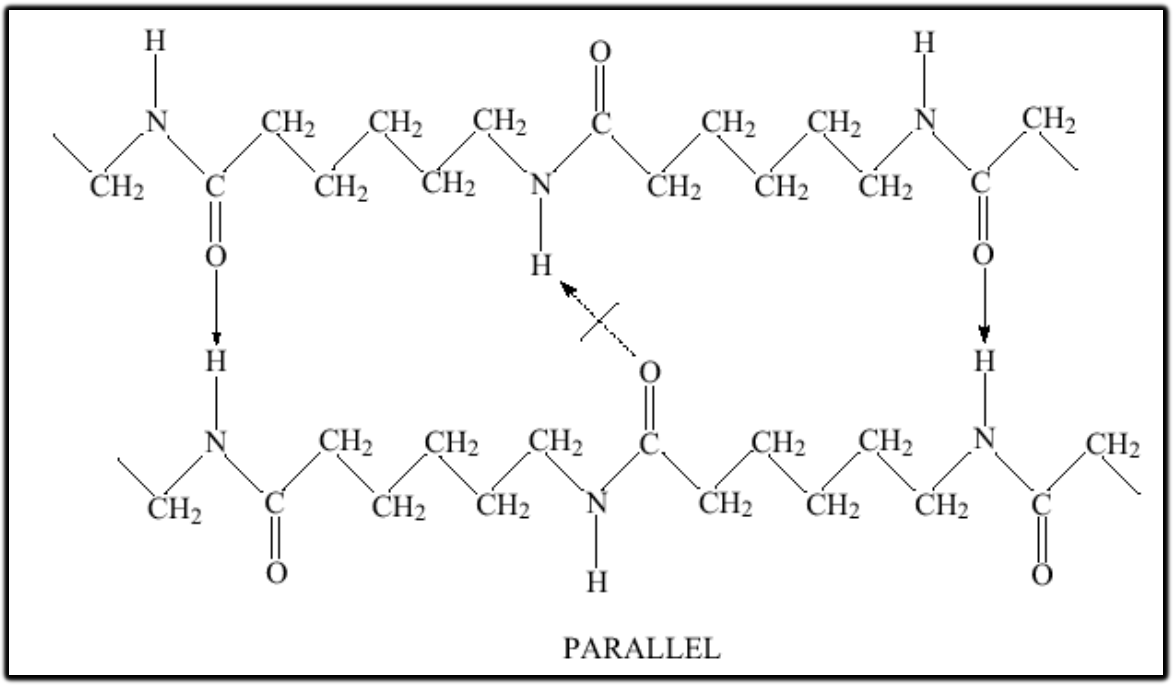

Figure 2- 8 The chain confirmation of gamma crystals of polyamide 6 [34]

The last one is beta crystal form of polyamide 6 that is generated from quenching, which is a mesomorphous state. It is similar to defect gamma structure, and also has a trend to transfer to the more stable alpha structure under thermal treatment. Till now there is still no accurate proof that if the beta crystal is a different crystal or just a kind of derivative from gamma structure [32].

High mechanical properties can be obtained from polyamide 6. Recycled polyamide 6 was used in this research project, so it is necessary to compare different mechanical properties between PA6 and RPA6. Different mechanical properties of PA6 from different supplier are summarized in Figure 2- 9.

Table 2- 1 Name and label of PA6 from different suppliers

Supplier	Name	Label
Solvay	TECHNYL® C 402 M PA6, DRY	S402
Solvay	TECHNYL® C 206 PA6, DRY	S206
Solvay	TECHNYL® C 216 PA6, DRY	S216
Ensinger	TECAMID 6 ID Blue	E6I
Ensinger	TECAMID 6 natural	E6N
Ensinger	TECAMID 6 MO Black	E6M
Unitika Ltd	A1030JR PA6, Dry	UJD
Unitika Ltd	A1030BRL PA6, Conditioned	UBC
Unitika Ltd	A1030BRL PA6, Dry	UBD

References:

http://www.ensingeronline.com/modules/public/datapdf/index.php?s1=0&s2=0&s3=SN2&s4=0&s5=0&L=0

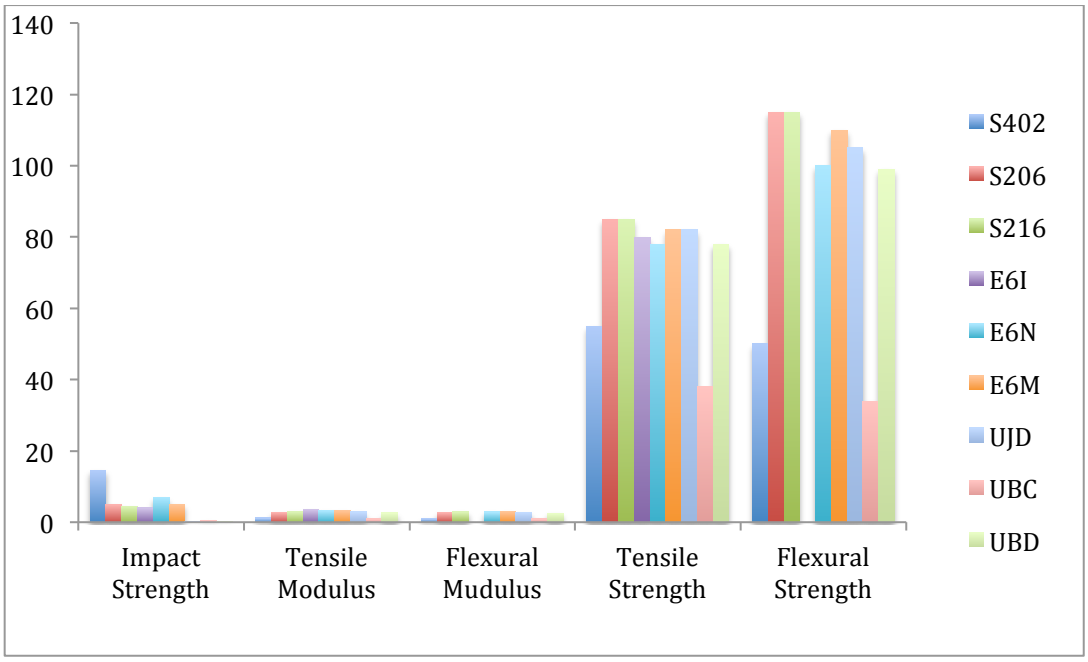

Figure 2- 9 Summary of mechanical properties of PA6 from different suppliers

2.4 Polyamide 6-10

Polyamide 6-10 is another commonly used nylon in different industries. There are different was to synthetize it: one is polymerization by ring opening from caprolactam, and the other one is through condensation reaction by binary acid and diamine. It is easy to have a general idea about the monomer of nylon directly by the number followed “nylon”. For example, polyamide 6 means it has single monomer caprolactam, and polyamide 6-6 means composite by hexane acid and hexamethylenediamine, and polyamide 6-10 means composite by hexamethylenediamine and sebacic acid, and the sketch map is showing in Figure 2- . So the first number followed “nylon” is the number of carbon of diamine and the second number means the number of carbon in the binary acid from the monomer. The word polyamide is the nomenclature for the polymer based on functional group formed during polymerization reaction, the amide is formed when the acid group reactes with the amine group. The word nylon is commonly used, but it was a trade name of Dupont company for its polyamide products.

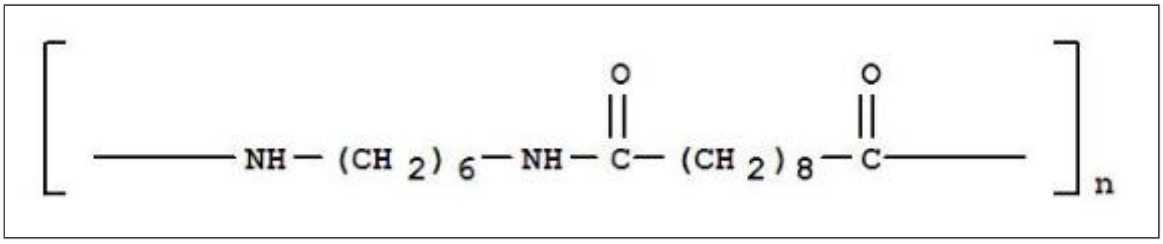

Figure 2- 10 Chemical structure of PA610

Polyamide 6-10 is similar to polyamide 6-6, while it has lower density and higher water absorption, shows better properties under low temperature. It has high resistance to alkaline and dilute mineral acid while not resistance to concentrate mineral acid. The chain conformation of polyamide 6-10 is showing in the following Figure 2- 11.

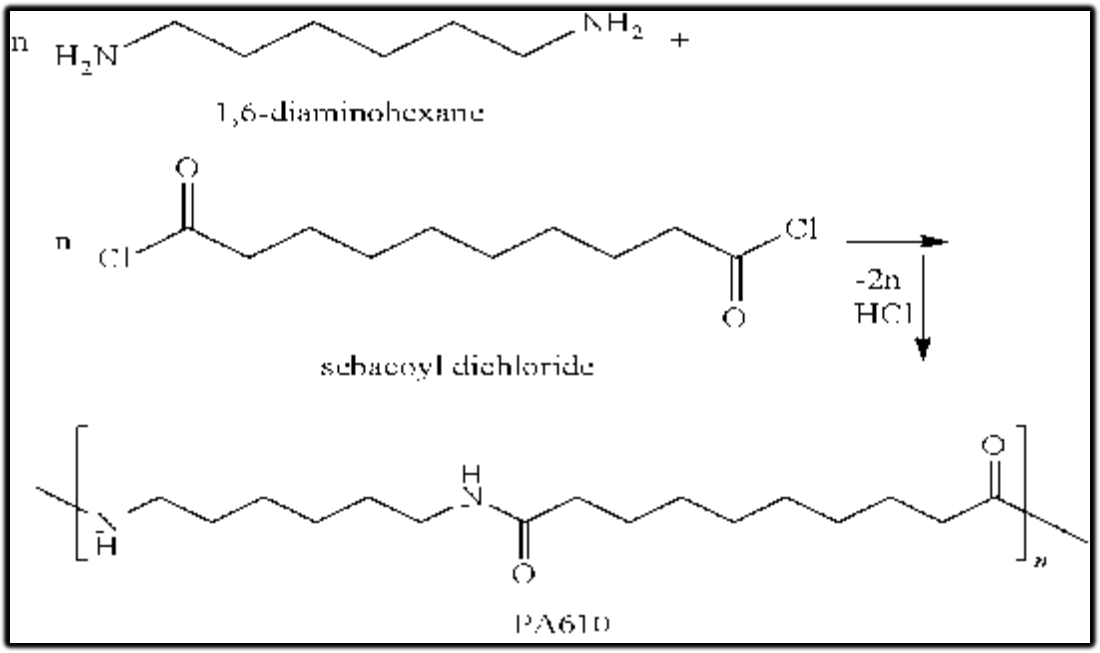

Figure 2- 11 Reaction and chain conformation of polyamide 610

2.5 Antioxidant Category And Mechanism

Polyamide 6 tends to react with oxygen just like other organic material, and this process usually being called "autoxidation". The autoxidation process always happened when polyamide 6 expose to heat, light, forces together with oxygen [35]. So it is essential to add antioxidant as a stabilizer to polyamide composite to get a better performance in different applications.

2.5.1 Polyamide 6 Oxidation

The lifetime and mechanical performance of thermoplastic are mainly determined by the ability of resist oxygen in the long term. Before learning the mechanism of different kind of antioxidants, it is important to have a good understanding of the oxidation mechanism of polyamide 6. The mechanism is described by a series of reactions in the following section.

The most weakness part of the polyamide 6 is the carbon-hydrogen bond of the methylene group which directly close to the nitrogen, and a series oxidation reaction may start from here [36]. Under high temperature and mechanical stress, the polyamide 6 will assimilate energy results in initiation reaction that will produce radicals. Then the major oxidation will start under the aerobic environment, and the radical (-CONHĊH-) reacts with oxygen lead to amide peroxy radical, this is the major oxidation step. The amide peroxy radicals react with polyamide 6 backbone generate more radicals (-CONHĊH-), this is the propagation step. Amide peroxy radical combination will lead to the termination reaction, which generate (-CONHCO-) and hydrogen peroxide. The schematic diagram of polyamide 6 auto-oxidation mechanism is shown in Figure 2- 12.

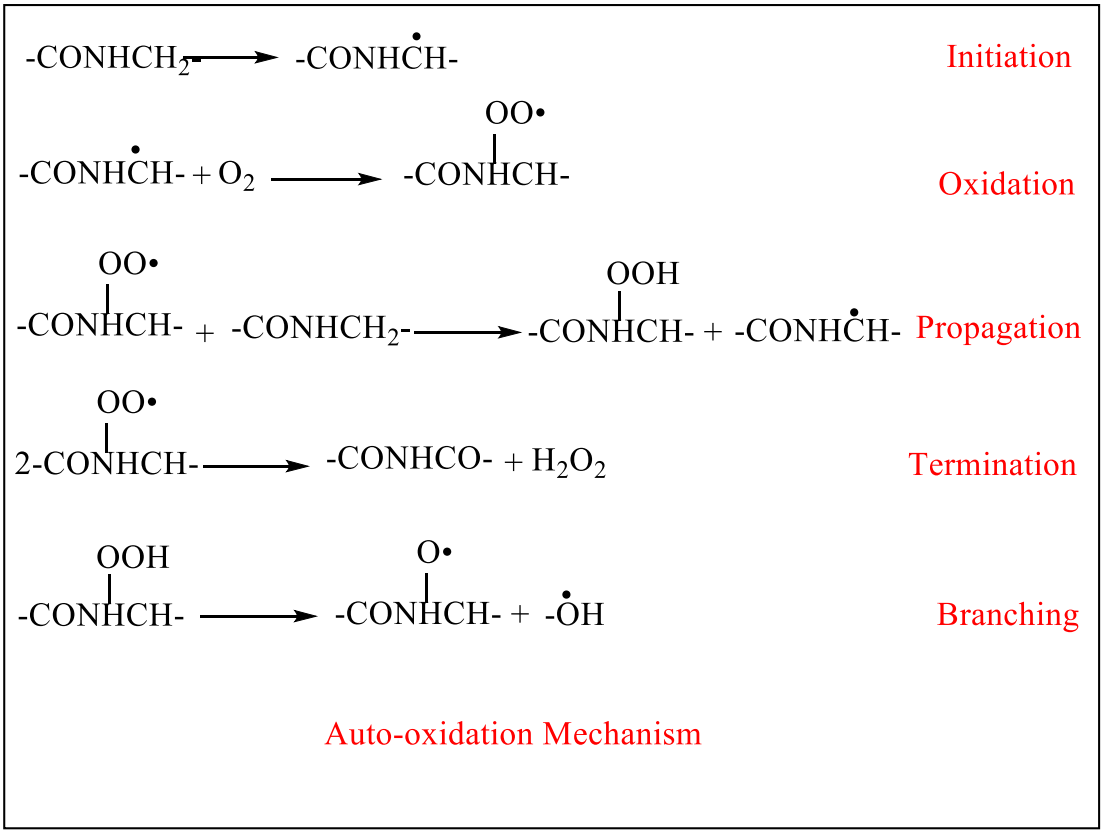

Figure 2- 19 The schematic diagram of polyamide 6 auto-oxidation mechanism [37]

2.5.2 Antioxidant Category And Mechanism

Antioxidants used in the polymers are usually organic compounds that can be classified into four types in chemical composition: phenol, amine, sulfur and phosphine [37]. It can also be classified by different functions: primary antioxidants, secondary antioxidant, multi-functional antioxidants hydroxylamines and carbon-centered radical scavengers [35].

2.5.2.1Primary Antioxidant

The first kind of antioxidant is primary antioxidant works as a chain breaker in the procedure, usually, react with peroxy radicals (ROO·). The mechanism of primary antioxidant is to stop the reaction by transfer (ROO·) to (ROOH). So primary antioxidant always have (OH) and (NH) groups [35]. The schematic diagram is shown in the following figure.

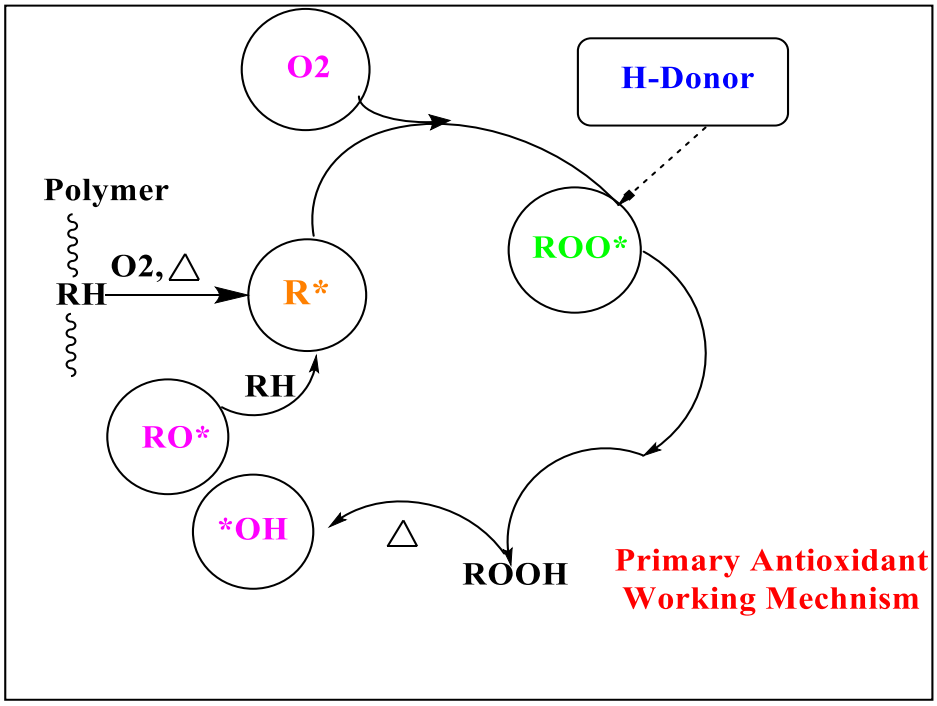

Figure 2- 12 The schematic diagram of primary antioxidants' working mechanism [35]

There are two kinds of primary antioxidant: Hindered phenols and secondary aromatic amines. Both of them work as a chain-breaking donor and at the same time

prevent radical to react with hydrogen from the main polymer backbone. As is known to us, the lifetime of polyamide products depends on their ability of oxygen resistance. Also the hindered phenolic antioxidant is widely used with secondary antioxidant during high-temperature processing. The reaction shows in the following Figure 2- 13 that shows the peroxy radicals (ROO·) abstract the hydrogen from the phenolic antioxidant instead of polymer backbone[35].

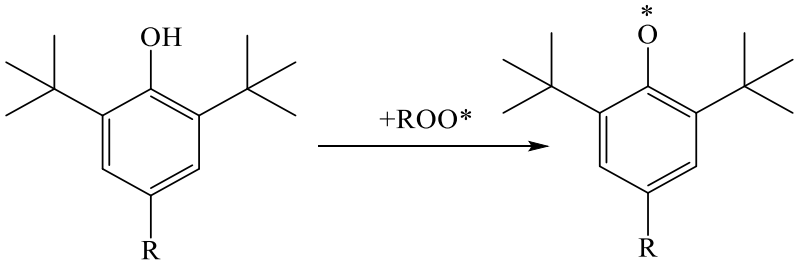

Figure 2- 13 The schematic diagram of hindered phenolic antioxidant working mechanism [35]

The left phenoxy radical is stable due to they can be transferred to a series of mesomeric forms present in Figure 2- 14.

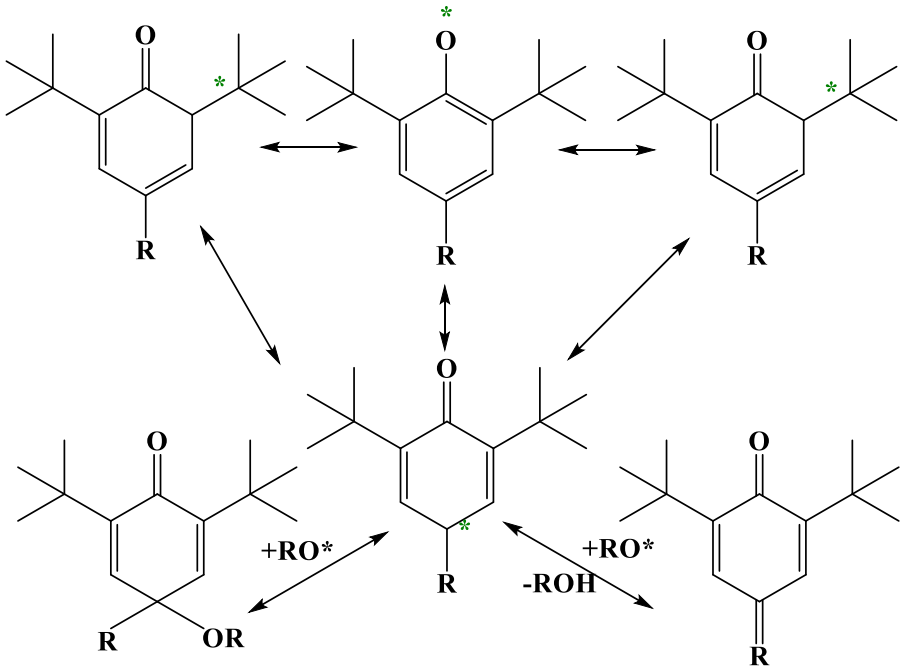

Figure 2- 14 The schematic graph of phenoxy radical transfer [35]

The other one, secondary aromatic amines antioxidant also works as a hydrogen donor and it is more reactive than hindered phenolic antioxidant because of less steric hindrance [35]. The reaction is showing in Figure 2- 15.

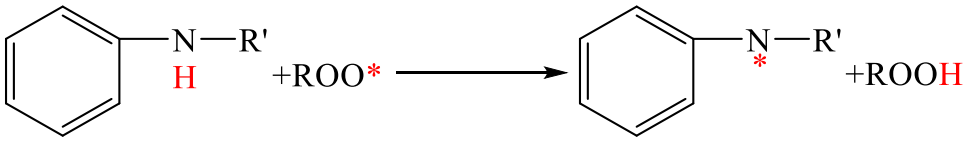

Figure 2- 15 The schematic diagram of secondary aromatic amines antioxidant working mechanism

2.5.2.2 Secondary Antioxidant

From the view of the mechanism, the secondary antioxidant is focused on decomposing hydroperoxide (ROOH) to stable forms. They always combined with

primary antioxidant to get a better performance by synergistic stabilization. The schematic diagram is showing in Figure 2- 16.

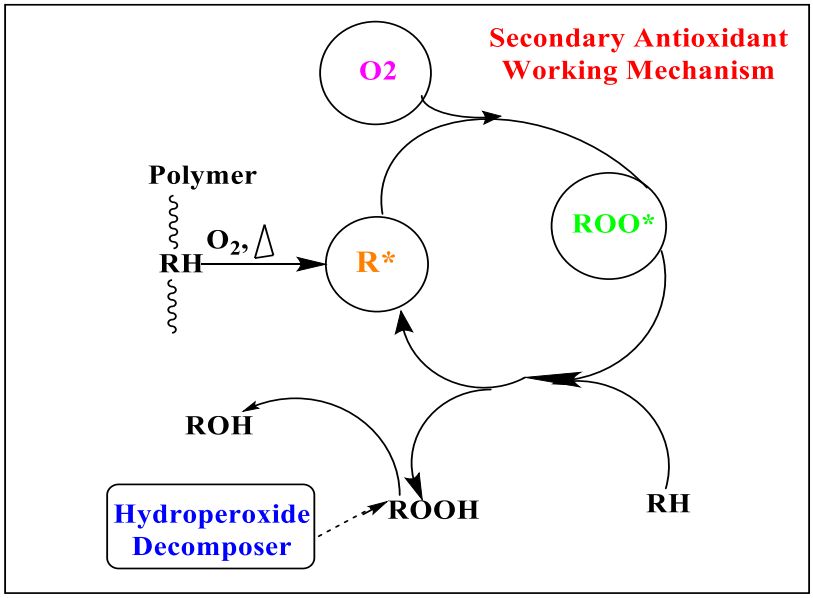

Figure 2- 16 The working mechanism of secondary antioxidant [35]

The main purpose of secondary antioxidant is to prevent the hydroxide transfer to reactive alkoxy and hydroxyl radicals. There are two kinds of secondary antioxidant: organophosphorus compounds and isosynergists antioxidants. The mechanism of organophosphorus compounds antioxidant is showing in the following picture. But this type antioxidant should not be used in the presence of water, because it can be hydrolyzed and produce acid [35].

$$(RO)_3{\bullet}P+ROOH \longrightarrow (RO)_3{\bullet}P{=}O+ROH$$

Figure 2- 17 Organophosphorus compounds antioxidants

Another one, the synergists antioxidants react as the following mechanism. The most famous one of this kind antioxidant is esters of 3,3-thiodipropionic acid. This type antioxidant is less effective to prevent melt fracture while effective in thermal

oxidation in the long run, and usually combined with hindered phenol antioxidants [35].

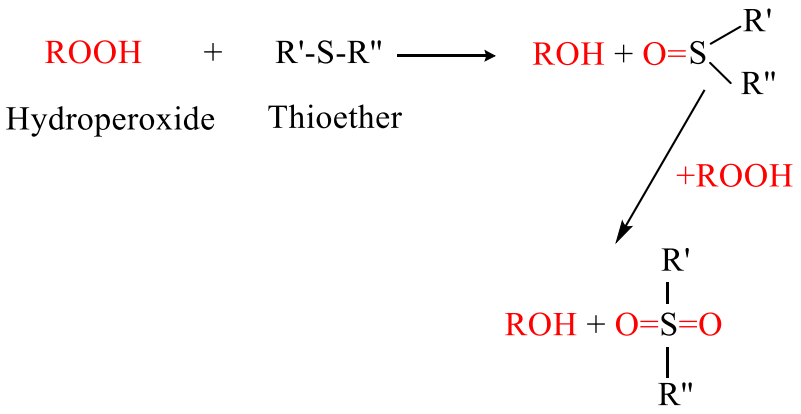

Figure 2- 18 Thioether antioxidants working mechanism [35]

2.5.2.3 Multifunctional Antioxidants

A multifunctional antioxidant is derived from the combination of primary antioxidants and secondary antioxidants according to a specific application. It simplifies the modification process by decreasing the number of stabilizers adding to the composite that also prevent many complicated processes of antioxidants storage. The schematic graph is showing in Figure 2- 19.

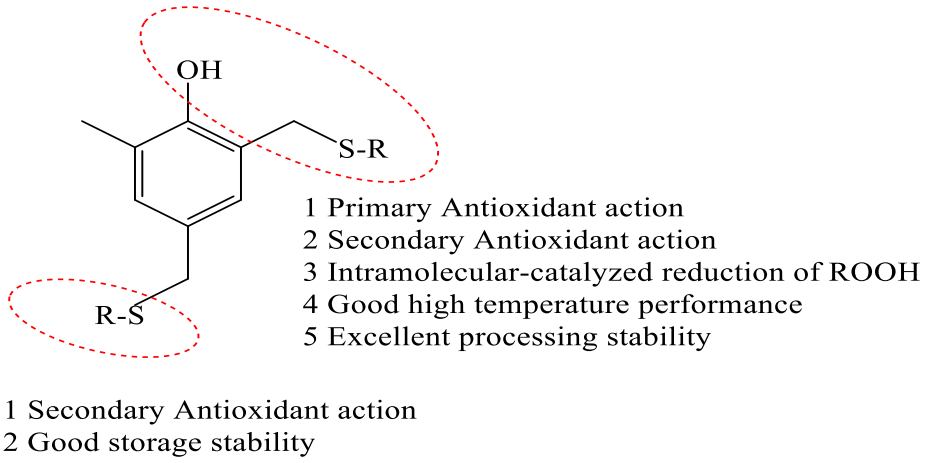

Figure 2- 19 Summary of multifunctional antioxidants working principle [35]

2.5.2.4 Hydroxylamine

Hydroxylamine works like a combination of primary and secondary antioxidant, it can improve processing stability and light stability [35]. The mechanism is showing in Figure 2- 20.

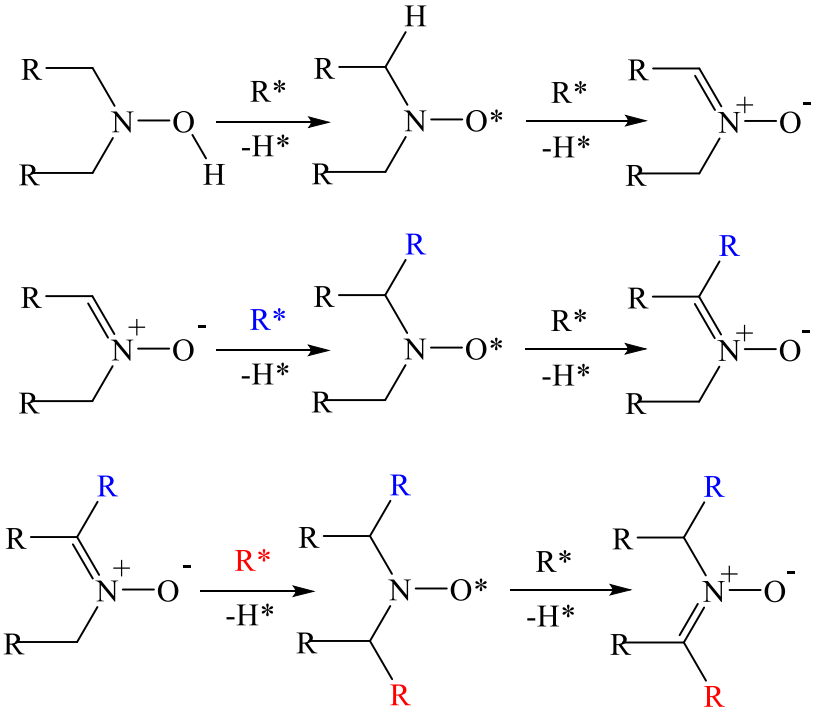

Figure 2- 20 Working mechanism of hydroxylamine

2.5.2.5 Radical Scavengers

It is easy to understand from its name, it is a sort of antioxidant effective by trapping radicals in the oxidation cycle. There are two major types: lactones and acrylated bis-phenols. The schematic diagram is showing in Figure 2- 21.

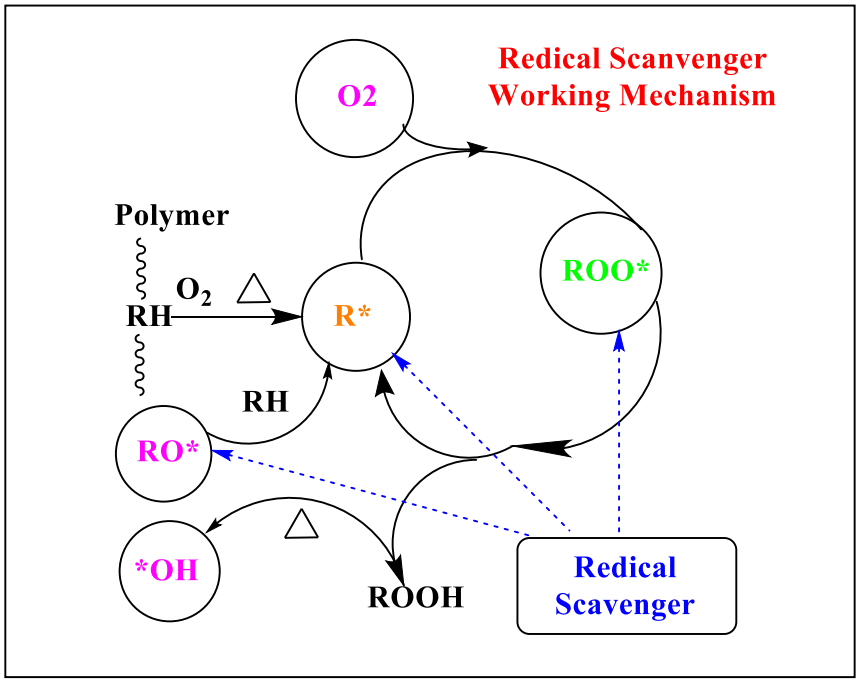

Figure 2- 21 The schematic graph of radical scavenger working mechanism [35]

The lactone is extremely effective in processing stability and is usually combined with phenolic compounds and phosphate as co-stabilizer. The working mechanism of it is showing in Figure 2- 22 [35].

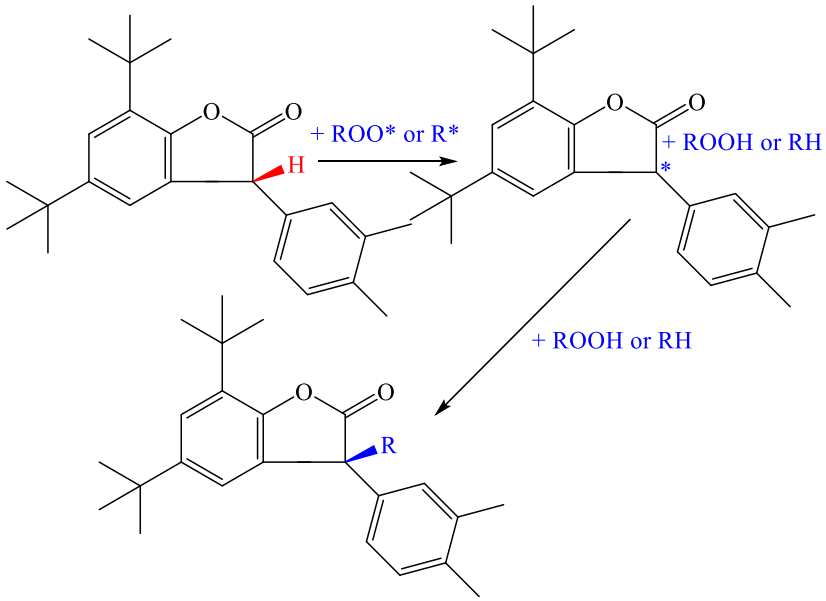

Figure 2- 22 The working mechanism of lactone [35]

2.5.2.6 Criteria Of Adding Antioxidant

Antioxidant suppliershave specific data sheet for each different antioxidant, which contains the recommendation for the amounts for a given specific material based on empirical values and internal research and development carried out by each supplier. The amounts of antioxidant used in the design of experiment applied in this research was based on the recommended amount as specified by suppliers. The amount of antioxidant and the antioxidant effect are not always positively correlated when it exceeds a certain concentration. Excess amounts may promote oxidation. Thereore, the experiments in this research adopted three different levels (low, medium, high) of a specific antioxidant according to the recommendation amount.

2.6 Attempts To Improve Mechanical Properties Of PA6/Natural Fiber

2.6.1 Fiber Treatment

Polyamide 6 reinforced by lignocellulosic fillers had already been used in automotive industries. But there is an obvious disadvantage, the water absorption, and dimensional changes, which may limit the lignocellulosic composites stability in the long run. As discussed earlier, the thermal stability of natural fibers is a significant challenge.

These disadvantages will lead to a decline of the mechanical property, so many treatment methods had been applied to lignocellulose as an attempt to mitigate the disadvantages. Compared with chemical modification, heat treatment is a more convenient alternative; it can be effective and it is a less time-consuming way to modify the lignocellulosic fiber. Heat treatment is an effective way to remove hemicellulose and lignin in cellulose fiber, it can also remove the major by-product, acetic acid, which will lead to a depolymerization of the polymer matrix. The heat treatment was processed in 212 ℃ for 8 hours in an air oven.

Aydemir used 20% heat-treated pine and maple reinforced with polyamide 6 to investigate the mechanical properties of the composite. The tensile strength

increased 109% for pine and 106% for maple cellulose fibers. The flexural modulus of elasticity of pine increased by 101% after heat treatment, and maple got 82% of increase. They also found that the crystallinity of the cellulosic fiber increased after heat treatment, thus contributing to higher modulus. So heat treatment is an effective modification to cellulosic fiber especially in automobile industries for improving the water absorption and stiffness [2].

The surface of the natural fiber contains non-cellulose waxes such as hemicellulose and lignin that will lead to a decrease of interfacial bonging between the polymer matrix and the natural fiber. So the chemical modification is necessary to improve the compatibility between the polymer and natural fiber. It is because the major obstruct of highly interfacial bonding is incompatible of hydrophobic polymer and hydrophilic natural fiber. The most common one is treated natural fiber with alkali, which also can be called mercerization. The sodium hydroxide (NaOH) is used to remove the waxes covered on the surface of the fiber and also reduced the amount of hydrogen bond to improve the surface roughness [3]. Applied mercerization under tension can effective decrease shrank level and improved tensile modulus of the fiber. Tae and Anil found that the fracture stress increased 12.2% and the stiffness increased 36.2% after the mercerization of sisal fiber under tension, which compared with unmercerized ones [38].

Praveen and Thomas found that after oxygen plasma treatment of natural coir fibers, the ability of water absorption increased from 39% to 100% compared with no plasma treated ones. They also confirmed a surface change by topographic measurement. It is possible to make use of this surface modification thereby to improve the interfacial bonding and improve the mechanical properties of the natural fiber and polymer composite [39].

He and Li did an experiment about using amino silicone oil to modify the ramie fiber reinforced polypropylene to improve the interfacial bonding. The result shows that after treated by amino silicone oil, the surface of ramie fiber change from

hydrophilic to hydrophobic especially confirmed by the contact angle changed from 0℃ to 112.6℃. Not only the contact angle but also the mechanical properties such as tensile strength increased by 15.89%, flexural strength increased by 7.04% and impact strength increased by 36.58% compared with ramie/ polypropylene composite without modifications [40].

In summary, from the review of several papers about the modification of natural fiber, the modification can be simple divided into three types according to the working mechanism: one is to remove the non-cellulose part such as hemicellulose and lignin in the natural fiber, the second one is to improve the thermal stability of natural fiber by different treatment, the last one is to help form better interfacial bonding between the polymer matrix and natural fiber fillers. All these modifications lead to an improvement of mechanical properties of the composite.

2.6.2 Additives

It is known to all that the major contradiction needed to be overcome during the process of polyamide 6 and natural fiber composition is the high melting point of polyamide 6 and the low degradation temperature of natural fiber. So the purpose of using additives is to lower the melting point of polyamide 6 and improve the thermal stability of natural fiber. Another sort of additives, antioxidant, is especially used to stop the autoxidation of the polymer chains, because of the weakness of the carbon-hydrogen bond of the methylene group which directly close to nitrogen result in a series of oxidation reaction during the process [36].

In 2012 Amintowlieh made a combination of lithium chloride with N-butyl benzenesulfonamide (N-BBSA) plasticizer to modify the 15% wheat straw composite with polyamide 6. The purpose of adding lithium chloride is to decrease the melting point of PA6 and lead to a lower processing temperature of the composition. N-BBSA is used as a lubricant agent to ease the processing [4].

Ng and Mohajerani tried to investigate the effect of several additives used in wood/polymer composite. One of them is azobisisobutyronitrile (AIBN), which is a sort of thermal initiator additives used to improve the radical concentration and give out an inert atmosphere by releasing nitrogen that is helpful to polymerization.

Other additives are crosslinking agents, diethyleneglycol dimethacrylate (DEGDMA) and divinyl benzene (DVB), which could increase the polymer loading and lead to an enhancement to the copolymerization and crosslink. By this investigation they found that DBV and DEGDMA are effective in improving the mechanical properties of wood/polymer composite even without other additives [41].

Adding plasticizer is an effective way to increase the processability when the polymers under extrusion and injection molding. Chavez and Aurelio attempt to detect the effect of three different plasticizers on cellulose acetate based biocomposites. They compared the effect of dioctyl phthalate (DOP), triethyl acetate (TEC) and glycerol triacetate (GTA) on mechanical properties, thermal conductivity and dimensional properties of biocomposites. The impact strength increased by DOP, while GTA helps to get a higher heat capacity and higher thermal conductivity in a specific temperature range. And TEC got the in-between performance of mechanical properties. From the results, the acetate cellulose based biocomposite modified by plasticizer could be a good choice for insulating materials which also biodegradable compared with traditional materials [42].

So, no matter which kind of additives used during the composition process, the major principle is to try to solve the limitations of the raw material such as the low degradation temperature of natural fiber, the high melting point of polymers, incompatibility of hydrophilic cellulose based fiber and hydrophobic polymers.

2.6.3 Processing Method

The common method used nowadays to prepare materials based polyamided filled with fiber of minerals uses two steps: the first step is meant to create a

homogeneous formulation (also known as compounding), the second step is meant to provide the shape of the product. As such, thermoplastic composites of polyamide 6 with natural fiber undergo extrusion in the first step followed by injection molding or compression molding (hot pressing) in the second step. It is well known that the melting point of polyamide 6 is around 220℃, much higher than the degradation temperature of natural fiber, which will lead to a loss of mechanical properties of the composite, so an improvement of the processing machine is necessary.

Jacobson and Caulfield invented a low-temperature compounding (LTC) method, and they installed a side-stuffer in the seven zone twin-screw extruder. The extruder is consists of seven heating zones at a total length of 32 mm. The extrusion process was divided into three phases: start-up phase, a transition phase, and steady-state phase. In this process, polyamide was first preheated before mixing with ultra-pure cellulose and cellulose was added through the side-stuffer in the forth zone, which aimed at lower the retention time of cellulose under high-temperature processing conditions. The result showed that through the LTC method produced less discoloration and better surface morphology of the composite [43] than one step compounding with extruder.

Maik and Andrzej tried a single-step pultrusion processing method instead of traditional two–step protrusion process to composite bio-based polyamides with cellulosic fibers. The single-step protrusion make use of a batch process that leads to a lower thermal and mechanical stresses under the processing procedure, results in a significant increase of tensile strength and notched impact strength [44].

Highly oriented polyamide 6 made from hot stretching investigated by Shi and Ye. The orientation factor and crystallinity increased as the increase of PA6 draw ratio. More alpha crystalline formed by hot stretching-oriented PA6 lead to a relatively high crystallinity and high-density structure composite. The high level of hydrothermal stability can be explained by low hydrolytic degradation due to high density of the composite [45].

2.6.4 Matrix Polymer Modification

Due to the advantages such as low cost, a large amount of resources, renewability, low density and high specific mechanical properties, natural fiber as an attractive reinforcement for polymer matrix. But sometimes the poor interfacial adhesion and not sufficient fiber dispersion will offset the flexibility and high aspect ratio to resist strong force processing method (extrusion and injection molding) [46]. Although natural fiber is attractive as reinforcement to engineering thermoplastic, there is still a major contradictory limitation need to be resolved during the composition. It is the incompatibility between the polar and hydrophilic cellulose-based natural fiber and the nonpolar and hydrophobic polymer matrixes. So in order to improve the compatibility between them, except the treatment of natural fiber, the modification of the polymer matrix is another effective way to solve the problem. Modification of the matrix with a coupling agent is a popular method to improve the adhesion in the interface by a good binding strength with both of the nonpolar thermoplastic and the polar natural fiber [46].

Maleic anhydride (MA) is shown to be the most effective coupling agent used in the reinforcement of polypropylene with natural fiber. Arbelaiz and Fernandez made an investigation on the effect of coupling agent MA on the mechanical properties and water absorption in polypropylene and short flax fiber composites. In a summary of their work, as the adding of the coupling agent both the tensile and flexural strength increased a lot. The molecular weight of maleic anhydride polypropylene (MAPP) is another important factor, longer MAPP chains with higher molecular weight lead to better tensile properties. They attribute this to the MA functional group grafted at the long polymer chain serves as a bridge between the natural fiber and polypropylene, and more entanglement among polymer chain also contribute a lot to this. After modification by MA, the composite also shows a slight improvement in resistance of water [46], [47].

Blend nonpolar polymer with polar polymer is also an attractive way of matrix modification. Manoj and Rakesh did a research on reinforcement of high-density polyethylene (HDPE)/ polyamide 6-6 with banana fiber. Blending the nonpolar polyethylene with polar polyamide 6-6 not only improved the adhesion between polyethylene and banana fiber and also combined the good mechanical properties inherit from all polymer matrixes. They found that by adding 30% treated banana fiber to the HDPE/ PA6-6 blends increased the tensile strength by 22%, tensile modulus by 31%, flexural strength by 3%, and flexural modulus by 43%. They attribute this improvement of mechanical properties to better interfacial bonding that confirmed by the SEM results [48].

CHAPTER 3 Materials And Methods

3.1 Materials And Instruments

Materials applied in this project and their suppliers are listed in Table 3- 1.

Table 3- 1 List of materials that were used in the project

Materials	Supplier	Comments
Recycled Polyamide 6	Kal-trading	MFI= 20.2g/10min
Polyamide 6-10	Ford	Polymer matrix
Irganox 10-10	BASF	Antioxidant
Irgafox 168	BASF	Antioxidant
Wood fiber compound	25%PA6+75%Suzano Cellulose	Pellet of PA6 and wood fiber
Wood fiber	Suzano Papel e Cellulose	Cellulose pulp fiber

Table 3- 2 shows the model and manufacturer of the instruments used in the project.

Table 3- 2 List of instruments used during the processing and testing experiments

Equipment	Manufacturer
Minilab Extruder Haake	Thermo Electron Corporation
Hot Press, Model3853-0, S/N 12000-937	CARVER, INC.
Injection Moulding Apparatus	Ray-Ran, UK
Testing machine 4467	TESTRESOURCES
Flexural testing machine 4465	TESTRESOURCES
Izod Impact machine43-02-01-001	TMI (Testing Machines Inc.)
Specimen Notch XQZ-I, Travel: 24 mm	Chengde JinJian Testing Instrument Co.,Ltd
FESEM gold coating unit Desk II with Argon	Denton Vacuum, USA
Field Emission Scanning Electron Microscope (FESEM) Leo 1530 with EDX/OIM PV9715/69 ME	Leo Gemini (Carl Zeiss AG, Germany); EDAX (AMETEK Inc.)

Tzero Hermetic low-mass pan and lid (DSC)	TA Instruments
MFI Dynisco Polymer Test D4001DE	Alpha Technologies
Mass Scale SP404D	Scientech
Grinder 5890A GC	IKA ®Werke
Oven 5890A GC	Hewlett Packard
TGA Q500	TA Instrument
DSC Q2000	TA Instrument
FTIR/ATR Tensor 27	Bruker Optik GmbH
Programmable Oven (Annealing)	HP Hewlett Paclard
Moisture Analyzer MB45	OHAUS
Laboratory Mill	Thomas-Wiley
Blender, Model 51BL32	Waring Commercial, USA
Air Oven	VWR PA 19087
XRD Instrument, 30 kV, 30 mA, with Cu Kα radiation	Bruker Instrument Inc.

3.1.1 Polymer: Recycled Polyamide 6

Recycled polyamide 6 (lots B#339236, L#12248) were kindly donated by company called Kal-Trading (Adress: 3440 Wolfedale Rd, Mississauga, ON L5C 1W4, Canada). The melting flow index of this kind of recycled polyamide 6 is 20.2 g/10-min and its

melting point is 219℃. The crystallinity of this recycled polyamide 6, measured by DSC, is 40.3% (without extrusion) and 42.3% (with extrusion).

3.1.2 Wood Fiber: Suzano Cellulose

The Suzano cellulose is provided by company Suzano Papel e Cellulose (Address: Av. Brg. Faria Lima, 1355 - Pinheiros, São Paulo - SP, Brazil, 01452-002). The raw material supplied is a cellulose sheet, the cellulose was produced using Kraft process. After cutting the sheet into small pieces (approximately 1 cm x 1 cm), a Thomas-Wiley laboratory mill was used to further disintegrate the sheet of cellulose into powder suitable for feeding the extruder.

3.1.3 Antioxidant: Irganox 1010

Irganox 1010 is a phenolic primary antioxidant used as a stabilizer for polyamide under long-term high thermal processing. Usually, the antioxidant level of Irganox ranges from 0.05% to 0.4% in different organic polymers (CIBA SPECIALTY CHEMICALS INC.)[49]. Irganox 1010 is a known as a sterically hindered phenolic antioxidant, which can protect polyamide from thermo-oxidative degradation. It has good compatibility with polyamide and can be used in combination with other additives. The structure of Irganox 1010 is shown in Figure 3-1.

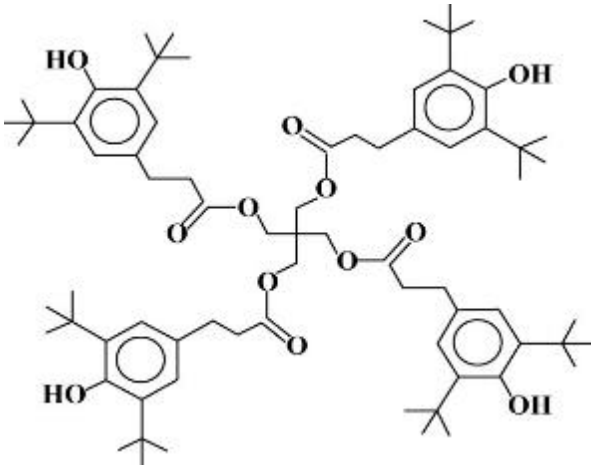

Figure 3- 1 Irganox 1010 chemical structure; copied from reference [50]

3.1.4 Antioxidant: Irgafox 168

Irgafox 168 is a phosphite secondary antioxidant, whose major purpose is to provide hydrolytic stability. Irgafox 168 is usually referred as a hydroperoxide decomposer, which will decompose the hydroperoxide into the unreactive product. The hydroperoxide is formed as the autoxidation of polyamide 6 over a long period of time. This secondary antioxidant always is used together with primary antioxidants to prevent hydroperoxide decomposition into reactive radicals which will lead to the propagation of autoxidation process and lead to a stability in thermal oxidation during the processing steps [35]. Irgafox 168 consists of organophosphate especially effective to hydrolysis. Usually, the antioxidant level of Irgafox is between 500 ppm to 2000 ppm [50]. The structure of Irgafox is shown in Figure 3- 2.

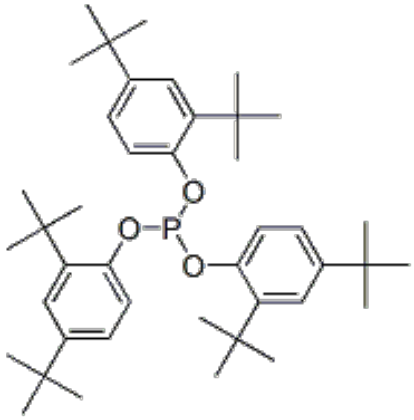

Figure 3- 2 Irgafox 168 chemical structure; copied from reference [50]

3.2 Processing Procedure

3.2.1 Extrusion

The granulated recycled polyamide 6 was dry blended with wood fiber (powder) and blended with different levels of antioxidant Irganox 1010, Irgafox 168 or a combination of the two. Then the lab-scale co-rotating conical twin screw extruder was used to compound the materials by melting and mixing them [Haake, Thermo Electron Corporation] (Figure 3- 3, Figure 3- 4).

Figure 3- 3 Thermo Haake minilab scale extruder

Figure 3- 4 Co-rotating conical twin screws

In order to detect the influence of the thermal degradation due to extrusion, samples of pure recycled polyamide 6 (RPA6) were prepared. Before using the extruder, the

ingredients of each formulation were mixed by shaking in a plastic bag (a process also known as dry blending). It was better to mix the antioxidant with RPA6 first and then mix together with cellulose powder. This is because if all the materials are mixed at the same time, the cellulose may trap the antioxidant which will lead to uneven dispersion into the composite.

The melting point of RP6 is about 220 ℃, while the extrusion temperature of the material is usually 30 ℃ higher than its melting point to ensure flowability, therefore 250 ℃ was selected as the processing temperature of extrusion. The rotating speed of the screw was set at 40 rpm for all the experiments. During the process, it is important to keep a constant pressure when feeding the raw material into the extruder and keep all the samples under same residence time in the extruder so that all the samples will undergo a similar thermal experience. Also it is important to make sure to not let the extrudate aggregate at the die. Since the objective is to test the optimal antioxidant level in the process so any other factor such as inconsistency of material should be avoided.

The resulting compounding material from the extruder was cut into small granules by using a commercial blender (Waring Commercial, USA) to more easily feed the injection molding machine. The materials were dried overnight. Figure 3- **5** shows the extrudate (left) and the pellets (right).

Figure 3- 5 Extrudate of 80%RPA6/20% Suzano Cellulose (left), pellets after grinded (right)

3.2.2 Injection Molding

In this project, a Ray Ran injection molding machine [Ray Ran,RR/TSMP] was used for making the testing bars. The barrel temperature was set to be 265℃ and the tool temperature was set at 80℃. Preheat the purging compound for 5 minutes at 265 ℃ and continuously pull it out. When the white purging compound came out without color changing, it means the feed barrel has already cleaned up. The pellets obtained from extrusion were dried and fed to the molding machine with 10 minutes preheating and melting. Testing bars were prepared for three tests: impact test, flexural test and tensile test. Rectangular bars are needed for impact and flexural tests and dumbbell shaped bars are required for tensile test. The shape and size of rectangular bars based on ASTM D256-10 (ASTM International 2015) and the dumbbell bars based on ASTM D1708-13 (ASTM International 2013). During the injection molding process, the pressure should be kept between 90 psi to 100 psi. Each sample is formed under this pressure for about 25-30s. If the processing temperature was decreased (to minimize thermal degradation), it was difficult to

melt the material and fill into the mold. The loading chamber was kept full of material to keep a constant residence time and reduce the thermal degradation level. The lab scale Ray Ran injection molding is shown in the following Figure 3- 6.

Figure 3- 6 The injection molding machine

The granules after the last step turned a light brown while the rectangular bars from undergoing the same step became almost dark brown or black (except pure RPA6). So the composite may already be degrading significantly during the injection molding process. As the amount of antioxidants was increased, the color of the rectangular bars became a little bit lighter, meaning the antioxidant effectively decreases the thermo-oxidative degradation of PA6.

3.3 Sample Preparation

The formulations of the samples are designed for detecting the influence of different levels of antioxidants on composite mechanical properties. The experiments with polyamide 6 were organized in three parts: the first part focuses on detecting the best antioxidant level of Irganox 1010, second part is to find the best antioxidant level of Irgafox 168, the third part is to find the best combination ratio of Irganox 1010 and Irgafox 168.

Finally, there is also an extra section of experiments to make a comparison of mechanical properties between different amounts of cellulose composite with polyamide 610. The thermal degradation caused by the extruder was also evaluated. Two samples without cellulose, just pure rpA6 was prepared with and without extrusion. The next 4 samples were prepared for antioxidant level test, with all of them keeping a 2:8 ratio of cellulose to RPA6. One of them prepared for the blank experiment where the sample did not contain antioxidants. The formulations of the remaining samples adding antioxidant Irganox 1010 in three levels: 50ppm, 500ppm and 5000ppm. The formulation of these samples is shown in Table 3- 3. Each series of composite prepared approximately 100g. The three levels of antioxidant Irgafox 168 is shown in Table 3- 4.

Table 3- 3 Design of sample formulations in part one

Run#	Label	Suzano cellulose (wt-%)	Recycled PA6 (wt-%)	Irganox 1010 (wt-%)
A	RPA6	0	100	0
B	RPA6 (E)	0	100	0
C	RPA6/CEL	20	80	0
D	RPA6/CEL-50IX	19.999	79.996	0.005
E	RPA6/CEL-500IX	19.99	79.96	0.05
F	RPA6/CEL-5000IX	19.9	79.6	0.5

"E" in the second run indicates the samples that will undergo extruder processing. After preparing the initial materials, they were dried in the air oven at 80℃ for 48 hours, and then dried by vacuum oven for another 5 hours. Before any processing experiment, moisture content should be tested three times and then an average was calculated.

Table 3- 4 Design of sample formulations in part two

Run#	Label	Suzano cellulose (wt-%)	Recycled PA6 (wt-%)	Irgafox 168 (wt-%)
1	RPA6/CEL	20	80	0
2	RPA6/CEL-250IF	19.995	79.98	0.025
3	RPA6/CEL-500IF	19.99	79.96	0.05
4	RPA6/CEL-1000IF	19.98	79.92	0.1

The combination formula of Irganox 1010 and Irgafox 168 is shown in the following Table 3- 5, four kinds of formulation used in this part, which are according to the mechanical properties from part one and part two.

Table 3- 5 Design of sample formulations in part three

Run#	Label	Suzano cellulose (wt-%)	Recycled PA6 (wt-%)	Irganox 1010 (wt-%)	Irgafox 168 (wt-%)
a	1000IX/250IF	19.975	79.9	0.1	0.025
b	250IX/1000IF	19.975	79.9	0.025	0.1
c	1000IX/1000IF	19.96	79.84	0.1	0.1
d	250IX/250IF	19.99	79.96	0.025	0.025

The last part is about polyamide 6-10 and wood fiber composite. The formulations are shown in the following Table 3- 6. These samples were molded by Ford Motors Company and sent to our research lab as part of research collaboration project; the analysis was done at the University of Waterloo.

Table 3- 6 Formulations of extra mechanical testing samples

Run#	Wood Fiber (wt-%)	Polyamide 610 (wt-%)
NF0	0	100
NF3	3	97
NF10	10	90
NF20	20	80
NF30	30	70

3.4 Processability

3.4.1 Melt Flow Index (Mfi)

The melting flow index (MFI) is a method to detect the processability of the material under thermal procedures. This MFI test followed the ASTM 1238-13 (ASTM INTERNATIONAL 2013). Each time a five grams sample was loaded to the heating chamber of the MFI instrument, processed under 260 ℃ for 240 seconds was taken to preheat the material before 60 seconds frequency of cutting the material. The weight of the piston was 2.06 kg, and the pushing bar was 0.1 kg, so in total the weight was 2.16 kg. Eight measurements were tested for each sample. The melting flow index is calculated as the amount of materials (grams) passing the die in 10

minutes. Higher MFI means a low viscosity and high mobility. Often grades for injection molding would have MFI values in the range of 3 to 40 grams/10min.

3.5 Mechanical Test

3.5.1 Annealing

All the samples after injection molding had already experienced a series of thermal procedures such as extrusion and injection molding. Annealing was carried to erase previous different thermal histories among the samples, which would lead to an effect on mechanical properties. Another reason to use the annealing process is that during injection molding, the melting materials rapidly cooling down in the molded lead to a suddenly freezing of the polymer chains that have not reached an equilibrium state. So the annealing process is necessary before evaluation of mechanical properties. During the annealing process, the atoms rearrange their position and decrease the amount of dislocation of the polymer chains, as a result, increase the order of the lattice and increase the crystallinity [51]. Annealing can also dry the samples to avoid the absorption of moisture that can cause a decrease in mechanical performance. The equipment used to process annealing is a programmable oven (Oven 5890A GC). The starting temperature of the annealing oven is 25 ℃ and the final temperature of this process is 120 ℃, this temperature is higher than the glass transition temperature of RPA6 and lower than its melting point. The rate of temperature increase is 1 ℃/minute, remaining at 120 ℃ for 600 minutes then cooling back to initial temperature at the same decreasing rate of 1 ℃/minute.

3.5.2 Conditioning

The conditioning process occurs in a lab environmental chamber. The reference standard is ASTM D256-10 (ASTM INTERNATIONAL 2015). The testing bars received from the injection molding after annealing were placed in the chamber for 48 hours. The relative humidity in the conditioning chamber was 50± 10% and the temperature kept at an indoor temperature of 23±**2** ℃ after setting all the

parameters in the environmental chamber, then sealing the chamber. The condition of the conditioning process is same as the following mechanical test.

3.5.3 Flexural Test

3.5.3.1 ASTM Standard

The flexural test was conducted according to ASTM D790-10 (ASTM INTERNATIONA 2010). The dimensions of the rectangular testing bar was 63.5mm × 12.7mm × 3.0mm made by injection molding. It is recommended for isotropic materials and molded samples that at least 5 specimens are required. The rate of cross head motion was 13.89 (mm/min) based on ASTM calculated by Equation 3-1:

$$R = \frac{Z \times L^2}{6d} \qquad \textbf{Equation 3- 1}$$

R (mm/s): Rate of crosshead motion, mm/min

L (mm): length of support span, 50mm

d (mm): depth (thickness) of sample, mm

Z (mm/mm/min): Straining rate of the outer fibers, which should be kept at 0.1 for method B [52]

3.5.3.2 IOS Standard

The flexural test of the polyamide610 and cellulose composite was molded according to ISO 178 (ISO 2010 E) at Ford. The flexural testing machine in our lab was set up to follow ASTM standard. The specimens received from Ford were adjustmented according to ASTM standard. The results got from this series of experiments should be limited to comparison among this series of samples, but it should be used to compare with other researchers result. The dimensions of the rectangular testing bar are 63.5mm × 10.0mm × 4.0mm made by injection molding. In total 5 specimens were measured for each sample [53].

3.5.4 Tensile Test

3.5.4.1 ASTM Standard

The tensile test was conducted according to ASTM D1708-13 (ASTM INTERNATIONAL 2013). The dimension of the dumbbell shape sample is described in the following Figure 3- 7. The testing speed of the process was 10 mm per minute [54]. For this test, 5 specimens were measured for each sample.

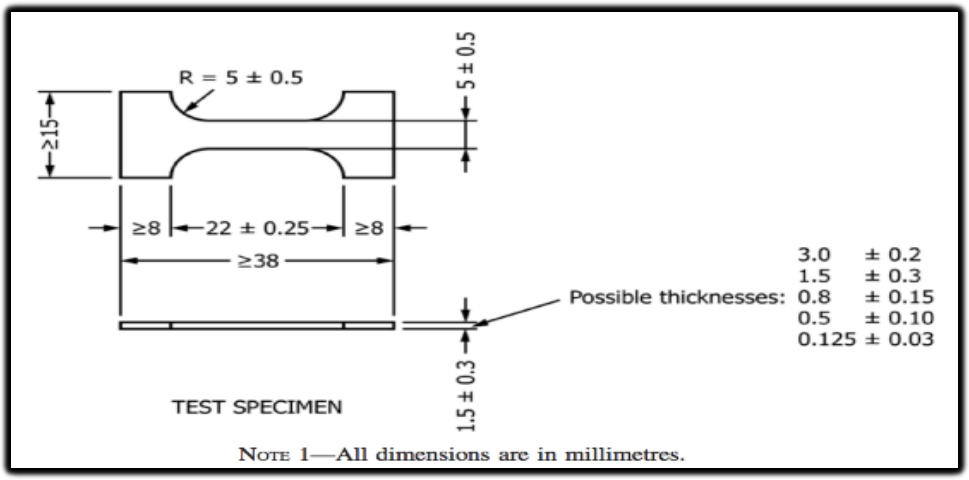

Figure 3- 7 Size of sample [53]

3.5.4.2 IOS Standard

The tensile test of polyamide 6-10 and cellulose composite was conducted according to ISO 527-1 (ISO 527-1:2012 E). The tensile testing machine in our lab set up to run ASTM standard test, therefore the specimens produced at Ford were adjusted to meet ASTM requirments. The testing speed of the process was 10 mm per minute. In total, 5 specimens were measured for each sample [55].

3.5.5 IZOD Impact Test

3.5.5.1 ASTM Standard

The Izod impact was conducted based on ASTM D256-10 (ASTM INTERNATIONAL 2010). The dimension of the rectangular bar is 63.5mm × 12.7mm × 3.0mm, and

notch of the bars should be done before testing. The notching process was done on a milling machine, and both the feed speed and the cutting speed were constant. The length of the un-notched part of the specimen was 10.16 ± 0.05 mm. Five specimens were measured for each sample [56].

3.5.5.2 IOS Standard

The Izod impact was conducted based on ISO 180 (ISO 180: 2000 E). The dimension of the rectangular bar was $63.5\ \text{mm} \times 10\ \text{mm} \times 4.0\ \text{mm}$, and notch of the bars should be done before testing. The notching process was done on a milling machine. The length of the un-notched part of the specimen should be 8.0 mm. Five specimens were measured for each sample [57].

The impact resistance of material is usually determined by Izod impact test. The impact test for this lab scale research is based on ASTM standard, while the impact test for sample prepared by industry was according to ISO standard. The impact strength is represented by energy lost per unit of thickness at the notch (J/m) in ASTM International standard. While, the impact strength is represented by energy last per unit cross-section area at the notch (kJ/m^2). The mechanical part that withstand impact load in practical work rarely damage due to one-time large energy impact, while mostly due to accumulation of multiple small energy impact results in initiation and propagation of the fracture [58].

Toughness is a measure of the energy required for fracture. There are two indicators for material toughness: Impact toughness and fracture toughness. The impact toughness is represented by aK (kJ/m^2). Impact toughness means the material resist to impact forces and without damage when it is under impact loading. It is the energy (kJ) consumed per unit area (m^2) in the cross-section.

3.5.6.Gardener Impact Test

The specimen consists of polyamide 6-10 and cellulose molded to follow the ISO 527-1(ISO INTERNATIONAL STANDARD 2012), however due to the limitation of instrument available in our lab the procedure followed the ASTM D5420-10 (ASTM INTERNATIONAL 2010). The diameter of the specimen was 74.30 mm and the thickness of the specimen is 3.05 mm. If the approximate mean-failure height for a given sample is known, 20 specimens are recommended for the gardener impact test. If it is unknown, 6 more specimens needed to determine the appropriate starting height of the test. There are six different type of failure of the testing specimen need to be identified after the test [55].

The measurement was conducted by precisely locating all the samples in the same position to ensure that the rod above hit the samples on the same area. The striker foot is raised out of the way and the specimen is located on the support plate. The weight up is raised to the desired value and released so that the weight can fall down in the guide tube and impact the specimen. Then a visual inspection is conducted to determine if the specimen has failed and record was made. If it is failed keep the mass of weight constant and decrease the height to which the weight was lifted, otherwise increase the drop height. Then repeat the test according to previous test results [59]. A diagram of instrument is shown in Figure 3- 8. This instrument is widely used in industry because the results are helpful in identifying the type of failure in the material when the specimen hit (impact) by a plunger in the shape of a blunt dart in the absence of previous defects in the specimen.

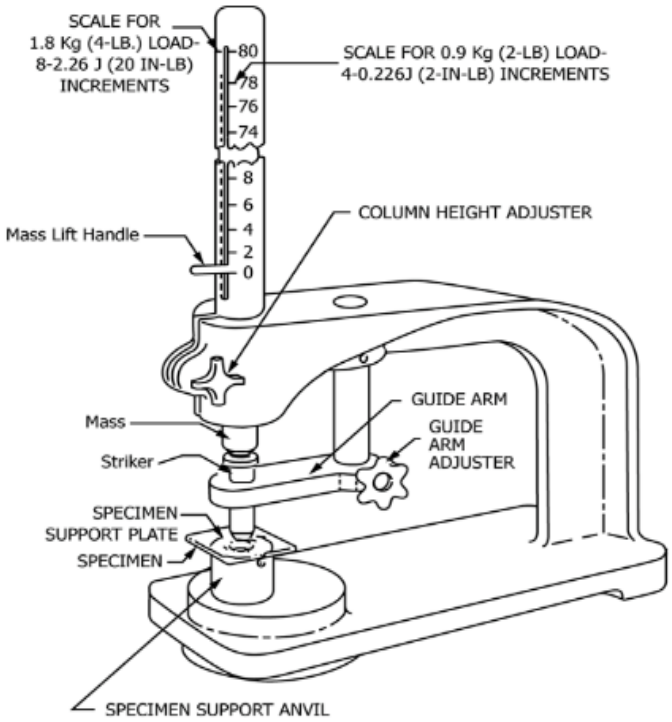

Figure 3- 8 Gardner impact tester [59]

The mean failure height and mean failure energy are calculated based on Equation 3-2 and Equation 3-4.

$$\boldsymbol{h = h_0 + d_h\left(\frac{A}{N} \pm 0.5\right)} \qquad \textbf{Equation 3- 2}$$

Where:

h = mean failure height (in)

d_h = increment of height (in)

N = total number of failure or non-failure, whichever is smaller. Call whichever a events in the following part

h_0 = lowest height where an event happened (in)

i = counting index from 0 for h or w

n_i = number of events happened at h_i

$$\boldsymbol{A = \sum_{i=0}^{k} i n_i} \qquad \textbf{Equation 3- 3}$$

The negative sign is used for h when the events are failure, positive sign is used for non-failure events.

$$MFE = hwf \qquad \textbf{Equation 3- 4}$$

Where:
MFE = mean-failure energy (J for Joule)
h = mean-failure height as applicable (in)
w = weight or mass (lb)
f = factor for conversion to joules
Use f = $9.80665*10^{-3}$ if h=mm and w=kg; Use 0.11299 if h= in. and w= lb; Use f= 1.0 for inch-pound units (in, lb)

Also the failure type can be classified into six types base on ASTM D5420:

- No crack (N)
- Complete shattering (C)
- Crack radiating towards edge of the plate (E)
- Radical crack within impact area (I)
- Hole in plaque (H)
- Brittle splitting (B) [59]

3.6 Thermal Property Characterization

The thermal properties such the melting point and crystallization temperature were obtained from the Differential Scanning Calorimetry (DSC) experiments. The percentage of the crystalline content in the material was also obtained from the same experiment by integration of the second melting peak in the curve and comparison of the enthalpy of heat measured in the specimen with a reference enthalpy of heating.

3.6.1 Differential Scanning Calorimetry (DSC)

DSC is a thermal analysis technology to detect the difference of heat flow for sample and reference to reach the same temperature. DSC is commonly used in polymer material for thermal property characterization. The melting point (Tm), glass transition temperature (Tg), crystallization temperature (Tc) could be obtained from the heating and cooling curve from DSC. This calculation follows Equation 3-5:

$$\boldsymbol{X_c}(\%) = \frac{\Delta \boldsymbol{H_c}}{\Delta \boldsymbol{H_m^0} \times \boldsymbol{f}} \times \mathbf{100} \qquad \textbf{Equation 3- 5}$$

ΔH_c is the enthalpy of the melting sample, ΔH_m^0 is the enthalpy of melting 100% crystalline PA6. Due to the most commonly crystalline form being α and γ in PA6, ΔH_m^0 was selected as an average value $190\,{}^{J}/_{g}$. And f is the weight percentage of matrix (PA6) in the composite [14].

The material used for DSC test is a piece of broken bar after impact test, the weight of the sample for DSC is between 5-8 mg. The DSC process included two heating, a short isothermal and two cooling cycles. The samples first heat to 280 ℃ at a rate of 10 ℃/min, then isothermal at this temperature for 5 minutes. Cooling at the same rate 10 ℃/min to 120 ℃, then isothermal for 5 minutes. The second cycle also heating the material to 280 ℃ at a rate of 10 ℃/min. Then cooling down at a higher rate of 50 ℃/min to 50 ℃.

3.6.2 Thermal Gravimetric Analysis (TGA)

Thermal Gravimetric Analysis (TGA) is is used to evaluate the thermal stability of the material according to the weight change (also known as weight loss) as the temperature increases or according to weight change at an isothermal condition. The evaluation of the decomposition can be investigated under nitrogen, air, and helium or other kinds of gasses. The TGA instrument is constituted with a programmable furnace, temperature measurement, weight measurement , sample

holder and references holder. A precise amount ranging often from 5 to 10 mg sample is placed in a platinum pan, and continuously weighted as the increasing of the temperature. The results of the TGA test can be present in two ways, one is the weight versus the temperature, , the other is to present the first derivative of weight versus the temperature is a better choice.

Here the samples were prepared by grinding bars after injection molding, and all the samples dried overnight in the air oven. The temperature of 1%, 5% and 10% weight loss for different samples were obtained from TGA curves. The measurement started at from 30℃ and finished at 650℃ at a heating rate of 20℃/min, and the flow rate of the nitrogen of the TGA machine is 40 ml/min.

3.7 Crystalline Identification

The crystalline forms of polymer and cellulose fiber were investigated by the X-ray diffraction (XRD). It is well known that the mechanical properties are closely related to different crystalline forms of the material that according to different chemical structure [60]. So it is necessary to investigate the transfer of different crystalline forms when polyamide 6 composite with cellulose or the effect of different natural fiber loading.

3.7.1 X-Ray Differaction (XRD)

The wide-angle X-ray powder diffraction is an application of X-ray crystallography, which is based on both the X-ray wave and the particle nature to investigate the structure and unit cell dimensions of the material. Identification of the material and different crystalline forms that existed in the samples were usually decided by diffraction pattern [61].

Usually the specimen used for XRD is a small amount of random powder loaded in a non-crystalline sample holder. But in polymers, a film or a plate are often used too. Here, the testing bar prepared by injection molding was directly put in the sample

holder for XRD measurement. The measurement was conducted by D8 Bruker XRD instrument. The samples were scanned from 3 ° to 45°, and they were conducted at 0.5°/step and stays for 3 seconds. The target metal used in XRD is copper and the strongest wavelength (Kα) is 1.54 $\mathring{A}$. Diffraction peaks are interpreted using Bragg's Law [66].

$$n\lambda = 2d \sin\theta \qquad \textbf{Equation 3- 6}$$

Where n: An integer, often 1

λ ($\mathring{A}$): The wavelength of X-ray

d ($\mathring{A}$): The inter-planar distance in diffraction

θ (∘): The diffraction angle

The X-Ray diffraction (XRD) is an effective structure analytical technology to identify the crystalline form of the material, to understand the interatomic or intermolecular distance and unit cell dimensions. It is widely used among crystalline material to identify the crystallinity and crystalline size. The diffraction patterns are obtained by scanning a specific range of incident angles that include the target peaks of identifying the material. The XRD could detect the intensity of the reflected area, which can be used to calculate the crystallinity of the material [61]. Another common use of XRD is to identify different type of crystalline forms by comparing the XRD data from the standard database of the same material.

3.8 Morphology Analysis

It is necessary to understand the surface properties of polymers since it is important for applications where employed composite. And inappropriate surface properties will lead to undesired mechanical properties [51]. The morphology of samples was investigated by scanning electron microscopy (SEM) such as the dispersion of cellulose fiber inside RPA6 matrix, interfacial bonding between RPA6 and cellulose fiber and the cracking mechanism.

3.8.1 Scanning Electron Microscopy (SEM)

Scanning electron microscopy is a technique to obtain the surface analysis of the materials through electron beam scanning the material. There are two major purpose of SEM used in this project, one is to investigate the interfacial bonding between the matrix and fillers, and another one is to see the status of dispersion of the cellulose fiber inside the polyamide.

The samples used in the SEM were made from fracturing samples immersed in liquid nitrogen. The samples were stuck to the SEM stub by conductive tape and coated two times by gold. The inert gas used during the coating is argon. The Field Emission Scanning Electron Microscope (FESEM) Leo 1530 with EDX/OIM PV9715/69 ME was used in my project. And the magnification used are 300, 500, 1000, 5000 and 10000. The voltage used during the test was 7.00kV.

3.9 Chemical Composition Identification

3.9.1 Fourier Transform Infrared (FTIR) Spectrocopy

Infrared spectrum shows unique absorption peaks of specific material based on the frequency of bonds and atom vibration, as a result used as a basic material identification (qualitative) technology. Also, the component percentage can be determined by comparing the size of absorption peaks, so that it can be used as a quantitative technology [62]. The spectrum is an output of infrared instrument. The x-axis is known as the wavenumber scale and the y-axis can be either presented by % transmittance or presented by % absorbance as an indication of bend intensity. The absorbance means how much incident light is absorbed when it go through the material while the transmittance means how much incident light transmitted. And transmittance is defined as the ratio of transmitted light intensity to incident light intensity [51]. The Bruker Tensor 27 FTIR was used to obtain the spectrum of RPA6 and PA6-10. The % transmittance was used as y-axis. The infrared spectrum was scanned from 400 to 4000 cm^{-1}. The resolution was 4 $cm^{-1}$and 32 scans was made for each sample. The thickness of sample film used in FTIR

was 0.03 mm.

3.10 Oxidation Induction Time (OIT) Test

OIT is short for oxidation induction time, it is often used to measure and to understand the oxidative stability of polymers. The application thermoplastic usually expose the material to environments with high working temperature, strong forces, light and oxygen that will lead to initiation of oxidation processes thus resulting in limited lifetime of the product or early failure due to oxidation. The OIT information is useful determining and choosing antioxidants and thermal stabilizers to extend the lifetime of the polymer products. The OIT measurement is done using a differential scanning calorimetry (DSC). The major purpose of this test is to evaluate the ability of antioxidants to resist and delay oxidation of the polymer. It can be used to detect the best amount of antioxidant to be included in a formulation for a given application of the polymer material. ASTM D3895-14 (ASTM INTERNATIONAL 2014) determines the condition for the setup for OIT test. It is important to note that this standard was originally developed to fit for polyolefin resin and there is no ASTM standard or other research paper published specifically for polyamide. The OIT is defined as the time from it switch to oxygen to the onset point of oxidation, which is exothermic showing in the DSC curve [63].

The choice of using OIT to evaluate thermal stability of polyamide with natural fibers as presented in this document is perhaps one of the first attempts in the literature. Polyamide and cellulose fibers samples were prepared by extrusion for OIT without injection molding to avoid excessive exposure and thermal history exerted during molding. The specimens used in this test were prepared by extrusion only and then hot pressed to 0.20 mm thick films for DSC measurement. The hot pressed film is shown in Figure 3- 9. The aluminium is made to 0.20 mm thick. The specimen was heated at 20 ℃/ minute to 180 ℃ at nitrogen atmosphere and

isothermal for 5 minutes. Then the inlet gas switched to oxygen to investigate oxidation induction time (OIT).

Figure 3- 9 The sandwich for OIT film hot press

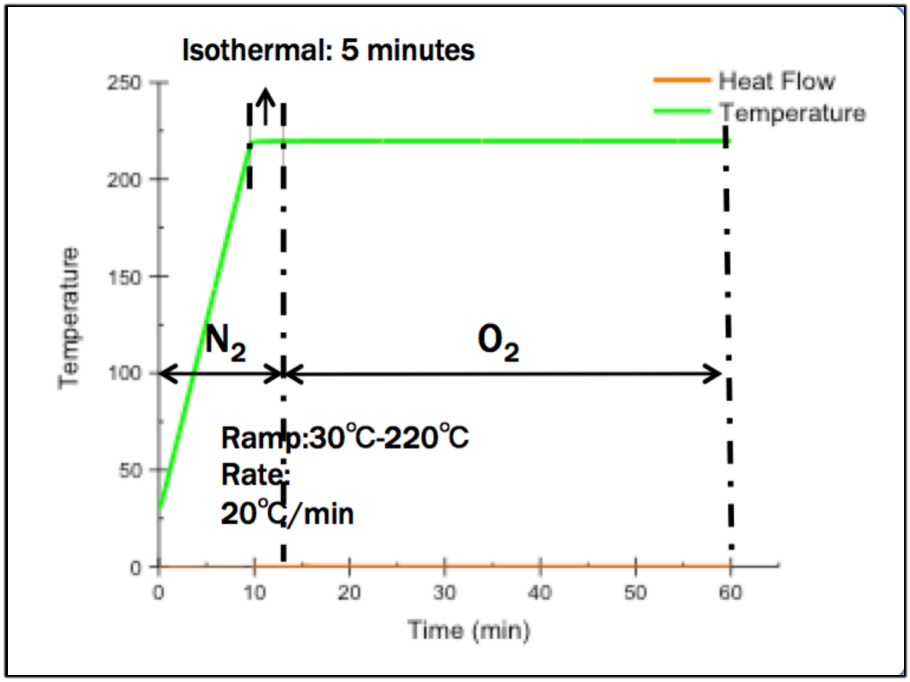

Figure 3- 10 The OIT procedure graph (temperature changes)

In the OIT test method, the sample disk was heated to a specific temperature in an open pan under N_2 atmosphere. Then isothermal at this temperature for 5 minutes before inlet gas switched to O_2. The time interval from the switching point to exothermic oxidation reaction is defined as OIT. The OIT test had already well established for polyethylene (PE), but never done for polyamide (PA), so the OIT test was tried to check is it possible to apply for PA6 composites.

CHAPTER 4 RESULTS AND DISCUSSIONS

4.1 Results And Discussion Of PA6/Suzano Cellulose With Irganox 1010

4.1.1 Specimens Color

The sample formulation of this part is in Table 3-3. The color of the specimen is an apparent representation of the degradation level of the material after different thermal processes. Figure 4- 1 shows the extrudate of pure RPA6 and the composite with 20% cellulose respectively.

Figure 4- 1 The extrudate recycled nylon 6(left), and the extrudate of 20%cellulose composite

After extrusion, the colour of the recycled polyamide 6 changed by becoming lightly yellowed while the cellulose composite turned to brown color, this means the thermal degradation was mainly a result of the cellulose. The higher degradation in the cellulose composite is due to the extrusion temperature being higher than the degradation temperature of the cellulose. Figure 4- 2 shows the rectangular bar after injection molding.

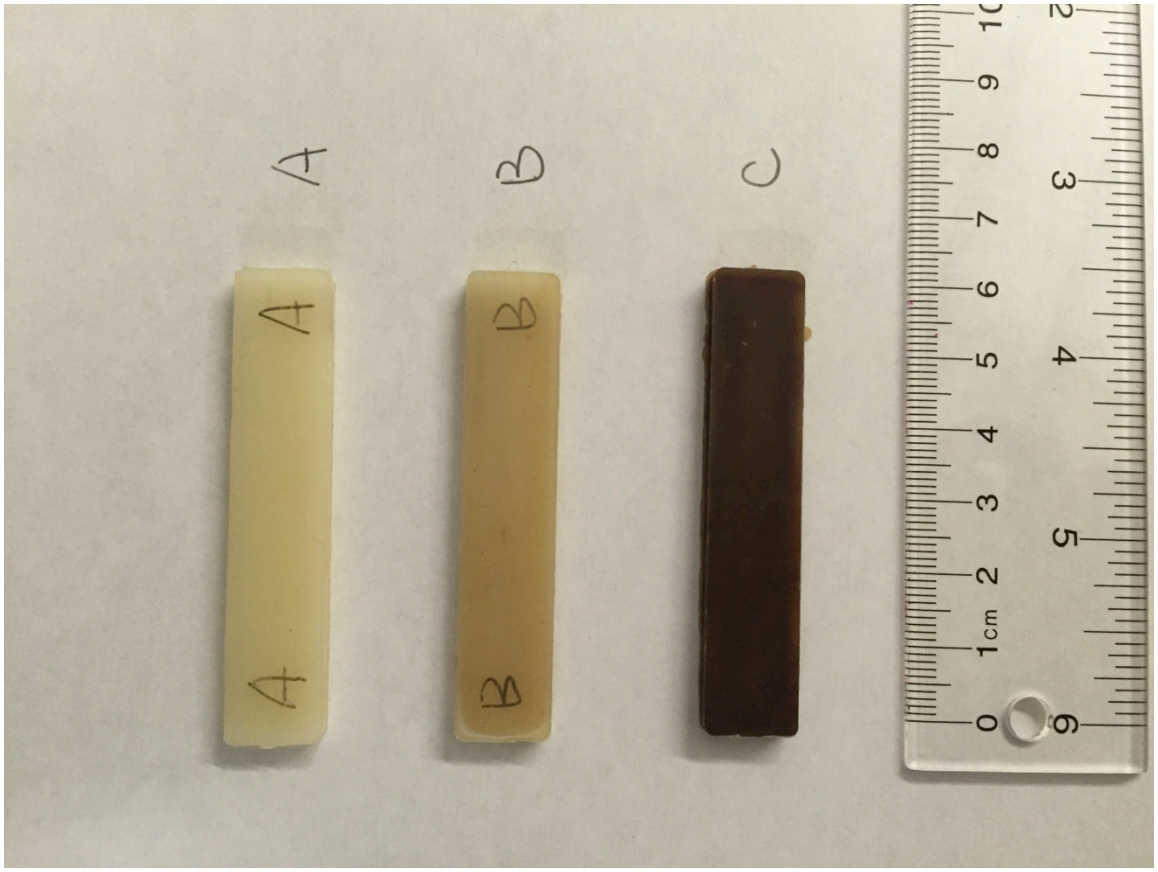

Figure 4- 2 (a) The injection bars of RPA6 (without extrusion) (b) The injection bars of RPA6 (under extrusion) (c) The injection bars of 20% cellulose composite

Comparing b with a, we can see a slightly deeper yellow when the recycled nylon 6 experienced extrusion, which means the extrusion will contribute to the degradation of RPA6. Compared to b, c took on a significantly darker colour, the deep brown indicates that the majority of the degradation is due to processing the Suzano cellulose under high temperatures.

4.1.2 Melting And Crystallization Temperature (DSC)

It is necessary to calculate the crystallinity of semi-crystalline thermoplastic because the crystalline form and crystallinity are easily changed under a series of thermal and mechanical processes that will result in a difference in mechanical properties [14]. Also the temperature of thermal processes such as extrusion and injection molding are closely related to the melting point of the material. A DSC test was

performed and the graph is used to obtain the crystallinity of the sample and obtain information on some thermal characteristics. Figure 4- 3 shows the DSC results of sample A to F, and also shows the second melting peak.

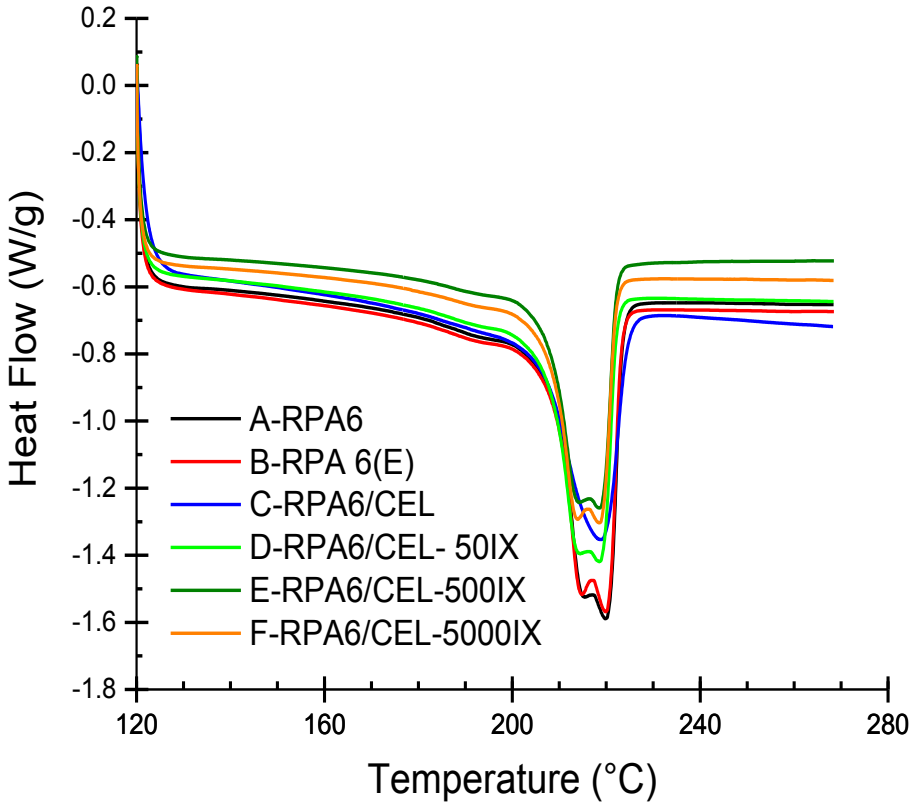

Figure 4- 3 Second melting peak of the sample

Equation 3-5 was used to calculate the crystallinity of each specimen. The summary of the second melting point T_{m2}, crystallization temperature T_c and the crystallinity X_c is shown in Table 4- 1.

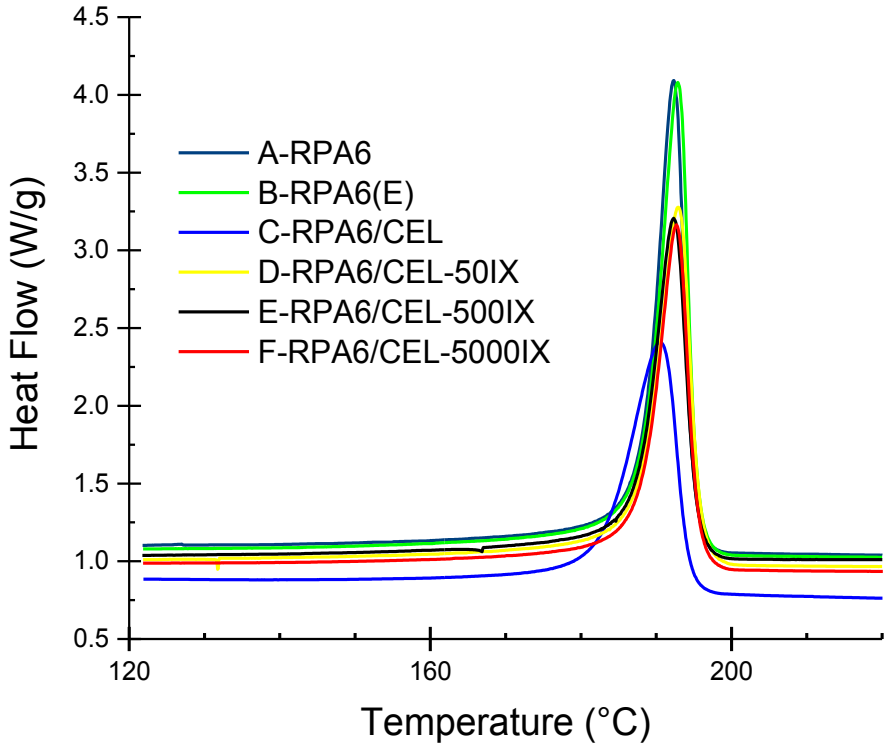

Figure 4- 4 Crystallization peak of sample A to F

Table 4- 1 Summary of DSC analysis results of sample A to F

Sample	T_{m2} (℃)	T_c (℃)	X_c (%)
RPA6	220	192	40.3
RPA6 (E)	220	198	42.3
RPA6/CEL	219	190	38.1
RPA6/CEL-50IX	219	193	41.8
RPA6/CEL-500IX	219	192	45.9
RPA6/CEL-5000IX	219	193	43.3

The two major crystalline forms of polyamide are α and γ and they are well documented from previous literature [32]. There is a less common β mesomorphic

phase. The more thermodynamically stable crystalline form is α crystal, which is a type of monoclinic antiparallel conformation. The relatively less stable γ structure is a parallel conformation leading to half hydrogen bonds between adjacent chains. So it is easy to explain that the major endotherm at melting point indicates more stable α crystalline and the minor endotherm beside it represents the γ structure [4].

Table 4- 1 shows a summary of melting point ($\boldsymbol{T_{m2}}$), crystallization temperature ($\boldsymbol{T_c}$), and crystallinity ($\boldsymbol{X_c}$) of different samples. Compared with RPA6, RPA6 (E) had a 2.0% minor increase of crystallinity ($\boldsymbol{X_c}$). The only difference between RPA6 and RPA6 (E) is that RPA6 (E) shows RPA6 undergo extrusion, which will lead to reorientation of the molecules in the screw rotation direction, which reaches a higher crystallinity.

After being compounded with cellulose, the crystallinity of the RPA6 decreased 4.2%. When using the DSC test to obtain the crystallinity, it is impossible to obtain information on the cellulose crystallinity in the composite due to the fact that the cellulose degrades before the crystal phase reaches melting point (cellulose does not melt). So the crystallinity recorded from the composite is completely derived from RPA6 , which explains the decrease in crystallinity by 4.24%.

Since the weight percentage of RPA6 decreased compared with pure RPA6, it is easy to understand the decrease of $\boldsymbol{X_c}$ in C RPA6/CEL. While from RPA6/CEL-50IX , RPA6/CEL-500IX and RPA6/CEL-5000IX it is possible to observer that Irganox 1010 increased the crystallinity of the composite especially when the concentration was 500ppm. It conforms to Bozena Lanska's perspective that it is difficult for oxygen going through crystalline phase compared with amorphous phase, so autoxidation is almost impossible in crystalline phase [64].

Irganox 1010 is a phenolic primary antioxidant used as a stabilizer for polyamide under long-term high thermal processing. It has reactive -OH groups and transfers protons to active ROO* which results in termination of the autoxidation process and production of stable ROOH.

The crystallization temperature $\boldsymbol{T_c}$ of RPA6 (E) changed mostly when compared with RPA6 that did not undergo extrusion, the $\boldsymbol{T_c}$ of other samples remained almost the same. The DSC procedure presented two cycles of melting and crystallization for each sample. The first cycle of heating erases the thermal history that may not be the same in different samples, even after samples were annealed. Figure 4- 5 First melting peak of the sample shows the DSC results of sample RPA6 to RPA6/CEL-5000IX, and also shows the first melting point and integration of the first melting peaks.

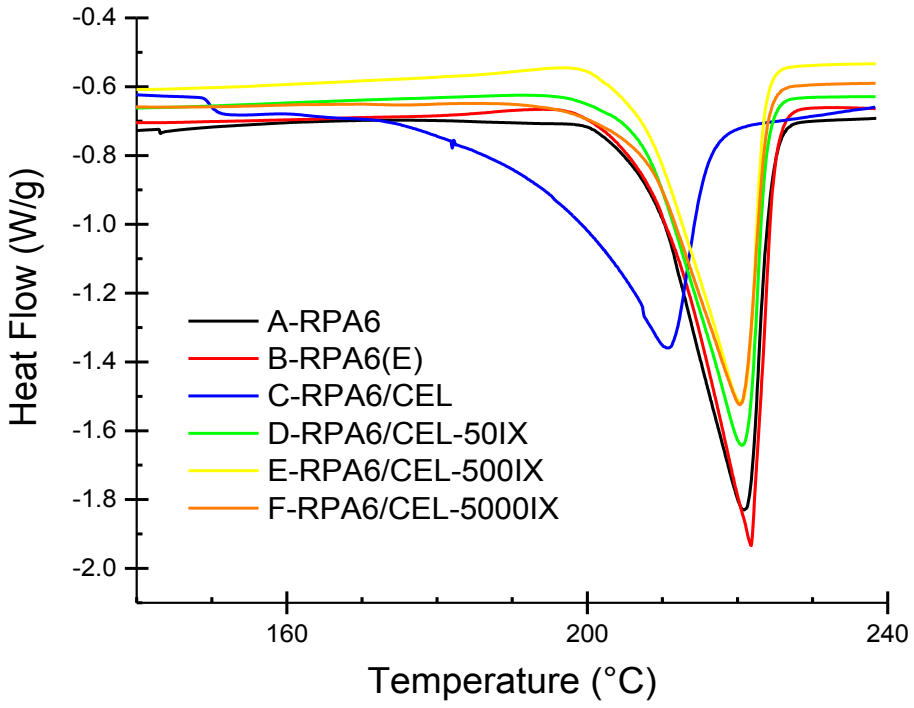

Figure 4- 5 First melting peak of the sample

Table 4- 2 Comparison of first melting peak and second melting peak

Sample	T_{m1} (℃)	T_{m2} (℃)	X_{c1} (%)	X_{c2} (%)
RPA6	219.90	219.73	39.09	40.27
RPA6 (E)	219.78	219.78	43.34	42.31
RPA6/CEL	210.71	218.87	49.88	38.07
RPA6/CEL-50IX	218.56	218.46	44.75	41.81
RPA6/CEL-500IX	218.64	218.64	46.10	45.91
RPA6/CEL-5000IX	218.51	218.51	43.66	43.31

The first melting peak and crystallinity reflect each sample's characteristics after the annealing procedure. From Table 4- 2 we can see that except for sample RPA6, all other samples obtained a higher crystallinity from the first melting peak compared to crystallinity obtained from the second melting peak. The starting temperature of the annealing oven is 25℃ and the final temperature of this process is 120℃, this temperature is higher than the glass transition temperature of recycled polyamide 6 and lower than its melting point. The rate of temperature increase is 1℃/minute, with the oven maintaining 120 ℃ for 600 minutes then cooling back to initial temperature at the same rate of 1℃/minute. So the speed of crystallization is 1℃/minute, while the speed of crystallization at DSC procedure is 10℃/minute which is much higher than the annealing procedure. So it is reasonable to obtain higher crystallinity when sample experience annealing, since it gives more time for the molecules to move around and crystallize. And the melting point of all the samples is around 219℃, which means there is no much difference of crystal size among each samples. It is also important to refer to the mechanical properties together with the crystallinity, which will discussed later in the mechanical properties section. Antioxidant can provide proton to peroxy radicals, so that peroxy radicals will not abstract hydrogen atom from polyamide backbone. As a result,

more hydrogen bond formed between polyamide chains lead to a higher crystallinity.

4.1.3 Processibility And Residence Time

The flowability of the material has significant influence on the processing conditions, it shows the mobility of the material in the extruder and injection molding. The melt flow index (MFI) value gives an idea of how the cellulose and different levels of antioxidants affect the fluidity of the composite. The results are collected in Table 4- 3.

Table 4- 3 MFI of different formula samples

Sample	Suzano cellulose (wt-%)	Recycled PA6 (wt-%)	Irganox 1010 (wt-%)	Melting Flow Index (MFI) (g/10 min)
RPA6	0	100	0	20.2
RPA6 (E)	0	100	0	48.60
RPA6/CEL	20	80	0	13.64
RPA6/CEL-50IX	19.999	79.996	0.005	8.80
RPA6/CEL-500IX	19.99	79.96	0.05	7.34
RPA6/CEL-5000IX	19.9	79.6	0.5	7.08

From Table 4- 3 it is possible to see that adding 20% of cellulose to recycled polyamide 6 lead to a significant decrease of MFI, which means an increase in viscosity and a decrease of processability. Moreover, lower MFI means a longer time that the sample would stay in the extruder or injection molding therefore resulting

in additional degradation of the material. On the opposite hand, a higher MFI means that the material would need less time to be processed and shorter exposure to the high processing temperatures.

Adding antioxidants to the composite resulted in an extra 10% decrease of the MFI, while there is not much difference of MFI between different levels of antioxidant compared with adding cellulose to RPA6 in the composite, so reinforcement with natural fiber is a major factor that decreased the MFI by 71.93%.

Although the differences in MFI due to addition of antioxidant are relatively small at about 10%, they can be interpreted as a result of the antioxidant decreasing the chain scission due to free radical generation and high temperature. This is seen as desirable effect of the antioxidant preventing a decrease in the molecular weight by chain scission, which could lead to decrease in mechanical properties of the composite.

4.1.4 Mechanical Properties

Mechanical testing is a general way to understand the performance of the material when it is under different type of mechanical stress. In this study, the results of mechanical properties are measured and used to make a comparison between different samples. There are four types of mechanical testing conducted in my study: flexural test, tensile test, notched Izod impact test and Gardner dart impact test.

4.1.4.1 IZOD Impact Test Results

Polyamide 6, as one of the most commonly used thermoplastics, can be applied in a large number of industries especially the automotive industry. Polyamide 6 is able to resist both physical abrasion and chemical abrasion while also having high heat deflection temperature (HDT), this means it has high thermal resistance when compared to polypropylene for example. But one of the most attractive properties of PA6 is its high impact resistance. Polyamide 6 will undergo a series of thermal

treatments during the composite process such as extrusion and injection molding that will contribute to thermal oxidation, chain scission and loss of impact strength. So adding antioxidant to the composite is a method to decrease the thermal oxidation of the polyamide 6, and as a result, keep a high level of impact resistance in the long term.

Amintowlieh found that one could decrease the impact resistance by adding untreated wheat straw to the polyamide 6 when working in our research group [4]. Deniz reported that whether the wood fillers were treated or not, the impact strength of PA6 decreased after compounding [2]. Usually, fiber reinforced polymer composites have a lower impact strength compared with pure polymers because adding fiber to the composite makes it easier for crack initiation, in other words it is more brittle. Addition of fiber also decreases the elongation-at-break, which is another important factor decreasing impact strength. Also the lower impact strength of the composite is affected by the poor adhesion of the interface between fiber and polymer matrix [1].

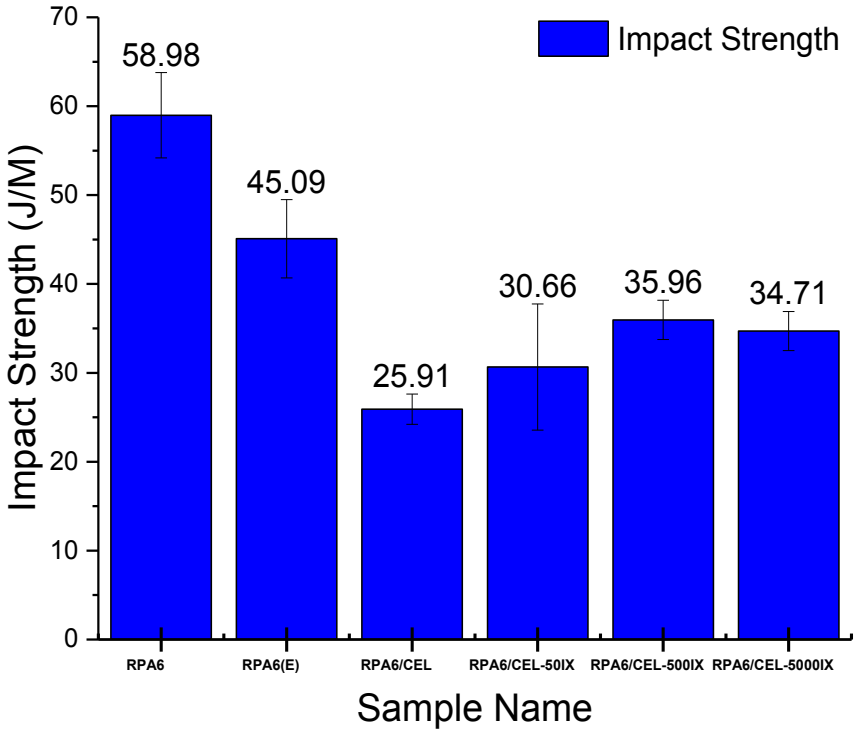

Figure 4- 6 Results of IZOD impact test for RPA6, 50, 500, 5000 ppm Irganox 1010 mixed in 20% cellulose reinforced RPA6

Compared with sample RPA6, sample RPA6 (E) had a much lower impact strength, it was decreased 23.56% after using the extruder. Adding 20% cellulose to the recycled polyamide 6 decreased the impact strength from 45.09 (J/m) to 25.91 (J/m) — about 42.52%. The result is consistent with other existing research that reported adding fibers to the polyamide 6 decreased the impact strength. This is attributed to the initiation of cracks becoming easier due to the high stress concentration on the fibers' ends and the weak adhesion between polymer and fiber. So when the composite suffers impact, less energy will be absorbed in the interface which will lead to a lower impact strength [1].

Adding antioxidant to the composite increased of the impact strength due to less thermal decomposition of the fiber surface. It is expostulated that oxidation or other

reactions on the surface of the cellulose fiber or polymer, such as abstraction of hydrogen from the polyamide 6 backbone, could decrease the interaction between polyamide 6 and the cellulose fiber. This mechanism is merely speculative at this stage.

The loading of cellulose was kept constant at 20% in this project because of previous research conducted in our laboratory recently which identified that this level was most suitable for a balance of properties [65]. As a consequence the effect of fiber content was not evaluated here.

It is known that the composite performance can be affected by many different factors and the fiber content is an important factor because the major purpose of adding fiber into the polymer matrix is to improve its mechanical performance (tensile properties). The mechanical properties of polyamide 6 composites with heat-treated or untreated wood fiber were investigated at four-fiber content levels by other authors: 5%, 10%, 20% and 30%. Their results showed that the tensile strength of 20% heat-treated maple and pine had the highest tensile strength [2]. And there are many other researchers who have found that around 20% natural fiber filler will lead to a better mechanical performance. Buchenauer investigated that 20% cellulose results in better tensile modulus and IZOD impact strenght when composite with wood fiber [65].

Sample RPA6/CEL-50IX, RPA6/CEL-500IX and RPA6/CEL-5000IX all had a higher impact strength compared with RPA6/CEL, so adding an antioxidant to the composite could improve the impact strength due to less hydrogen to abstract from the backbone of polyamide 6. And 500 ppm Irganox 1010 has the highest value among these three formulations, it is 35.96 (J/m) which is a 38.79% improvement compared with RPA6/CEL whose composite did not include any antioxidant.

4.1.4.2 Tensile Test Results

Figure 4-14 and Figure 4-15 present the effect of different levels of antioxidant (Irganox 1010) on tensile modulus and tensile strength of recycled polyamide 6 composites with cellulose (20%).

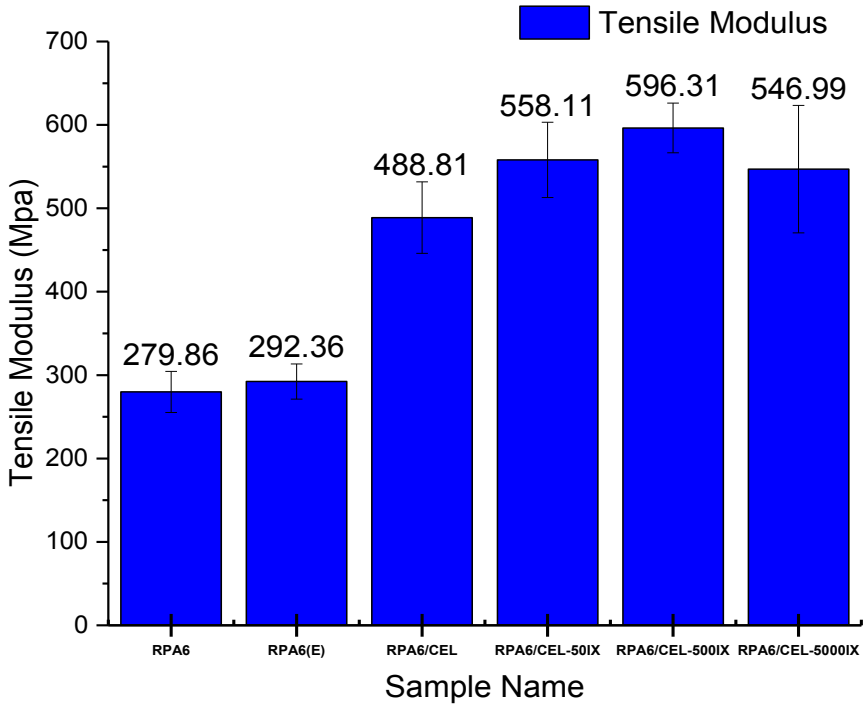

Figure 4- 7 Tensile modulus got from RPA6, 50, 500, 5000 ppm Irganox 1010 mixed in 20% cellulose reinforced RPA6

From Figure 4- 7 we can find that compared with single recycled polyamide 6, all the other samples (RPA6 reinforced by cellulose) had a higher tensile modulus. When reinforced by 20% cellulose, the composite made a 67.2% improvement compared with pure recycled polyamide 6. Although this is already a large improvement, what is surprising is that after adding a different level of antioxidant one can still achieve further significant improvements. The most significant improvement was achieved by adding 500 ppm of Irganox 1010, which lead to an extra 22% increase compared with the polyamide 6 composite with 20 percent cellulose. It is a 104% increase compared with pure recycled polyamide 6.

The improvement of tensile modulus is due to a good compatibility between the matrix and the fillers, and the composite achieves a better performance of stress transfer from polyamide 6 to cellulose, which leads to a high tensile modulus [66]. Due to the methods of using a series of high temperature processing, the composite mechanical performance is also closely related to thermal degradation. When the polyamide 6 is under conditions of high temperature, light, and mechanical processing, it also initiates a series of oxidation reactions. The cellulose would degrade during processing such as during extrusion and injection molding. All these factors may lead to a loss of tensile property. From the results of Figure 4- 7, sample D, E and F had all improved compared with C. This reinforcement of tensile modulus may be because PA6's better resistance of thermal oxidation after adding antioxidant, since the oxygen reacts with the hydrogen from the antioxidant instead of abstracting it from the backbone of polyamide 6. So it leads to more hydrogen bonds and good adhesion between polymer and cellulose, which results in good energy transfer when receiving stress.

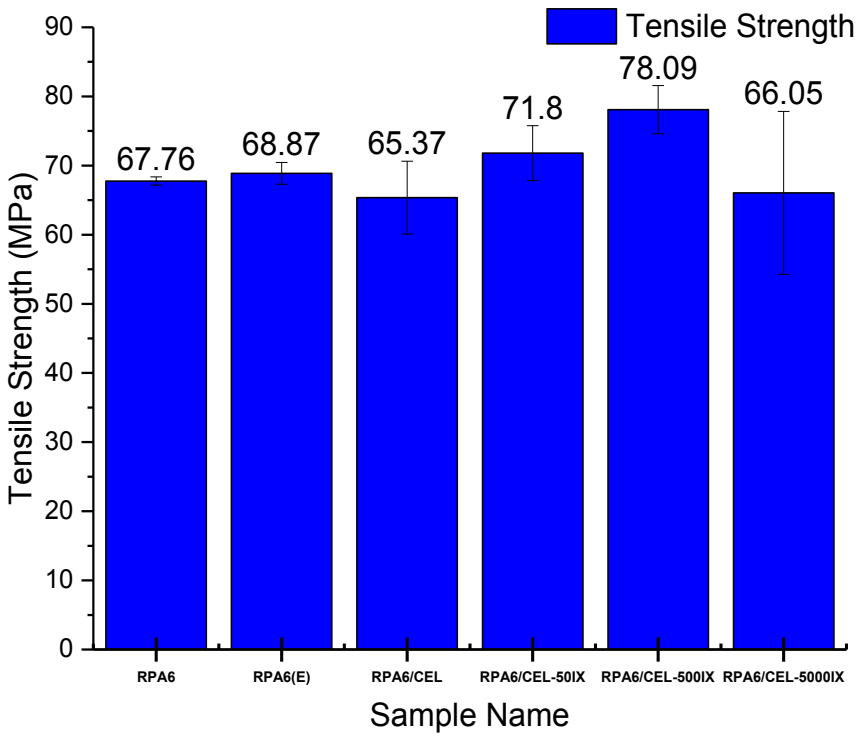

Figure 4- 8 Tensile strength got from RPA6, 50, 500, 5000 ppm Irganox 1010 mixed in 20% cellulose reinforced RPA6

From Figure 4- 8, the composite tensile strength decreased by 5.10% compared with pure RPA6. The result according to Amintowlieh's report, the composite with wheat straw would decrease the tensile strength [4]. Khoathane investigated the tensile properties of bleached hemp, cottonized hemp and long fiber hemp reinforced polypropylene (PP). He found that the tensile strength of these three composites were on an increasing trend except the bleached fiber reinforced PP which decreased in tensile strength from 10% to 20% fiber loading [67]. Lee investigated detecting the mechanical performance of polypropylene reinforced by kenaf and jute long- discontinuous natural fiber, which he found that both the tensile strength and the strain at the break decreased compared with the pure polypropylene which is due to bad interfacial adhesion between the matrix PP and the natural fiber [68].

In this case, the decrease in tensile strength could be due to the poor interfacial adhesion between the RPA6 matrix and the cellulose filler and also the bubbles in the composite that results from moisture evaporation or volatile compounds formed during thermal decomposition. The interfacial adhesion is largely dependent on the intermolecular connection (hydrogen bond), which is not as strong as covalent bonds, as a result it cannot hold the matrix and filler together when suffering large tensile forces. Also the bubbles in the composite lead to a higher stress concentration that will result in easier breakage [68].

While the tensile strength of sample D, E and F were all improved compared with composites without antioxidant. Adding 500ppm antioxidant resulted in the best performance, it is a 19.46% increase from the tensile strength in sample C. This means a better adhesion of the interface between polyamide 6 and cellulose, so the antioxidant may enhance the interfacial bonding of the composite. It is because less abstraction of hydrogen from the backbone of PA6, so more hydrogen bonds was formed between matrix and cellulose.

4.1.4.3 Flexural Test Results

The effect of different levels of antioxidant on flexural properties of recycled polyamide 6 and cellulose are shown in Figure 4- 9 and Figure 4- 10.

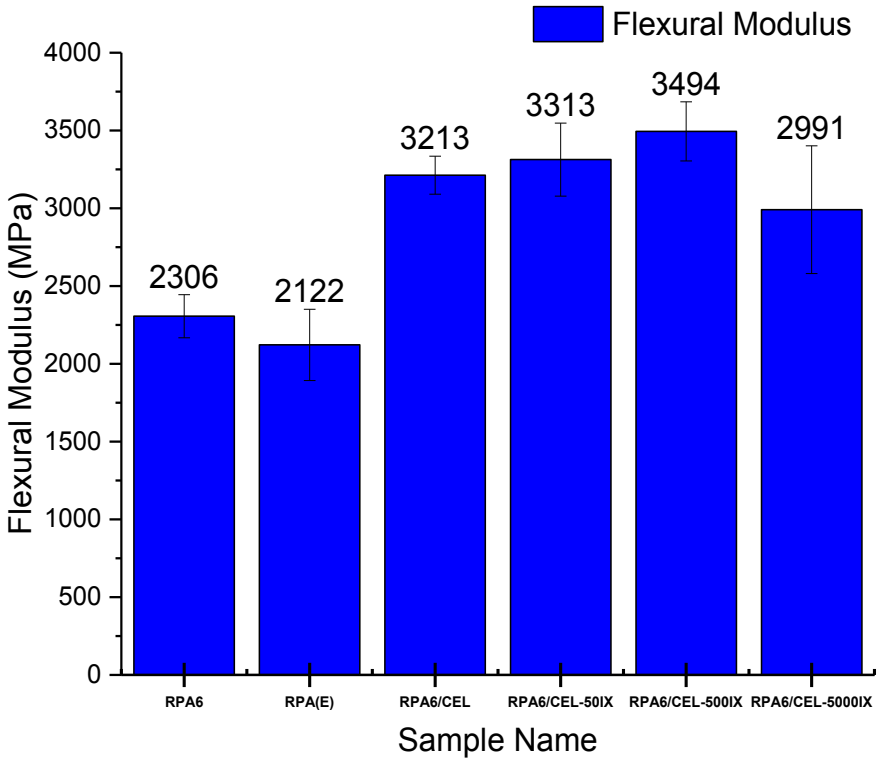

Figure 4- 9 Flexural modulus for RPA6, 50, 500, 5000 ppm Irganox 1010 mixed in 20% cellulose reinforced RPA6

From Figure 4- 9 shows that the flexural modulus increased from 2,122 Mpa to 3,213 Mpa (51.4% improvement) with addition of cellulose. After adding 50 ppm Irganox 1010 there was an extra 3.11% increase. Adding 500 ppm Irganox 1010 to the composite further benefit by an extra 8.75% compared with samples without antioxidant. But sample RPA6/CEL-5000IX with 5000 ppm of Irganox 1010 had a loss of tensile modulus. The reason for this behavior is not well known yet, one possible explanation could be the poor dispersion of the antioxidant.

Aydemir found that with the increase of the cellulose content, the flexural modulus increased linearly which means an increase in stiffness. This is also in accordance with another research which found that adding wood fiber, mix of natural fiber, MCC and alpha cellulose fiber all improves the flexural performance of composite [1]. The flexural test shows a similar trend as the tensile test. On the other hand, the improvement of mechanical property means less thermal degradation, it is because even a small amount of antioxidant significantly prevents the polyamide from autoxidation during the processing procedure.

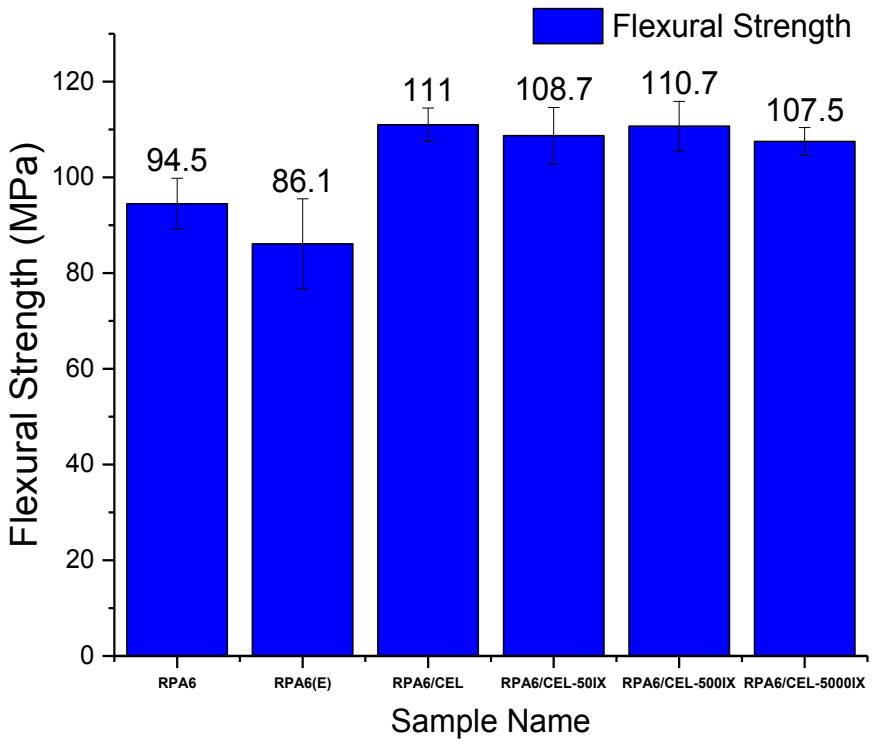

Figure 4- 10 Flexural strength for RPA6, 50, 500, 5000 ppm Irganox 1010 mixed in 20% cellulose reinforced RPA6

Figure 4- 10 shows that after reinforcing polyamide 6 with cellulose, the flexural strength increased by 28.92%, while different levels of antioxidant did not make

much difference in flexural strength since all differences are within the experimental error.

4.1.5 Degradation (Thermal Gravimetric Analysis)

Polyamide 6 is a semi-crystalline thermoplastic, which means that it has a melting point and can only be processed after this temperature is reached. However, cellulose does not have a melting point, and degradation occurs at around 260℃, which is lower than polyamide degradation temperature 312℃.

This gap between the onset of thermal decomposition of cellulose and the temperature needed to process polyamide represents a major technical challenge. It is necessary to understand the degradation character of both the pure material and the composite. The summary of 1%, 5% and 10% weight loss temperature and the maximum first derivative temperature is shown in Table 4- 4. The TGA graph and DTGA graph shown in Figure 4- 11 and Figure 4- 12. Note that the slight weight loss up to 160℃ is due to water evaporation [34], all TGA curves shown here excluded the moisture content.

Table 4- 4 TGA analysis summary

Run#	T1% (℃)	T5% (℃)	T10% (℃)	Tmax1 (℃)	Tmax2 (℃)	Tmax3 (℃)	T onset (℃)
RPA6	312.8	400.2	420.5	-	-	468.9	351.1
RPA6 (E)	275.1	389.8	411.2	-	-	463.1	337.9
RPA6/CEL	299.2	359.8	377.8	398.4	412.6	456.7	300.9
RPA6/CEL-50IX	282.1	347.8	368.5	391.1	-	457.9	279.6
RPA6/CEL-500IX	281.7	348.0	369.3	400.2	-	462.4	280.8
RPA6/CEL-5000IX	296.0	355.4	374.4	402.9	-	463.1	296.6
Cellulose	259.2	299.9	319.5	374.8	-	-	240.1

The thermal stability of the composite is investigated by using TGA running under nitrogen atmosphere. The TGA graph of different levels of antioxidant composite and pure cellulose are shown in Figure 4- 11. It can be easily observed that the degradation of pure cellulose happens much earlier than the other samples, while the RPA6 degrades later. No matter whether the RPA6 or pure cellulose, both have just one major degradation stage, however with composite added they now have two major degradation stages. Normally, RPA6 has almost no residue left at 650 ℃, but adding cellulose filler resulted in much more residue at the same temperature. Sample A had the highest temperature for 1%, 5% and 10% weight loss and also the highest degradation onset temperature, which means a much better thermal stability. The main reason is because undergoing just injection molding may decrease thermal degradation more significantly than other samples which underwent extrusion before injection molding. There are no much differences in TGA graph for the composite, except the 5000 pp shows a slightly better thermal stability.

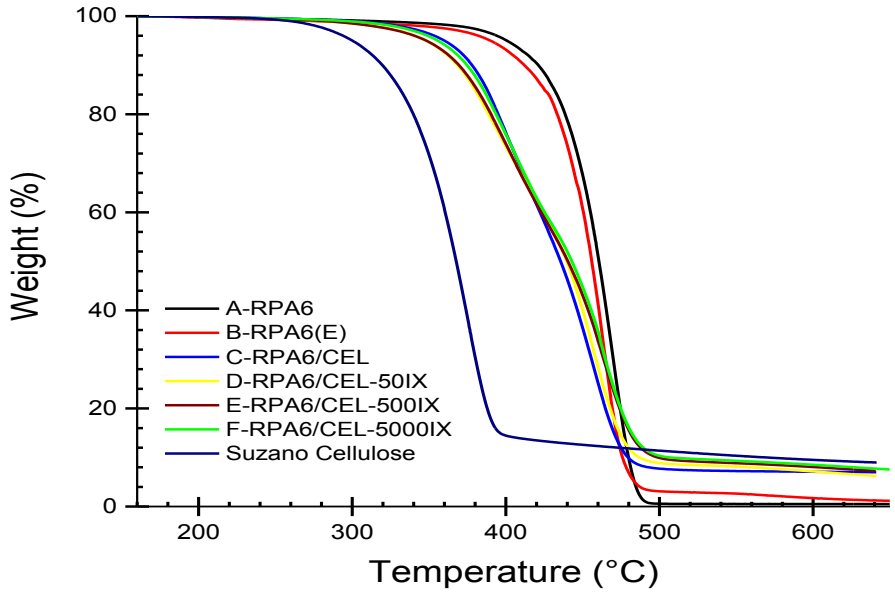

Figure 4- 11 TGA graph of RPA6, 50, 500, 5000 ppm Irganox 1010 mixed in 20% cellulose reinforced RPA6

Table 4- 4 TGA analysis summary , the behavior of samples can be divided into three groups: Cellulose, Composite and RPA6. The highest degradation speed of cellulose happens at the peak position in DTGA graph. Although cellulose degrades

earlier, the rate is much lower than RPA6's highest degradation rate. The DTGA curve of the composite presents an overlap of cellulose and RPA6.

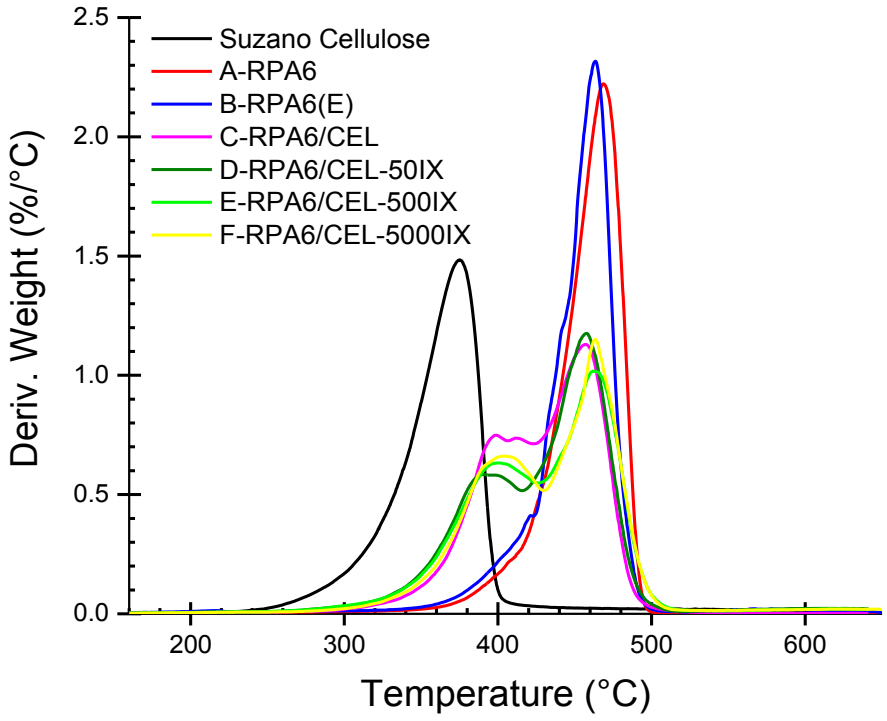

Figure 4- 12 DTGA graph of RPA6, 50, 500, 5000 ppm Irganox 1010 mixed in 20% cellulose reinforced RPA6

4.1.6 Indentification Of Crystalline Form

As it is widely known, the crystalline form, crystallinity and morphology are the critical factors on physical and mechanical properties of semi-crystalline thermoplastic [68]. XRD spectrum is widely employed to identify the crystalline form of materials. The XRD curves overlay and crystalline identification shows in Figure 4- 13.

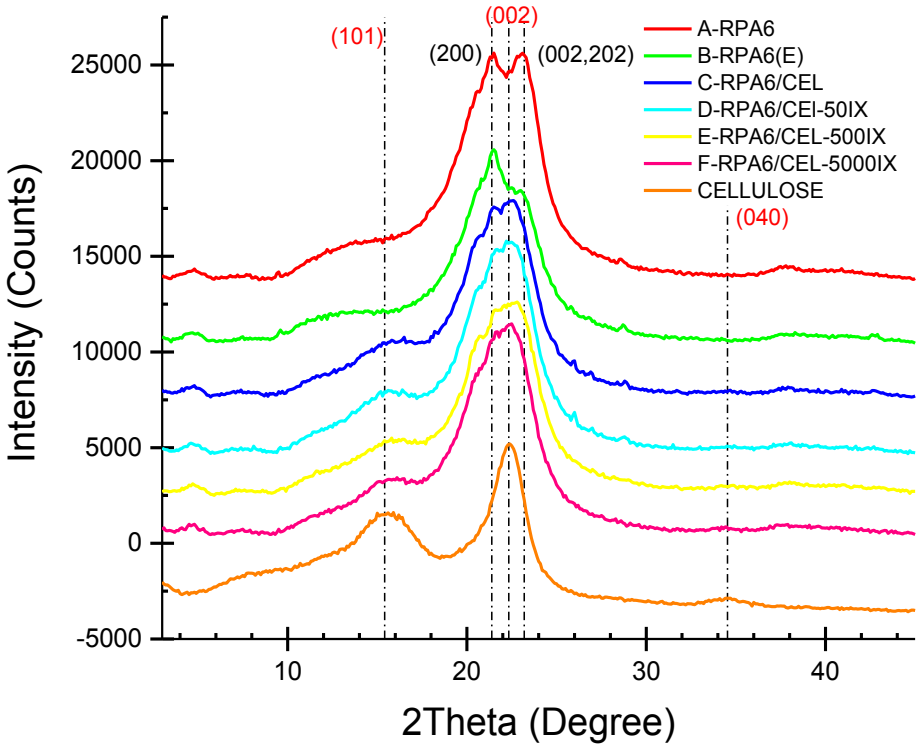

Figure 4- 13 XRD curves of pure cellulose, RPA6 and composite

The deconvolution of the XRD curves are shown in the appendixs. This deconvolution is used to calculate the amount of crystalline phase in each material. Appendix 4- 1 to Appendix 4- 6 shows the peak fit results of Sample RPA6 to Sample RPA6/CEL-5000IX, while Appendix 4- 7 and Appendix 4- 8 shows the peak fit of un-dried cellulose and dried cellulose.

For polyamide 6, it has already been reported that the value of 2θ of α crystals were detected at 18°-20° (200) and 23.6° $\pm$ 0.1(202/002) and the values of 2θ of γ crystals were detected at 9°-13° (020) and 21.3° $\pm$ 0.1 (001) [14]. Also the major crystalline form of cellulose are well known in the literture, cellulose I crystals were detected at 14.81° (101), 16.54° (10$\underline{1}$), 22.8° (002). Cellulose II were detected at 12.04° (101), 19.95° (10$\underline{1}$), 22.17° (002) [69].

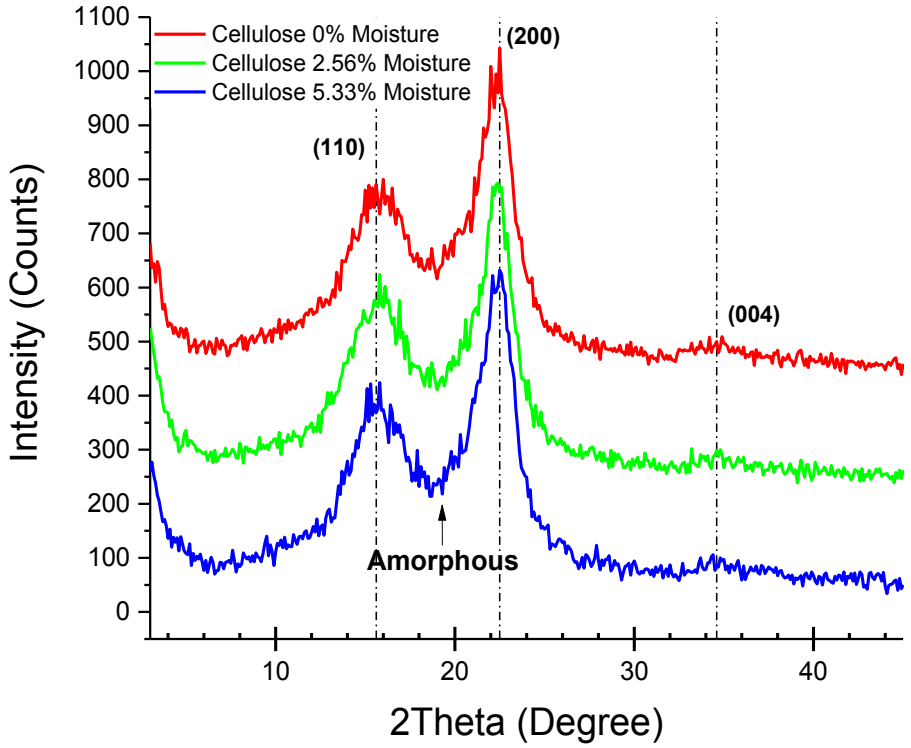

Figure 4- 14 XRD curves of different moisture cellulose

Appendix 4- 1 and Appendix 4- 2 shows that RPA6 both α and γ crystalline phases are present in RPA6 that was molded with or without the extrusion The peak deconvolution process in not able to find differences in the amount of crystalline phases for these two samples.

Appendix 4- 7 and Appendix 4- 8 demonstrates that the deconvolution of Suzano cellulose contains both Cellulose I and Cellulose II regardless of if it is dried. According to the Segal Method using the relative intensity of I_{200} and I_{AM} calculated the crystallinity of un-dried cellulose is 59.8%, while the crystallinity increased a little of dried cellulose equals to 60.9%. The calculation of cellulose crystallinity is in Appendix 4- 9. It may also have some differences in the percentage of Cellulose I and Cellulose II, but it is difficult to tell via XRD. And Figure 4- 14 shows the XRD offset curves for cellulose with different moisture contents.

4.1.7 Morphology (SEM)

The effect of cellulose filler and different levels of antioxidant on the composite morphology was studied using the scanning electron microscope (SEM). The major purpose of SEM analysis is to investigate the interfacial bonding and degree of interaction between the polymer matrix and the cellulose filler of different samples. The SEM analysis started on a low magnification to get a general idea of fiber dispersion level across the polymer matrix and then went in high magnification to observe details about the cellulose fiber and its interface, including the fiber pull out, fiber cut-off and the interfacial bonding when there was a break.

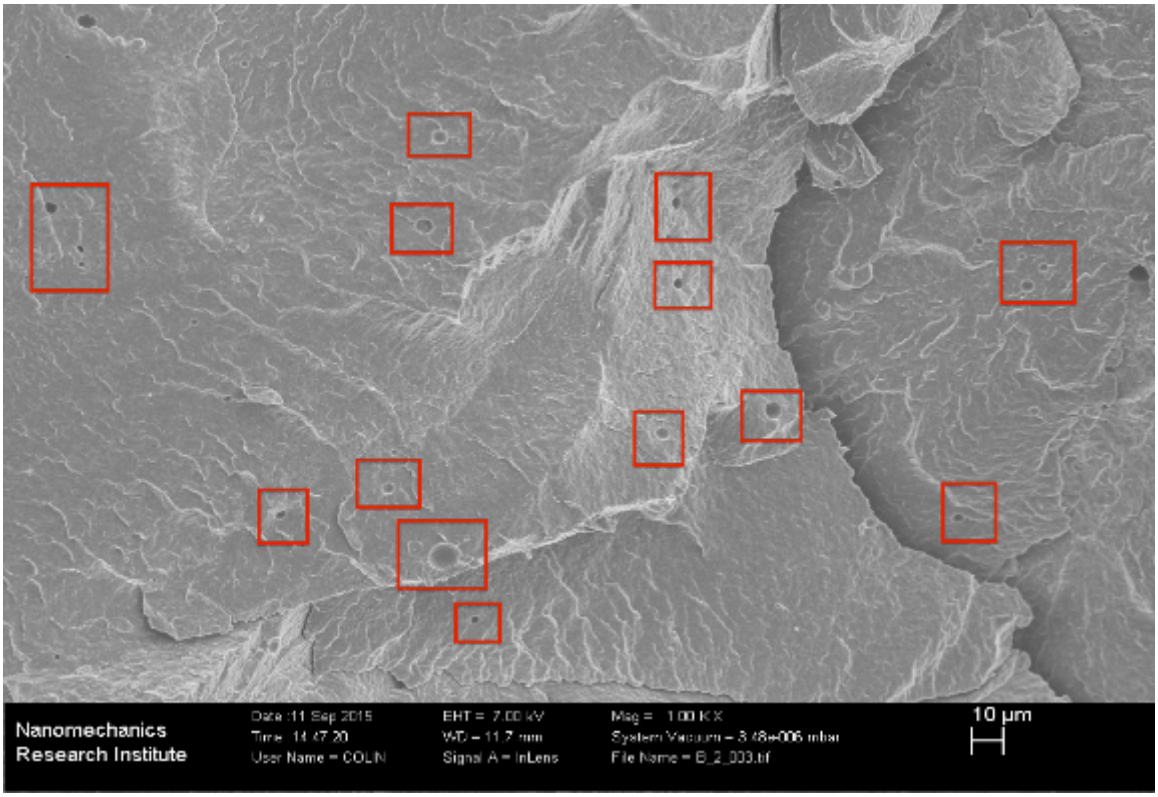

Figure 4- 15 Sample RPA6 (E) (RPA6 experience extrusion) at 1K magnification

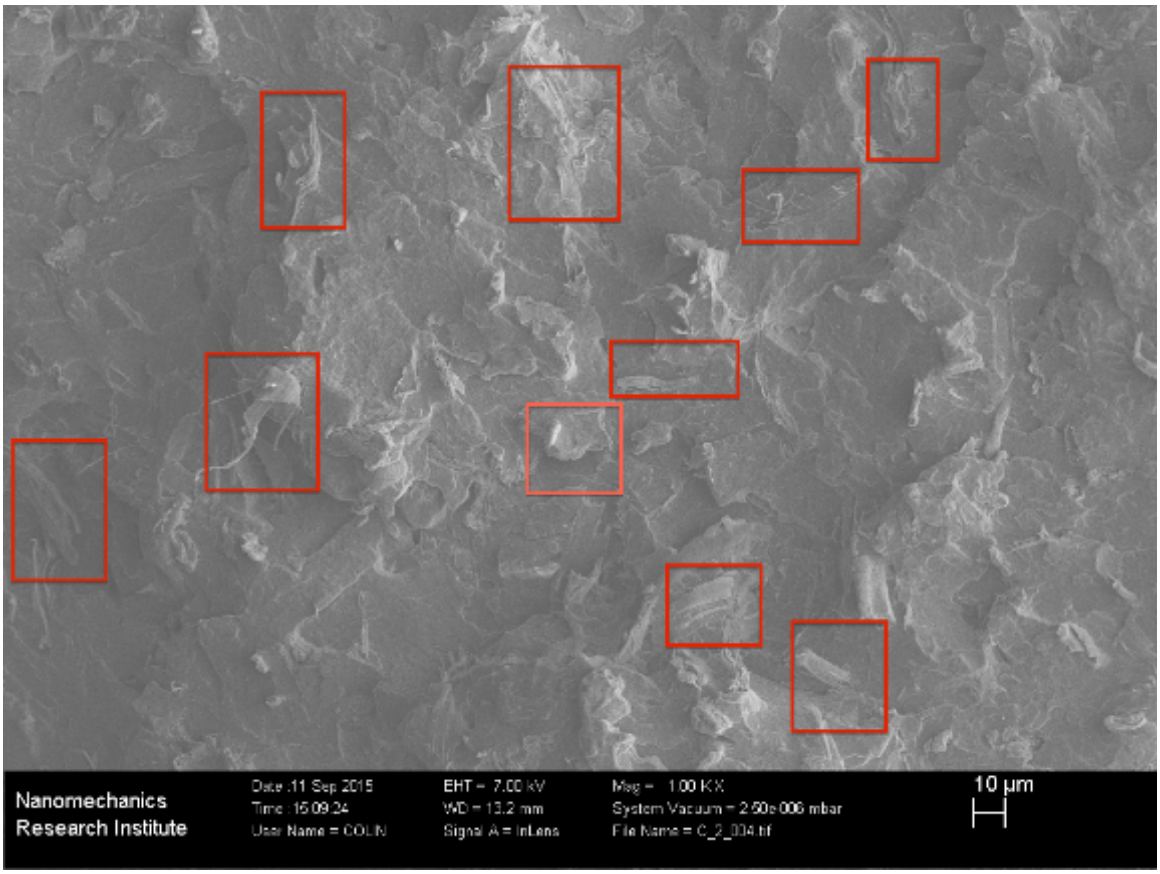

Figure 4- 16 Sample RPA6/CEL (RPA 6/ 20% cellulose) at 1K magnification

Figure 4- 15 shows the cross section of RPA6 that experiences extrusion, it is possible to observe many cavities in the shape of dimples (rounds sink marks) in the sample, which may be due to the gas being trapped in the sample. This evolution of gas during injection molding may be due to evaporation of the moisture in the specimen. However a more closely observation of this dimples reveals a different outcome. It is possible to obseve that the dimples are filled with another type of material. Another research in our group [65] working with the same sample of recycled polyamide 6 has identified this as a second polymer present as a contamination in the recycled polyamide 6. The polymer contaminant could possiblty be polypropylene.

Figure 4- 16 shows the cross section of RPA6/ 20% cellulose composite, and it presents a good dispersion of cellulose fiber in polyamide. It displays a good wetting

of the surface of the cellulose by polyamide and a relatively smooth morphology character. This homogeneous distribution of cellulose will lead to a better stress transfer and better modulus. This observation supports the improvement of modulus discussed in the previous section.

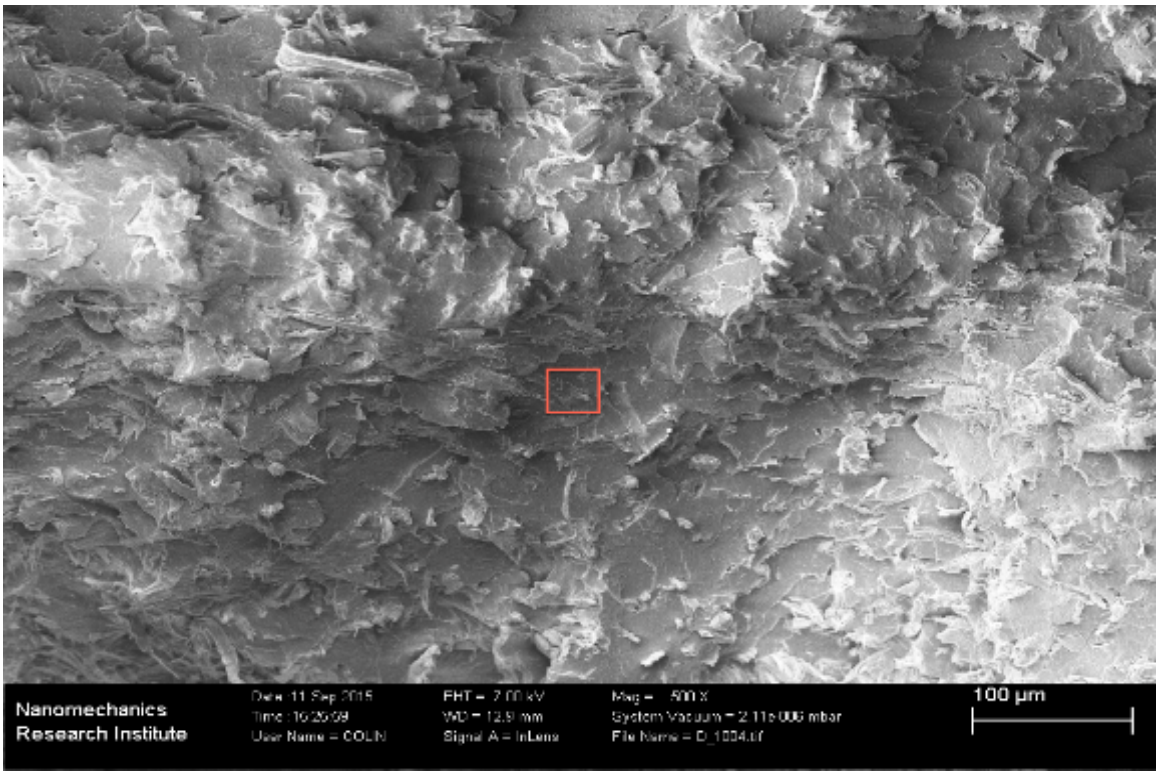

(a) Mag=500X

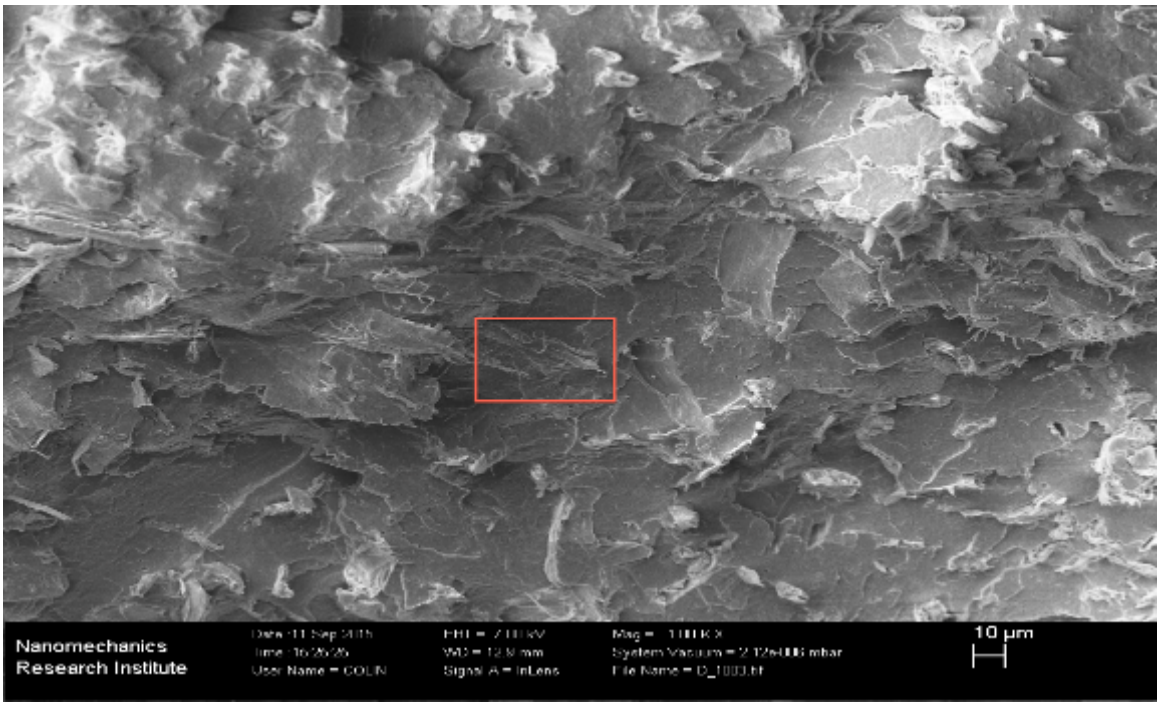

(b) Mag= 1000X

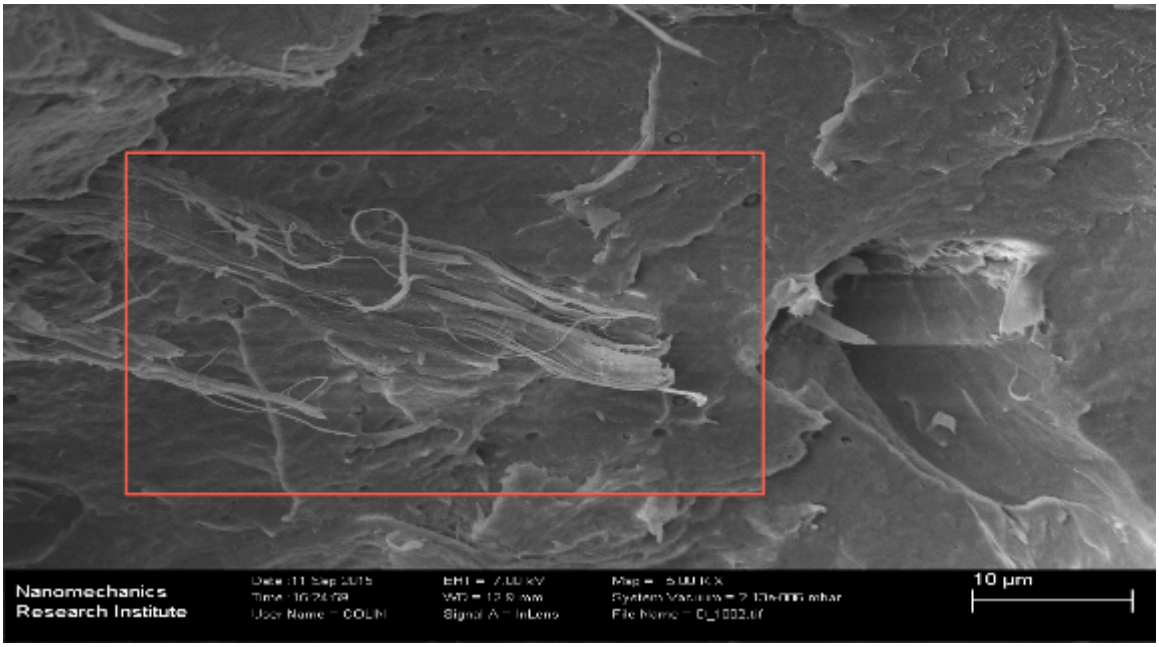

(c)Mag=5000X

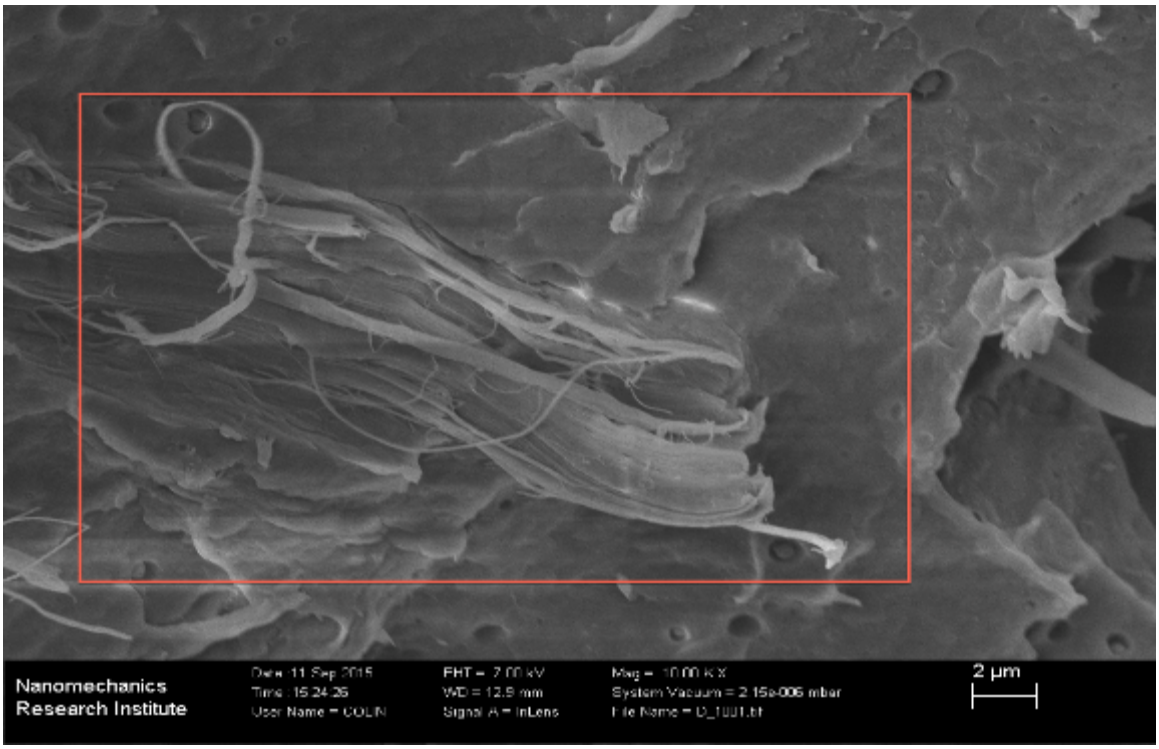

(d) Mag=10000X

Figure 4- 17 The cross section of Sample RPA6/CEL-50IX (50 ppm Irganox 1010). Magnification (a):500X (b):1KX (c):5KX (d):10KX

Figure 4- 17 shows the cross section of composites with 50 ppm Irganox 1010 in 500X, 1KX, 5KX and 10KX respectively. From low magnification (a) and (b) present a fibers dispersed well in RPA6 matrix. This good dispersion and wetting of natural fiber in polymer matrix and minimal agglomerations of fiber observed in the cross section explains the improved tensile and flexile properties compared with RPA6. And when it goes to high magnification (c) and (d), it shows a very good interfacial bonding, and there is almost no gap between the fiber and polymer matrix, which will lead to a good energy transfer when it is under stress. This domain fiber cut-off in the composite means a better adhesion and interfacial bonding compared with the fiber pull out phenomenon [70].

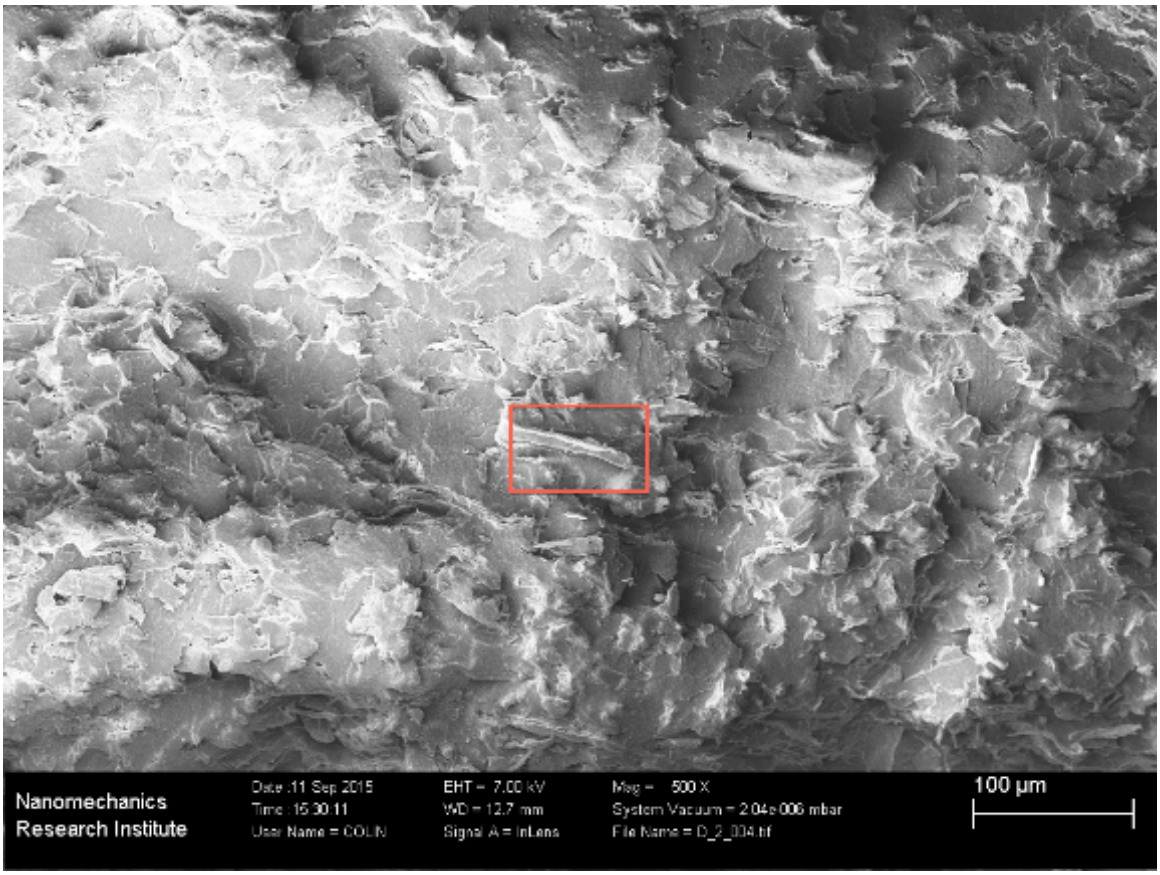

(a) Mag=500X

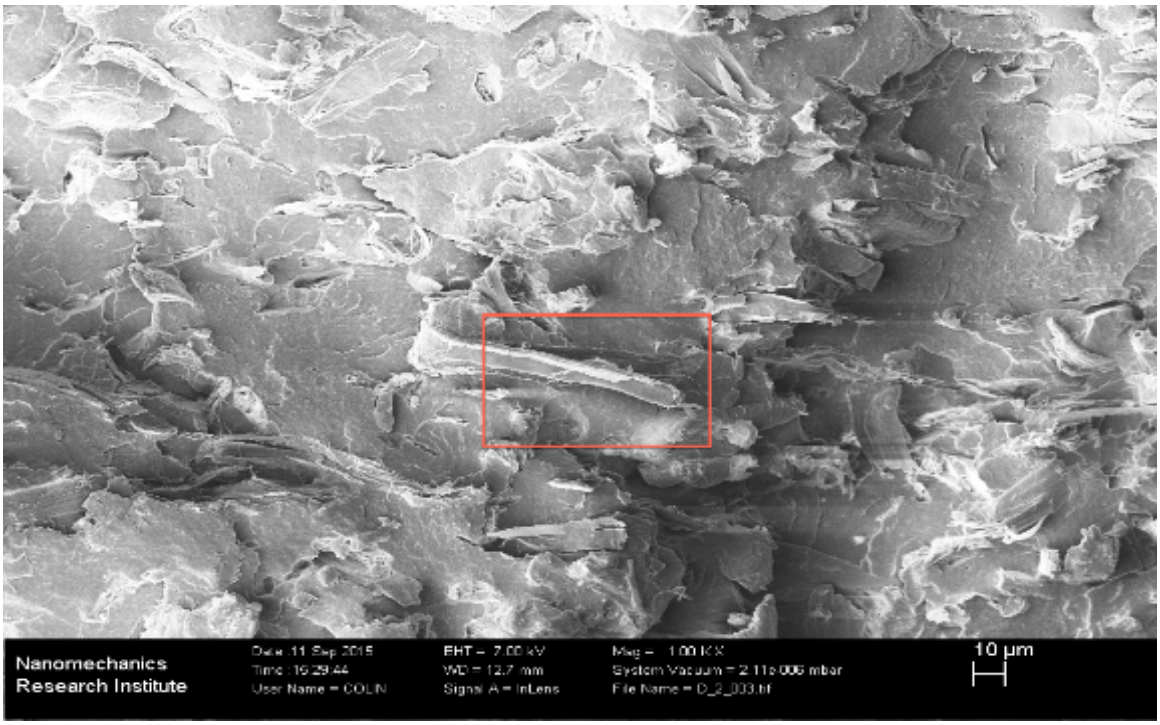

(b) Mag=1000X

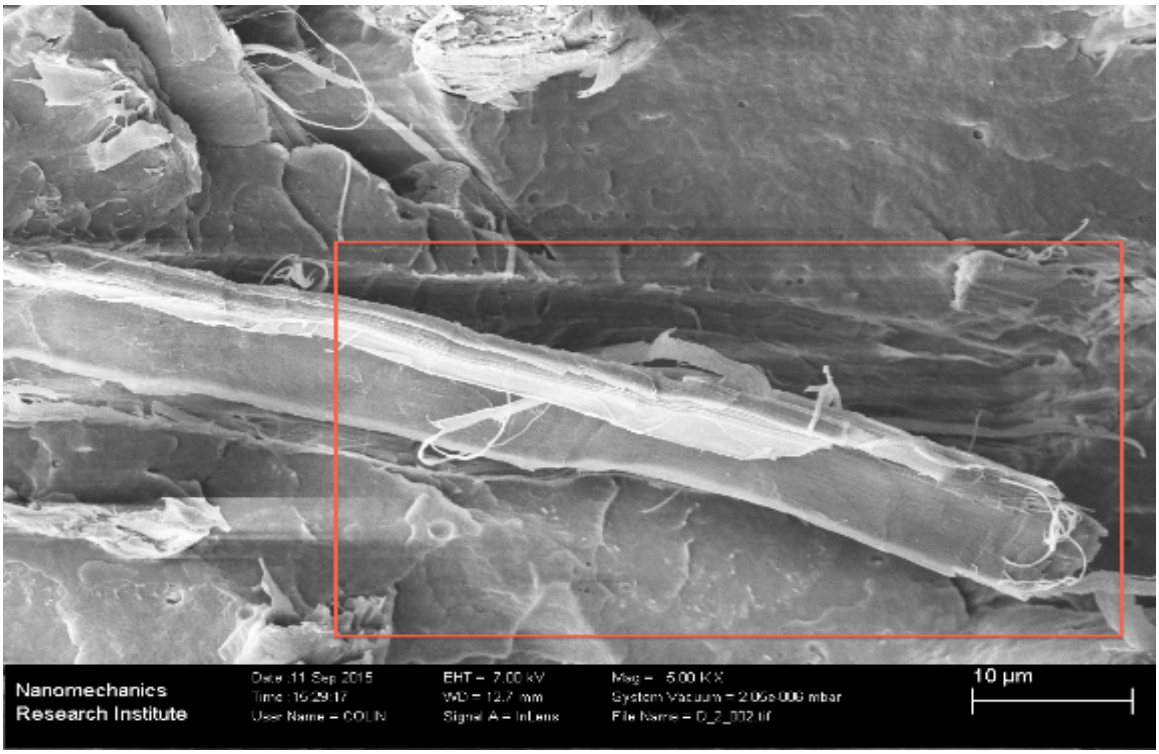

(c) Mag=10000X

(d) Mag=100000X

Figure 4- 18 Another point of Sample RPA6/CEL-50IX (50 ppm Irganox 1010). Maganification (a):500X (b):1KX (c):5KX (d):10KX

Figure 4- 18 shows another point of sample RPA6/CEL-50IX (Composite with 50 ppm Irganox 1010). From the magnification of 500X (a), it shows a good dispersion of fiber in the polymer matrix except one part in the middle. This part was examined at a 10000X magnification (d), an obvious fiber pull out can be seen, which leads to a bad adhesion. This shows that in some points the cellulose is aggregated in the polyamide matrix and dispersion could be further improved. These points where cellulose agglomeration is observed represent a minimal fraction of the sample.

(a) Mag=500X

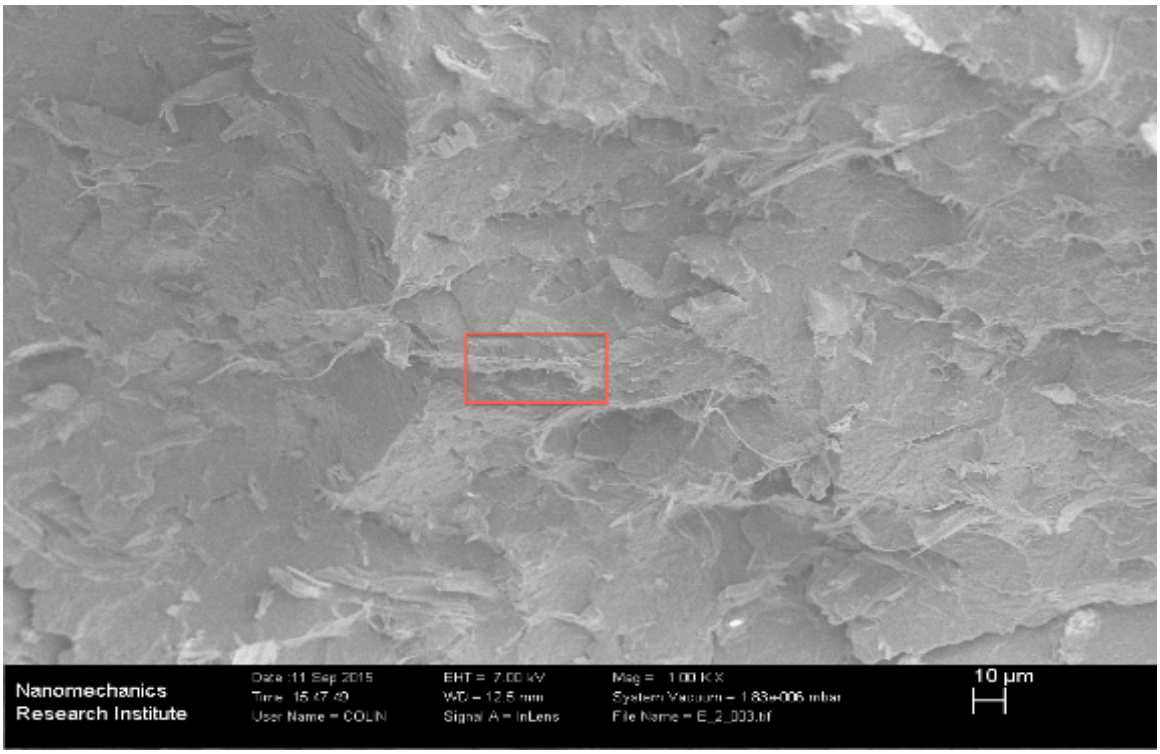

(b) Mag=1000X

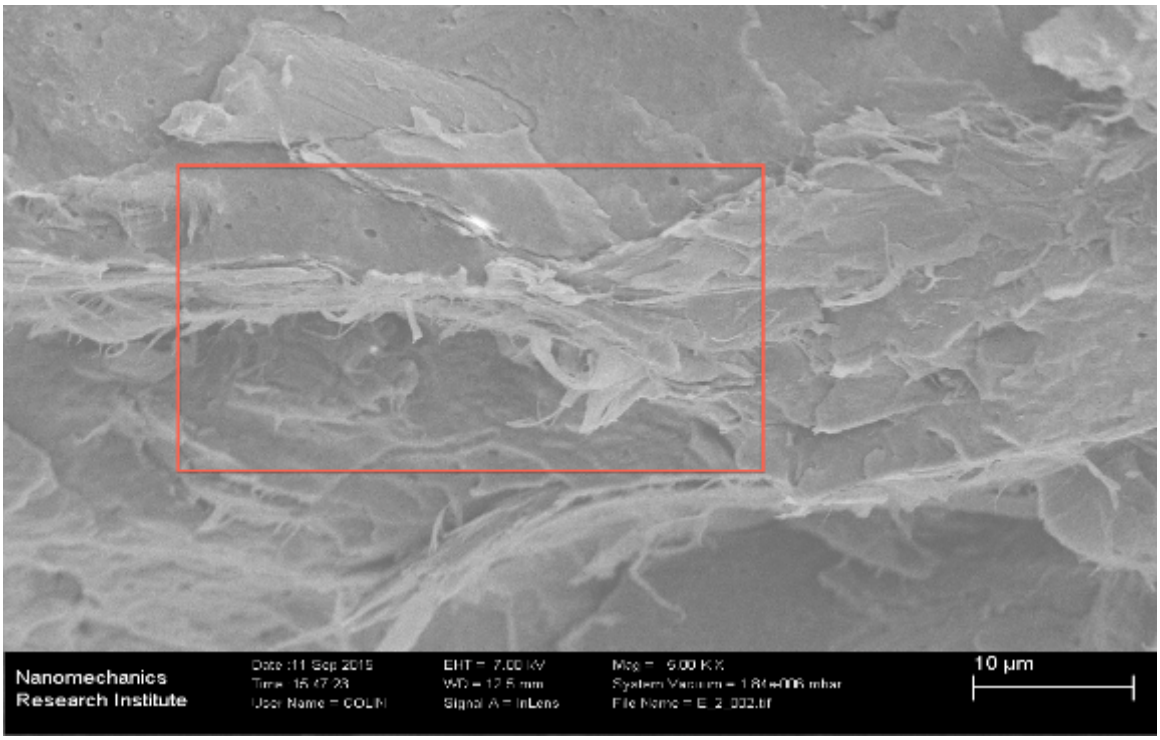

(c) Mag=5000X

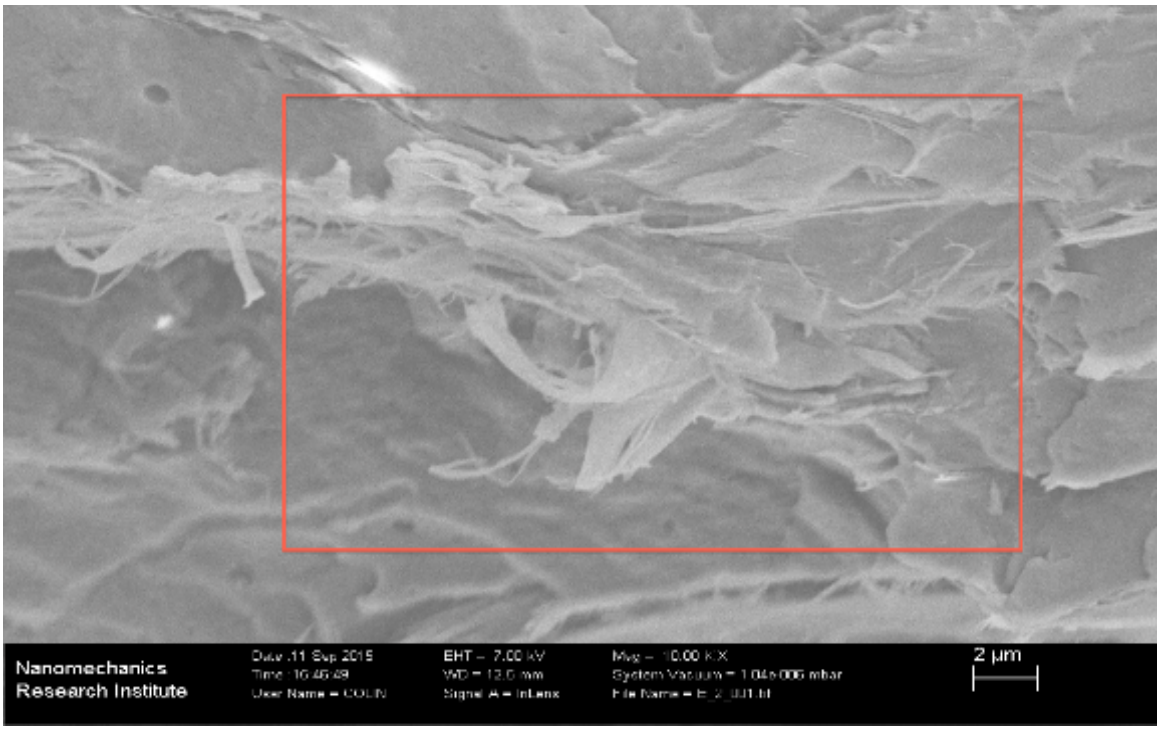

(d) Mag=10000X

Figure 4- 19 The cross section of Sample E (500 ppm Irganox 1010). Magnification (a):500X (b):1KX (c):5KX (d):10KX

Figure 4- 19 shows the cross section of sample RPA6/CEL-500IX (composite with 500 ppm antioxidant) showing a good dispersion like sample RPA6/CEL-50IX . When moving to higher magnification, a coarse and unclear surface can be seen, which represents a good interfacial adhesion in the composite. Sample E had the best performance among all the formulas which also fits the results of the mechanical properties. It may be due to the appropriate amount of Irganox 1010 provide enough hydrogen for autoxidation process instead of abstraction of hydrogen in PA6 backbone, so that more hydrogen bonds formed in the composite.

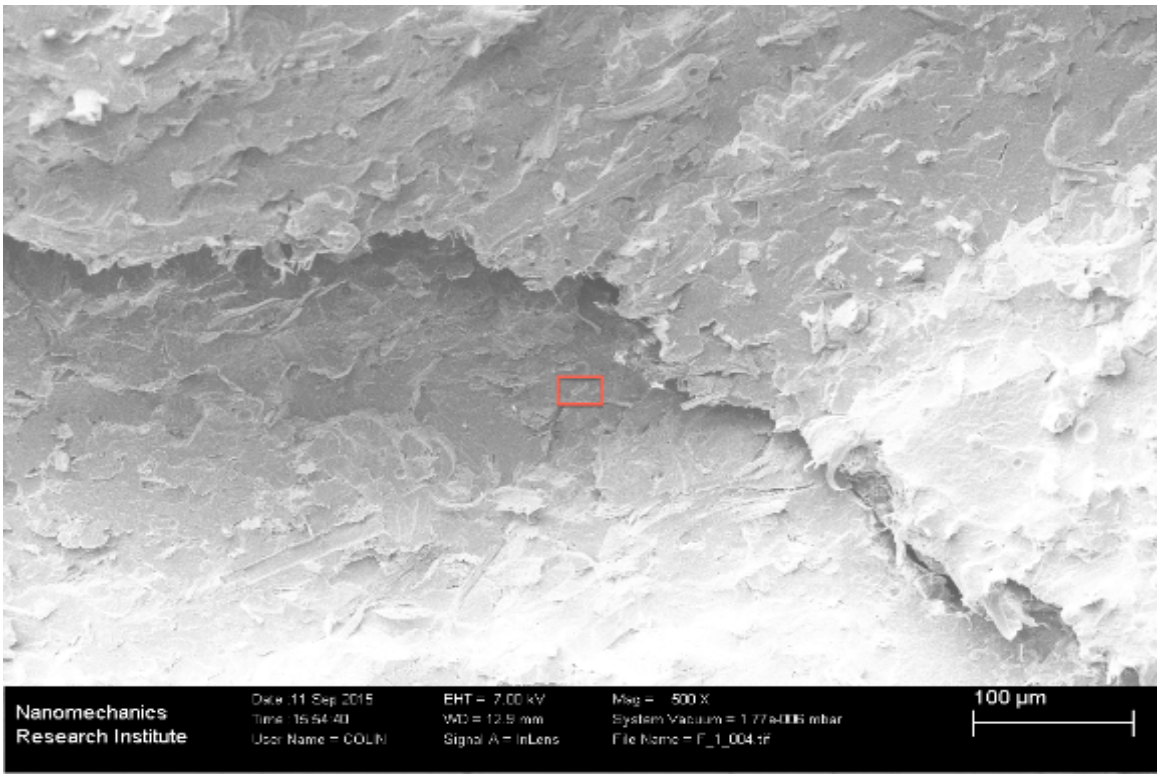

(a) Magnification= 500X

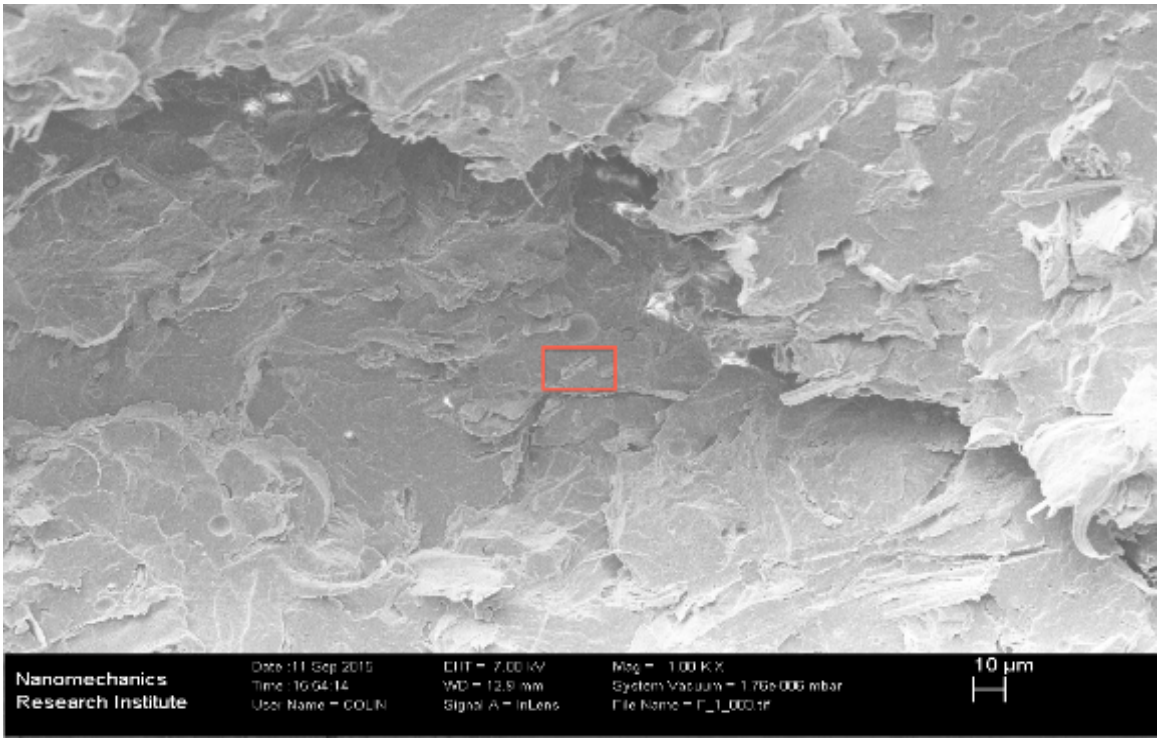

(b) Magnification=1000X

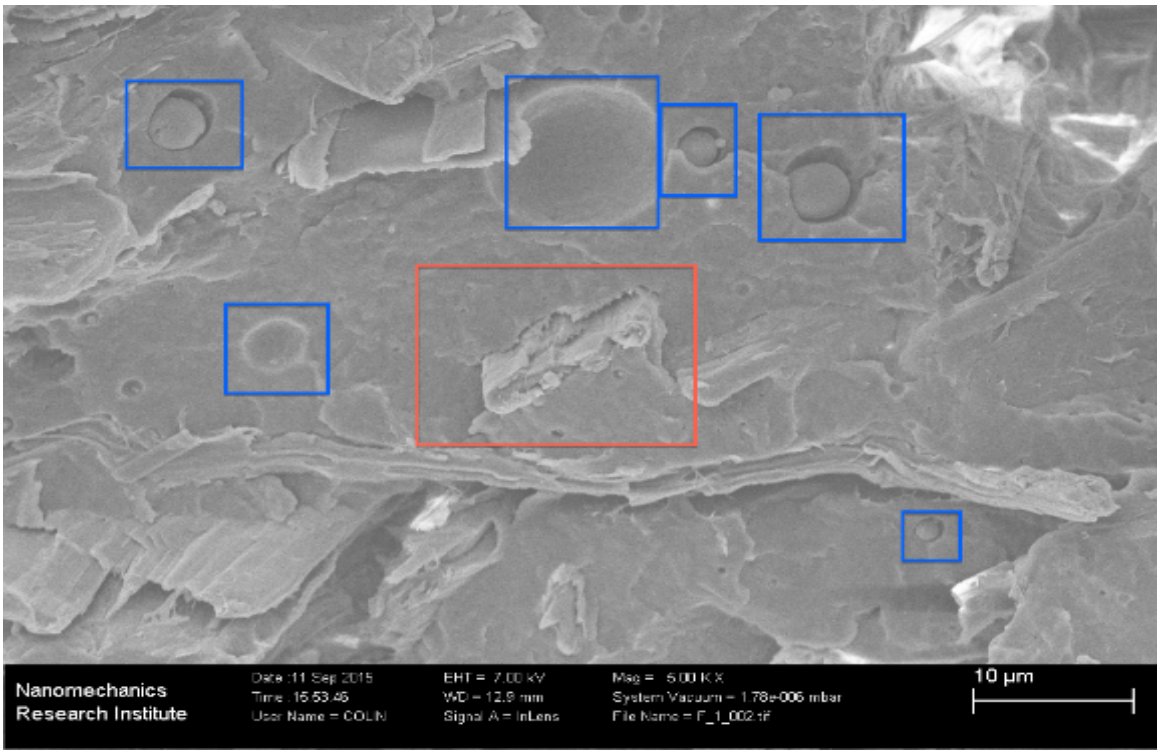

(c) Magnification=5000X

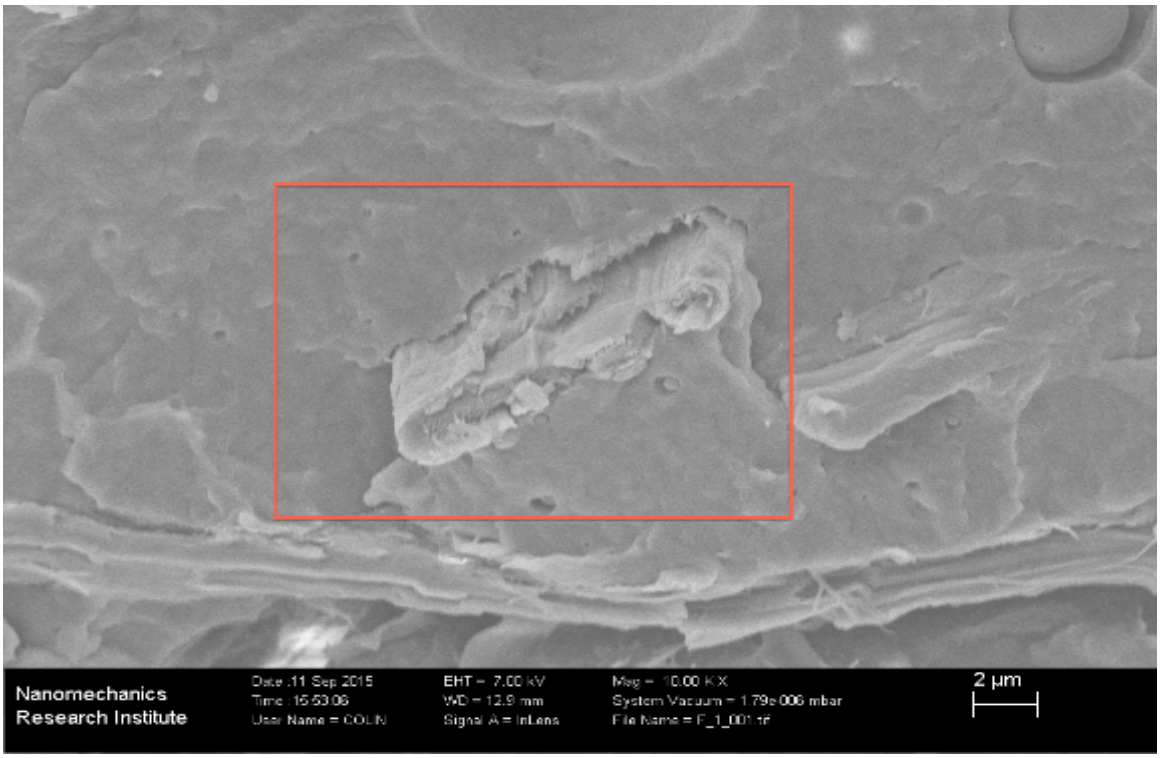

(d) Magnification=10000X

Figure 4- 20 The cross section of sample RPA6/CEL-5000IX (composite with 5000 ppm Irganox 1010)

From Figure 4- 20 it is possible to see that a crack is present in low magnification that leads to a poor stress transfer inside the composite. Higher magnification shows some small droplets in the polymer matrix, which represents small amount of another polymer in the recycled polyamide 6. The mechanical property of this sample is showing a small decrease compared with sample RPA6/CEL-500IX , this may be perhaps a result of the uneven dispersion of the antioxidant or adding too much antioxidant.

4.1.8 Chemical Composition Identification (FTIR)

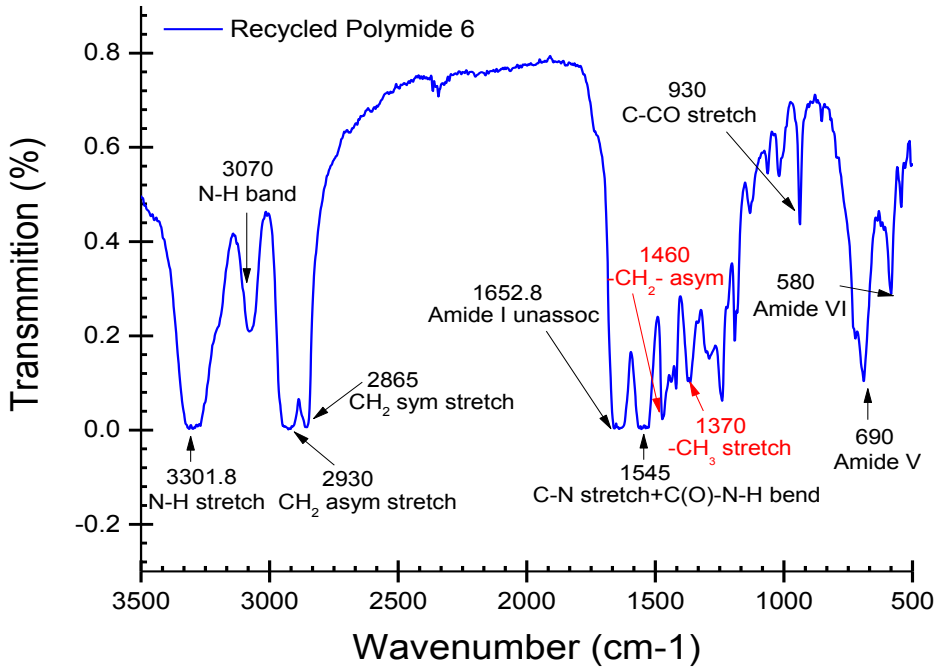

Figure 4- 21 FTIR curve for RPA6

FTIR is a good way to identify the main contents in the recycled polyamide 6 and also to investigate other components in the matrix materials by checking the wavenumber of the functional groups in FTIR spectrum. From the spectrum, amide I band appears at 1652.8cm^{-1}, amide V band appear at 690 cm^{-1} and amide VI appears

at 580cm^{-1}. The N-H stretch and N-H band appears in 3301.8 cm^{-1} and 3070 cm^{-1} respectively. The characterization part C-N stretch and C(O)-N-H bend appears in 1545 cm^{-1}, the CH_2 (asymmetric stretching) and CH_2 (symmetric stretching) appears in 2930 cm^{-1} and 2865 cm^{-1}. The wave number of C-CO stretch stands at 930 cm^{-1} in the spectrum. So the major content in RPA6 proved to be PA6[71]. On the other hand, the FTIR spectrum also shows a peak at 1460 cm^{-1} and 1370 cm^{-1} representing CH_2 (asymmetric stretching) and CH_3 (symmetric stretching), while the CH_2 bend from PA6 at 1371 cm^{-1} could overlap with CH_3 stretching, so considering the recycle procedure of polymer and the SEM image, RPA6 may contain small amounts of polypropylene [72].

4.2 Results And Discussion Of Polyamide 6/Cellulose With Irgafos 168

4.2.1 Mechanical Properties

4.2.1.1 IZOD Impact Test

The most widely used strategy to maximize antioxidant effectiveness is to combine antioxidants of different functions so that they can get a synergism and increase the onset temperature for oxidation. The working mechanism of primary antioxidant (Irganox 1010) is to terminate the free radicals and combine with hydroperoxide decomposer (Irgafox 168) that will decompose hydroperoxide into non-reactive matter. Before combination of these two antioxidants, an evaluation of a proper amount of Irgafox 168 was performed. Figure 4- 22 shows the results of impact strenght of three levels of Irgafox 168: 250 ppm, 500 ppm, and 1000 ppm together with a blank composite without antioxidants.

Compared with the blank sample RPA6/CEL , all the other three samples increased in impact strength after adding Irganox 168 to the composite; the samples increased by 9.2%, 7.0%, and 16.0% respectively. Usually, fiber reinforced polymer composite has a lower impact strength compared with pure polymers because adding fiber to the composite make it easier for crack initiation. However, after adding Irganox 168 to the composite changed this behavior of impact strength induced by adding fiber.

The primary purpose for the composite with cellulose is to achieve a balance of properties by increasing both modulus and impact strength.

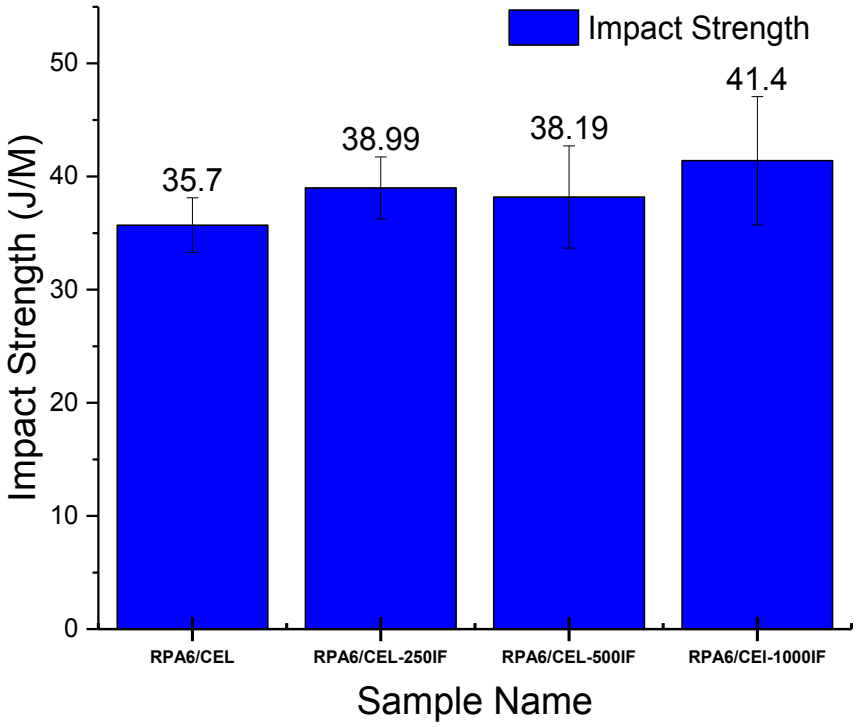

Figure 4- 22 Impact strength of 250, 500, 1000 ppm Irgafox168 adding to 20% cellulose reinforced RPA6

4.2.1.2 Tensile Test

Figure 4- 23 and Figure 4- 24 shows the result of tensile measurements. Both the tensile strength and tensile modulus showedthe same trend as impact strength, all these three samples increased in stiffness (modulus) and strength compared with the blank composite with a respective 6.2%, 3,1% and 18.9% increase for tensile modulus and a 14.9%, 9.1% and 18.91% increase perspective for tensile strength. Compared with the results from the first part, they are showing a similar ability at improving the tensile properties, since the 500ppm Irganox 1010 shows a 22.0% increase compared to the blank composite. So it is appealing to test the stabilization ability by combining these two antioxidants.

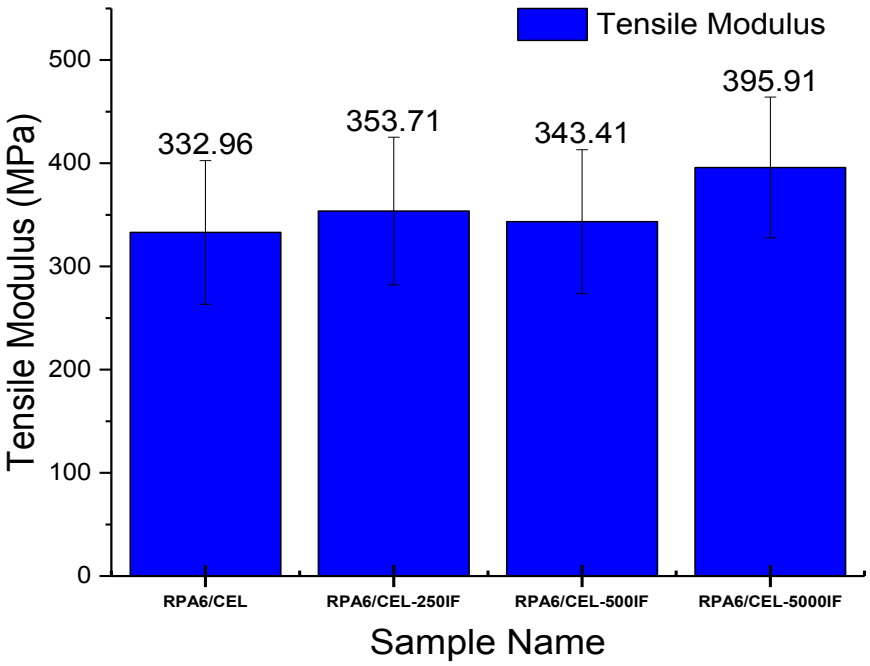

Figure 4- 23 Tensile modulus of 250, 500, 1000 ppm Irgafox168 adding to 20% cellulose reinforced RPA6

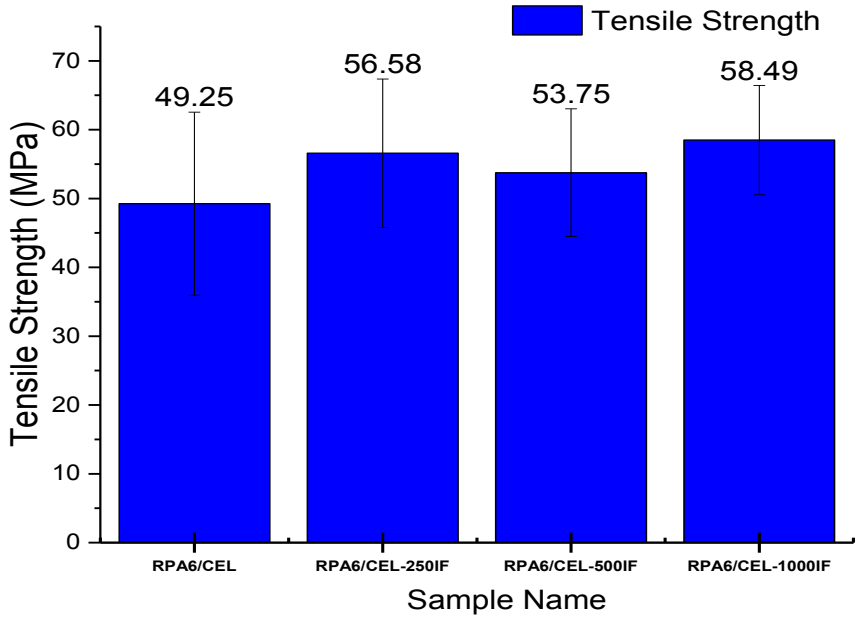

Figure 4- 24 Tensile strength of 250, 500, 1000 ppm Irgafox168 adding to 20% cellulose reinforced RPA6

4.2.1.3 Flexural Test

The effect of different levels of Irgafox 168 on flexural properties of the composite shows on Figure 4- 25 and Figure 4- 26.

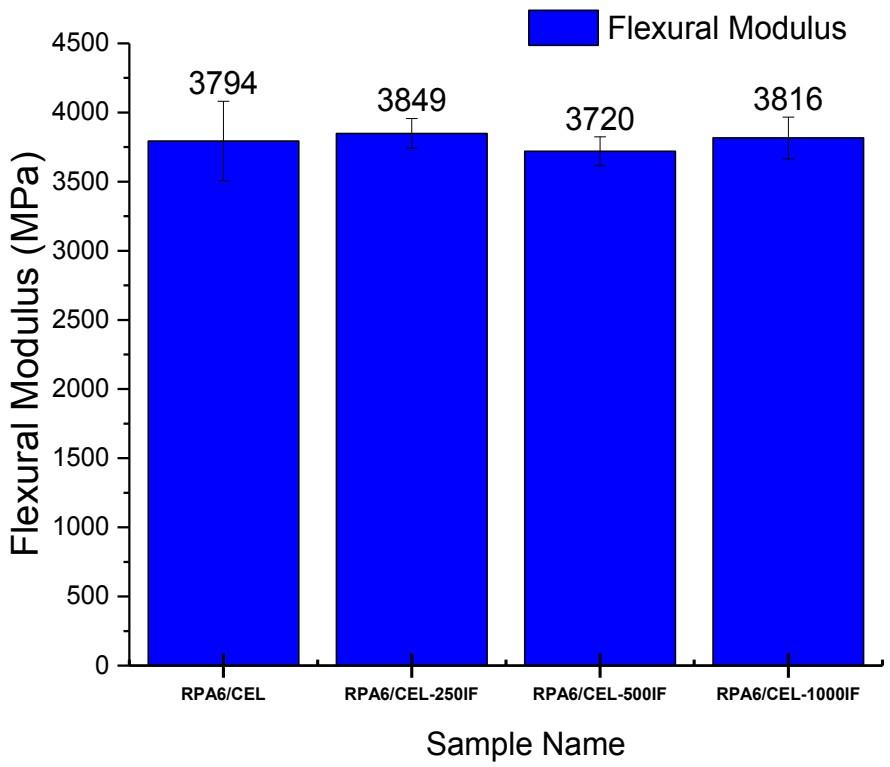

Figure 4- 25 Flexural modulus of 250, 500, 1000 ppm Irgafox168 adding to 20% cellulose reinforced RPA6

From Figure 4- 25 we can see after adding Irgafox 168 to the composite, there is almost no change in the flexural modulus and moreover 500 ppm Irgafox resulted in a decrease of the modulus compared with the blank composite. Also from Figure 4- 26, we can observe a similar situation with the modulus results. So the adding of Irgafox 168 to the composite does not affect the flexural properties while a consideration of synergism and combination test still needs to be performed.

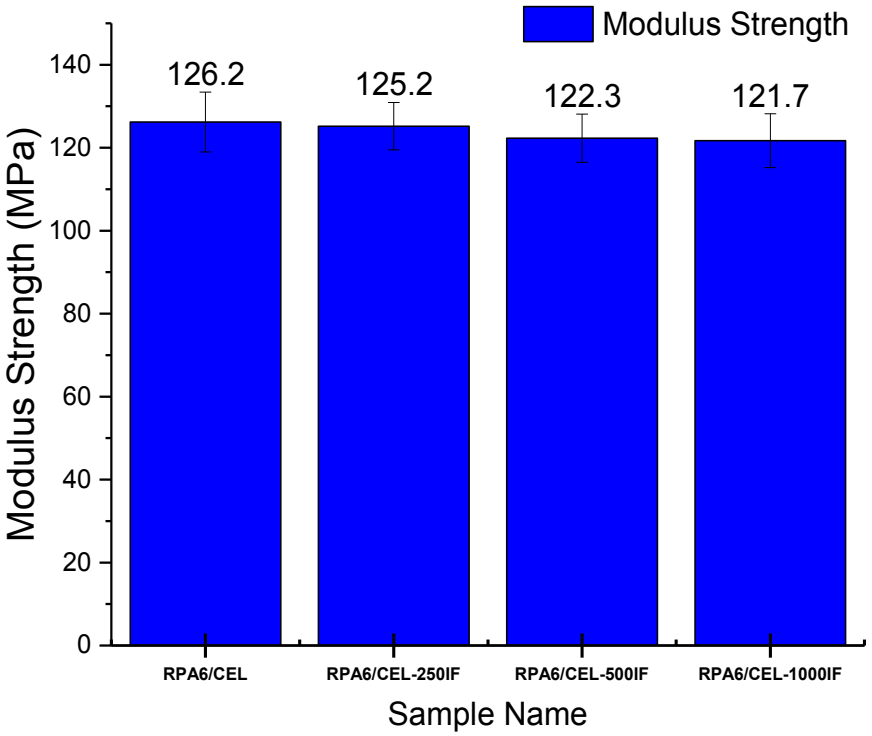

Figure 4- 26 Flexural strength of 250, 500, 1000 ppm Irgafox168 adding to 20% cellulose reinforced RPA6

4.2.1.4 The Summary Of Different Mechanical Properties For Irganox 168

The mechanical properties: Impact strength, tensile modulus, tensile strength, flexural modulus and flexural strength are shown in Figure 4- 27. The radar graph clearly represent that there are small improvements of different mechanical properties compared with blank composite (does not contain Irgafox 168.)

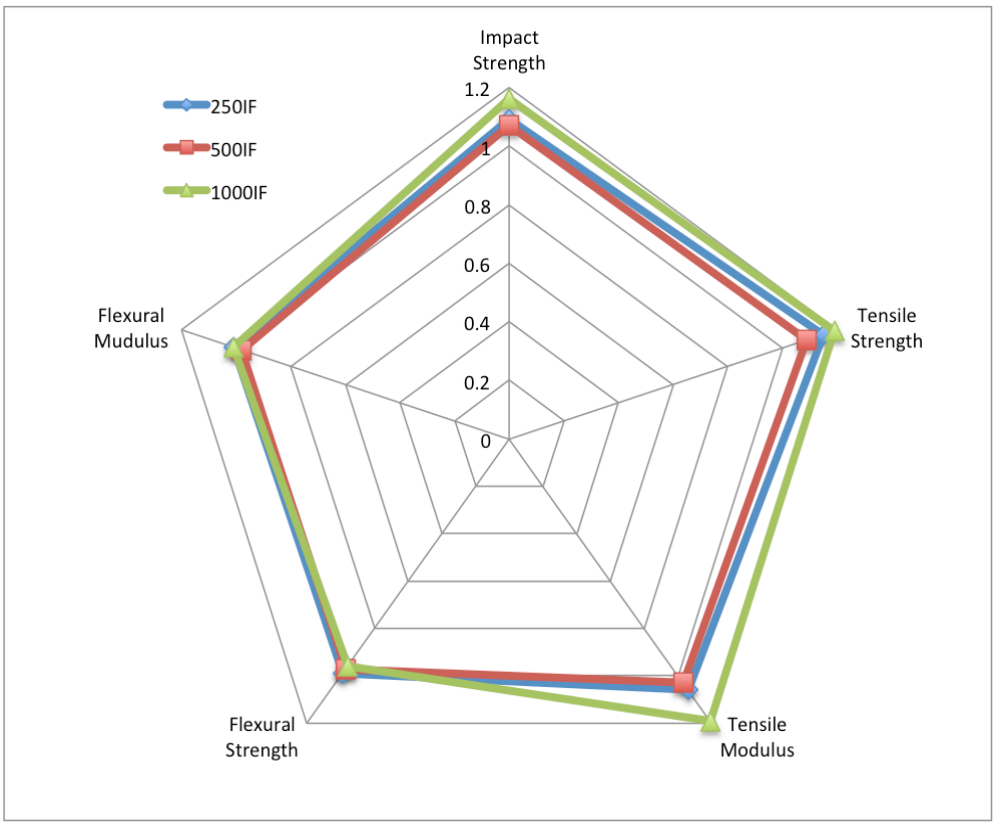

Figure 4- 27 Mechanical properties for 250, 500, 1000 ppm Irgafox168 adding to 20% cellulose reinforced RPA6

4.2.2 Degradation (Thermal Gravimetric Analysis)

The summary of 1%, 5% and 10% weight loss temperature and the maximum first derivative temperature is showing in Table 4- 5. The overlay TGA graph of this series of samples presented in Figure 4- 28 and DTGA graph shows in Figure 4- 29.

From the overlay TGA graph, we can easily observe sample 1000IX/250IF has a lower weight percentage of residues at 650℃. This means the blank sample has a much higher level of degradation, at the same time proved the antioxidant is effective in stabilization of high temperatures. During the processing procedure, polyamide/cellulose composite will undergo a series of high-temperature processes such as extrusion, injection molding and compression, which will lead to thermal degradation, so this thermal test proved that it is effective to stabilize the composite.

Table 4- 5 TGA analysis summary

Run#	T1% (℃)	T5% (℃)	T10% (℃)	Tmax1 (℃)	Tmax2 (℃)	Tmax3 (℃)	T onset (℃)
RPA6/CEL	289.7	351.5	370.8	391.0	408.5	454.5	289.5
RPA6/CEL-250IF	283.5	347.4	367.5	391.1	421.6	459.0	280.6
RPA6/CEL-500IF	279.3	354.7	374.7	392.8	406.2	457.3	288.5
RPA6/CEL-1000IF	288.6	350.2	369.9	392.2	413.1	457.9	284.7

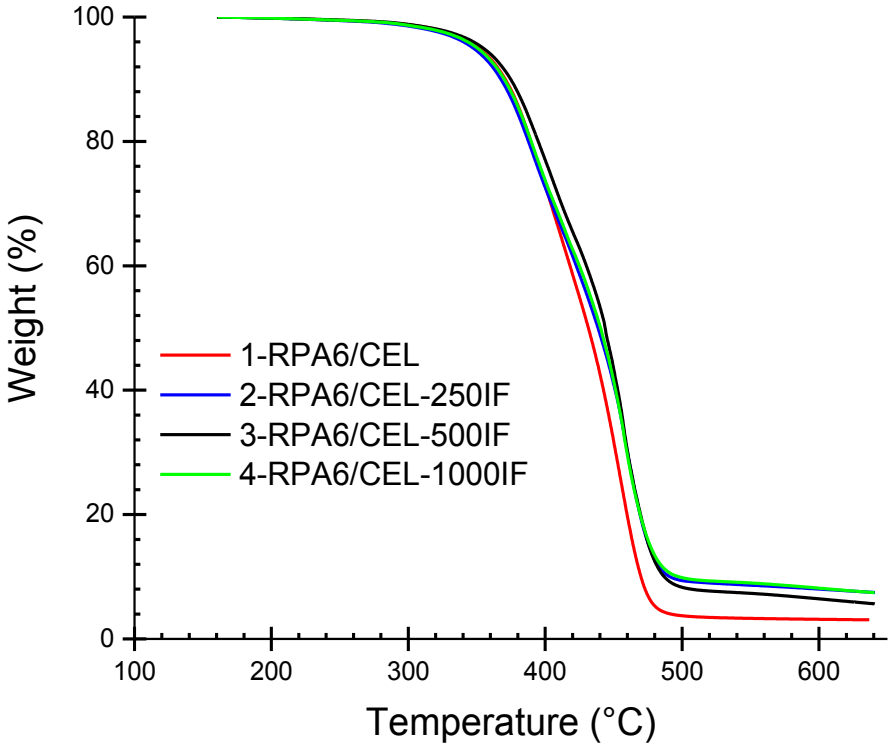

Figure 4- 28 TGA curves for 250, 500, 1000 ppm Irgafox168 adding to 20% cellulose reinforced RPA6

From the DTGA results we can separate the degradation process into three steps or two major steps, the first two steps are very close and happen at around 380 to 400 ℃, the second major degradation occurs at 480 ℃. Also from the DTGA graph, we can clearly observe that the blank composite had a higher degradation rate in the first degradation step than other samples, which demonstrates that without antioxidants the composite will be less stable at the onset of thermal degradation. At about 480 ℃ (the peak of the second degradation step) they show the same level of degradation, but there is a noticeable shoulder just before the peak at 480 ℃ for the sample without antioxidant. Overall it is very clear the trend that the antioxidant is reducing the rate of thermal degradation.

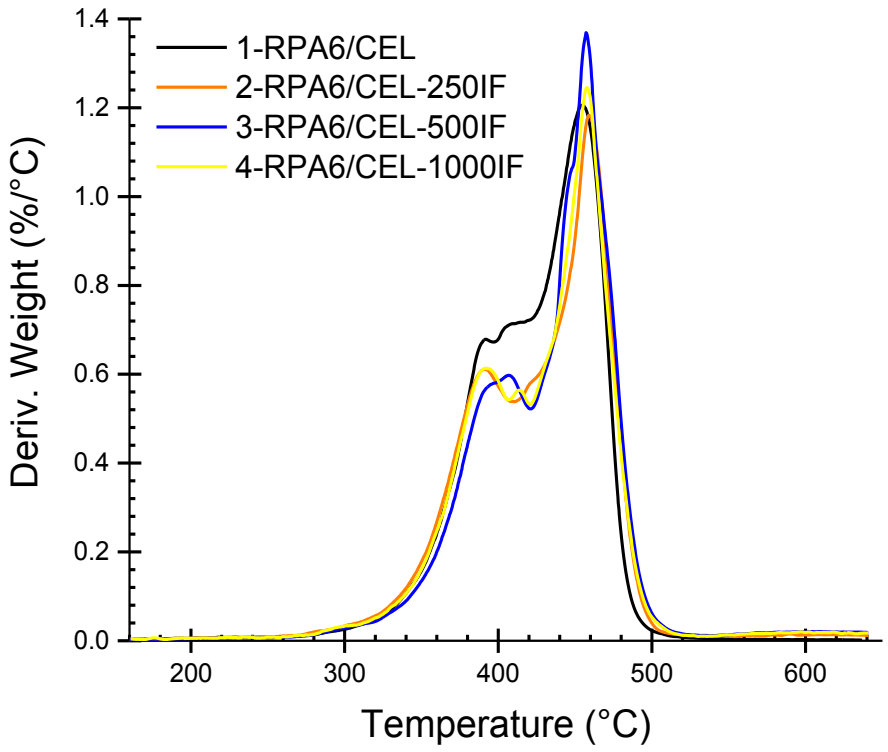

Figure 4- 29 DTGA curves for 250, 500, 1000 ppm Irgafox168 adding to 20% cellulose reinforced RPA6

4.3 Results And Discussion Of Polyamide 6/Cellulose With Antioxidant Irganox 1010 & Irgafox 168

4.3.1 Mechanical Properties

4.3.1.1 IZOD Impact Test

Figure 4- 30 presents the impact test results of four different formulations of the Irganox 1010 and Irgafox 168 combination mixed in the composite. The results indicate that the combination of these two antioxidants did not affect the impact strength of the composite, especially when taking the error bar into consideration.

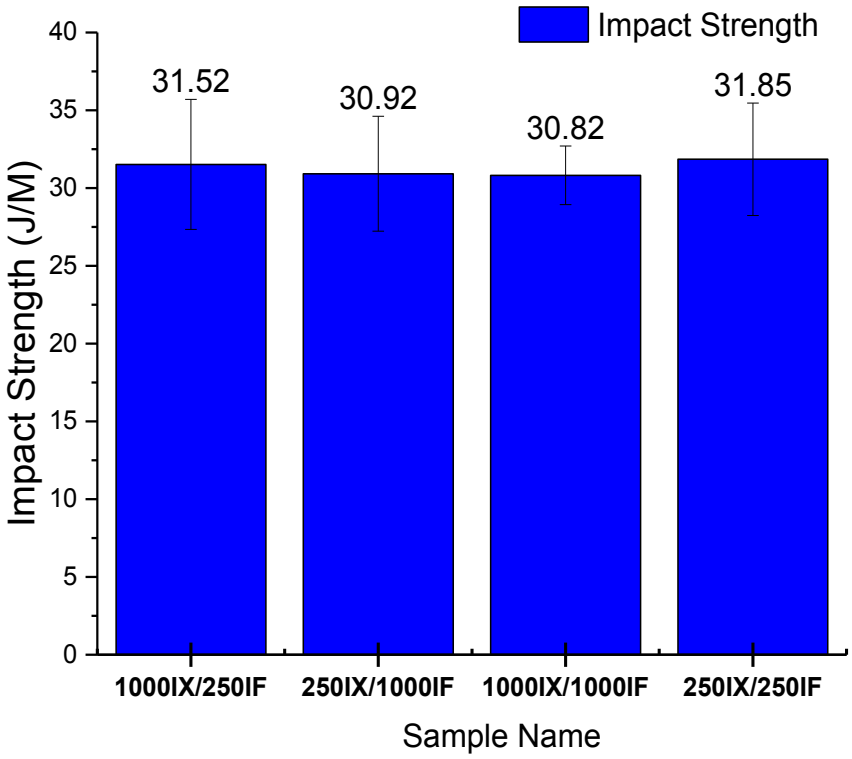

Figure 4- 30 Impact strength of 20% cellulose reinforced RPA6 contains combination of 250 and 1000 ppm Irganox 1010 and Irgafox 168

4.3.1.2 Tensile Test

Figure 4- 31 and Figure 4- 32 are the results of tensile properties of Irganox 1010 combined with Irgafox 168. The major purpose of this part is to evaluate the combination of types of antioxidant in the formulation. Sample 250IX/250IF (250 ppm Irganox 1010/ 250 ppm Irgafox 168) had the best performance in tensile modulus. Also, sample 250IX/250IF showed a higher value of tensile strength. The improvement of the tensile modulus is attributed to a good compatibility between the matrix polymer and natural fiber filler so that the composite inherits the good tensile modulus from cellulose and achieves a better stress transfer [66].

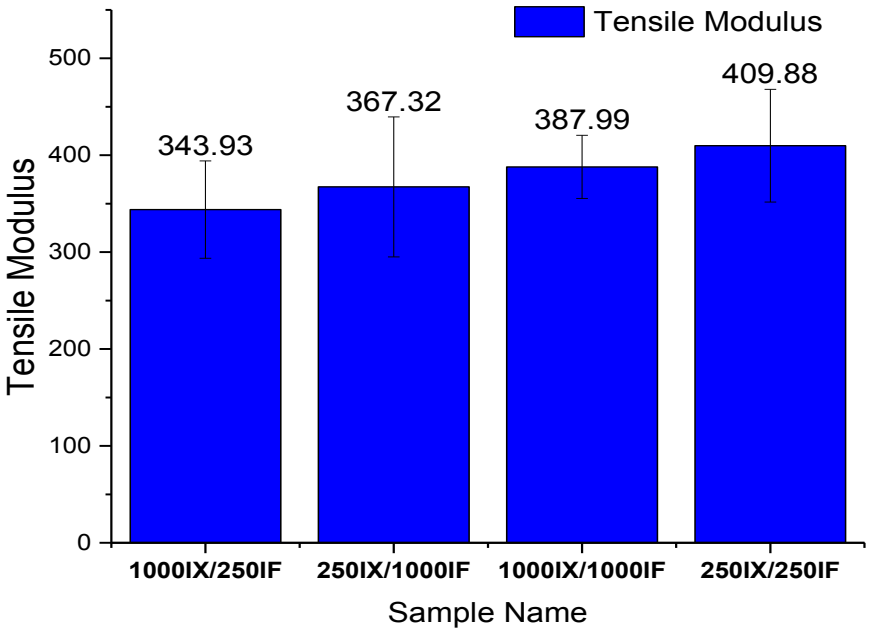

Figure 4- 31 Tensile modulus of 20% cellulose reinforced RPA6 contains combination of 250 and 1000 ppm Irganox 1010 and Irgafox 168

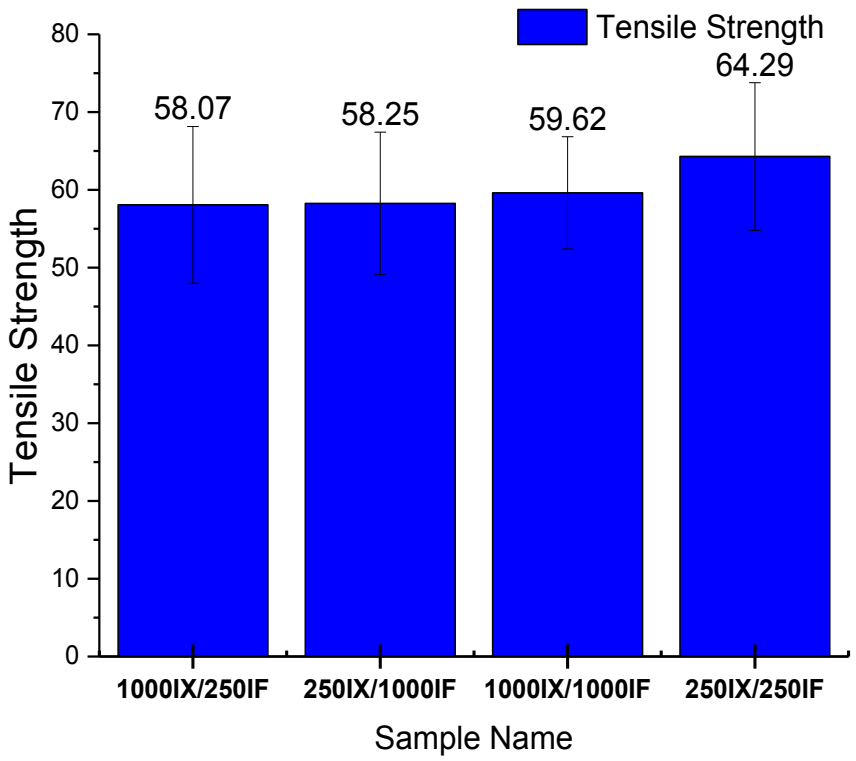

Figure 4- 32 Tensile strength of 20% cellulose reinforced RPA6 contains combination of 250 and 1000 ppm Irganox 1010 and Irgafox 168

4.3.1.3 Flexural Test

The effect of the different level antioxidant combinations on flexural properties of the composite is shown in Figure 4- 33 and Figure 4- 34. From these results, it is possible to observe that there is almost no difference between different formulations, and compared with the previous two sections there is no advantage over using a single antioxidant.

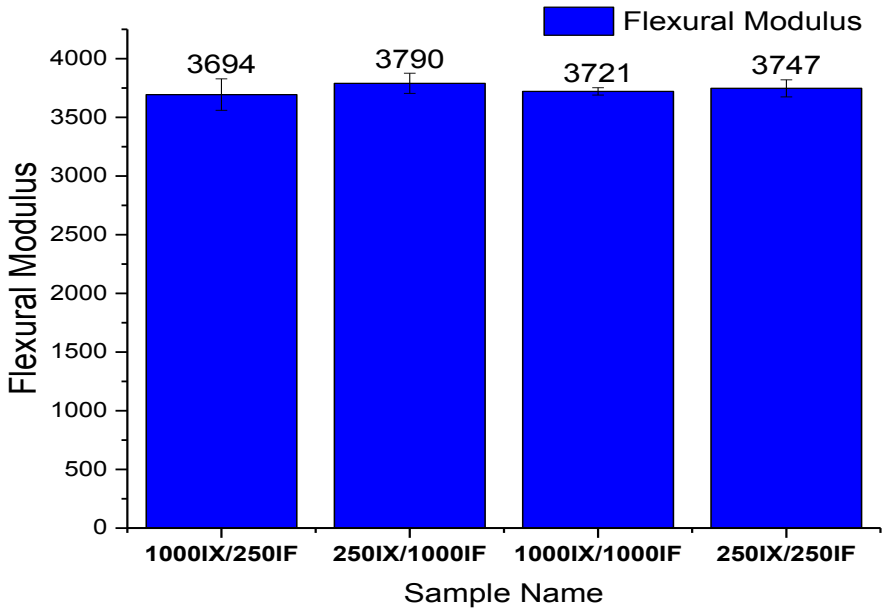

Figure 4- 33 Flexural modulus of 20% cellulose reinforced RPA6 contains combination of 250 and 1000 ppm Irganox 1010 and Irgafox 168

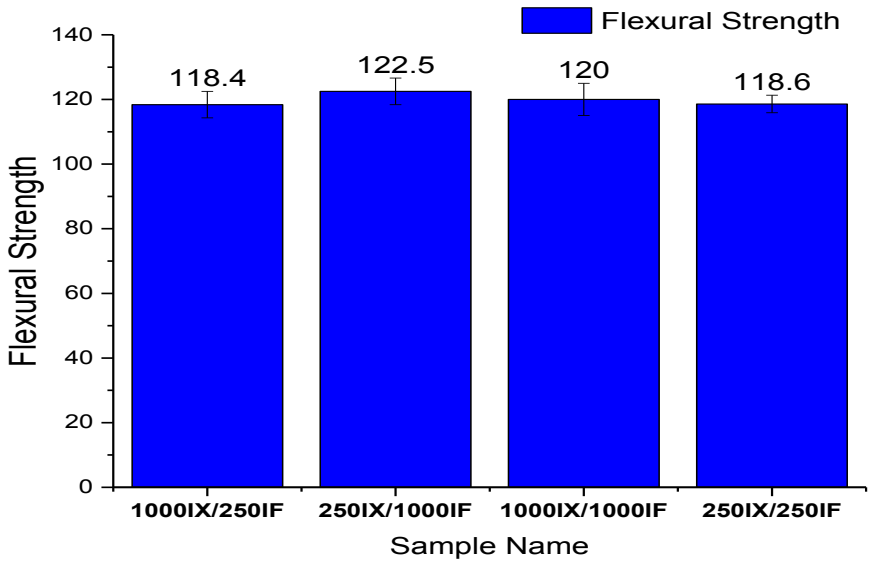

Figure 4- 34 Flexural strength of 20% cellulose reinforced RPA6 contains combination of 250 and 1000 ppm Irganox 1010 and Irgafox 168

4.1.3.4 The Summary Of Different Mechanical Properties For Irganox 168/ Irganox 1010

The mechanical properties for irganox 1010/ Irgafox168 are shown in the radar graph. It clearly represents that there different improvements of impact strength, tensile strength, flexural strength and flexural modulus, while tensile modulus got the highest value when the combination was 250 ppm Irganox 1010 and 250 ppm Irgrafox 168.

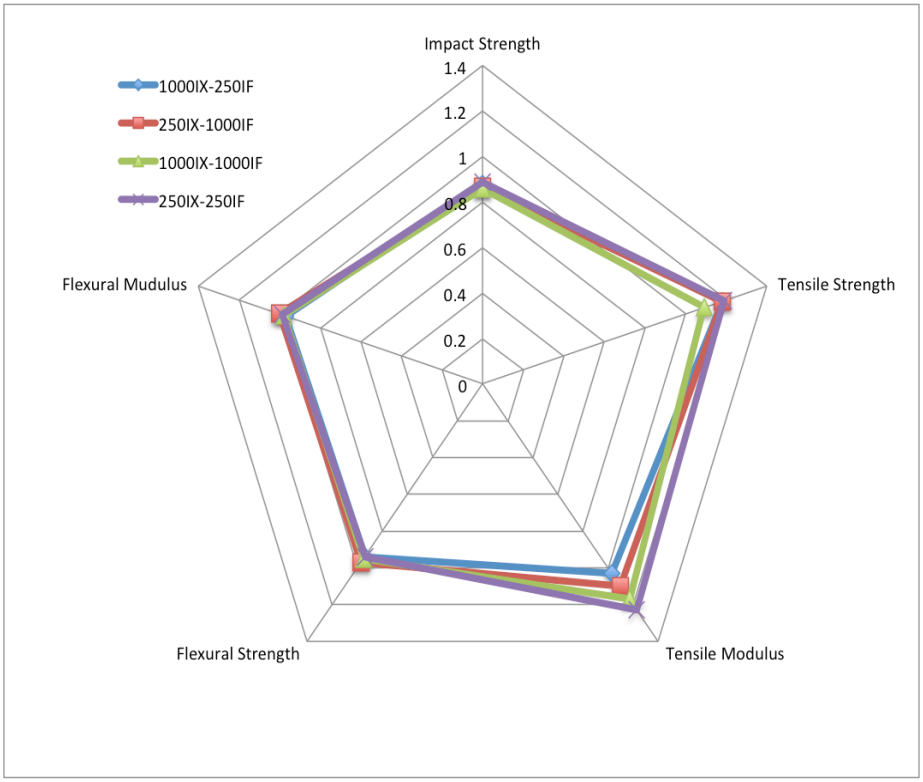

Figure 4- 35 The summary of mechanical properties for the combination of these two antioxidant

4.3.2 Degradation (Thermal Gravimetric Analysis)

The summary of 1%, 5% and 10% weight loss temperature and the maximum first derivative temperature is shown in Table 4- 6. The TGA and DTGA graph is shown in Figure 4- 36 and Figure 4- 37.

Table 4- 6 TGA analysis summary of Irganox1010/ Irgafox 168 composite

Run#	T1% (℃)	T5% (℃)	T10% (℃)	Tmax1 (℃)	Tmax2 (℃)	T onset (℃)
1000IX/250IF	287.2	353.8	373.4	405.8	452.8	293.7
250IX/1000IF	286.0	348.6	368.0	391.1	461.3	279.1
1000IX/1000IF	286.7	350.7	371.1	275.7	459.0	275.7
250IX/250IF	289.0	350.0	369.4	393.3	457.9	282.7

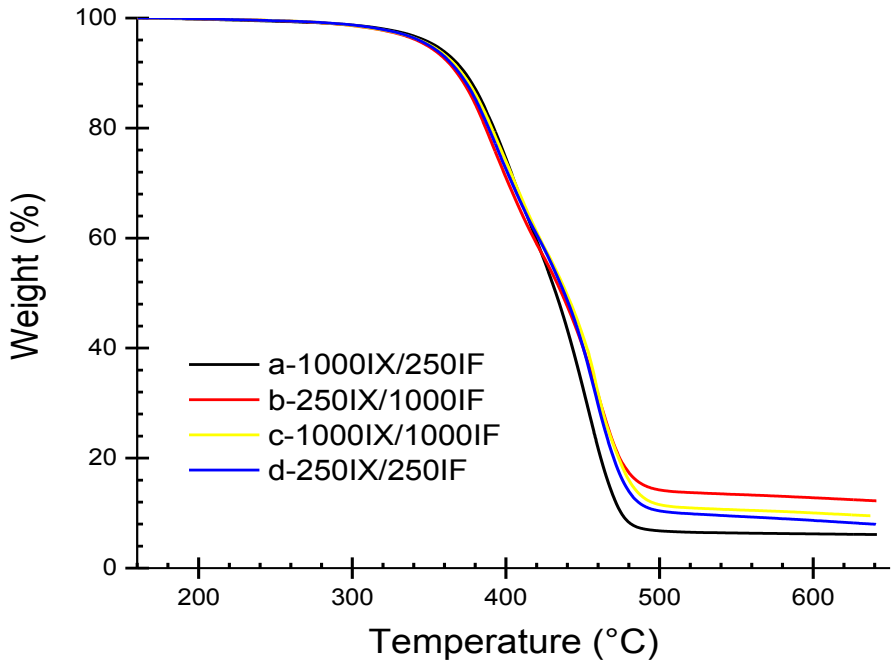

Figure 4- 36 TGA curves for 20% cellulose reinforced RPA6 contains combination of 250 and 1000 ppm Irganox 1010 and Irgafox 168

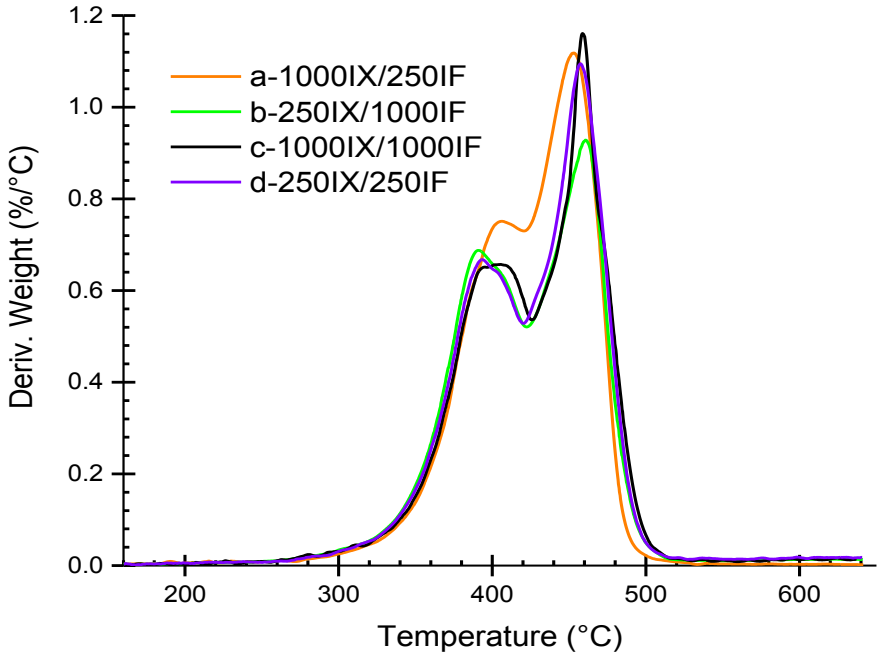

Figure 4- 37 DTGA curves for 20% cellulose reinforced RPA6 contains combination of 250 and 1000 ppm Irganox 1010 and Irgafox 168

According to the summary table, we can tell that this composite material can be stable until 350℃, so that can be applied in high working temperature. The weight loss of 1%, 5%, and 10% happened at a similar temperature for different samples so that different combinations of Irganox 1010 and Irgafox 168 have no obvious effect on the thermal stability of the composite. The DTGA graph indicates it is also two-stage degradation, the first degradation peak happened at 380℃ and the second major degradation peak happened at 460℃. The differences in residue at 650 ℃ of different runs is obvious, sample A (1000 ppm Irganox 1010/250 ppm Irgafox 168) has more residue than others, the residue sequence being: A>C>D>B. Both sample A and sample A contains 1000 ppm Irganox 1010 in the composite, which agrees with the results from the first part that the 500 ppm Irganox 1010 is more fit for the composite. On the other hand, it reflects Irgafox 168 was not that effective for this composite, and this is also in accordance with the results from the second part of the

study that the Irgafox 168 makes almost no difference to the composite performance.

However, in order to obtain a more accurate test for the oxygen resistance ability, further testing such as the oxidation induction time is recommended.

4.4 Results And Discussion Of Polyamide 6-10/ Wood Fiber

The previous sections evaluated the effect of antioxidants on recycled polyamide 6 compounded with cellulose fiber. Recycled polymer has a significant environmental appeal because a significant amount of material can be diverted from landfill by using recycled polymers. Another perspective to increase the sustainability of materials is to use polymer based on renewable feedstock, like polyamide 6-10 (PA-610). The objective of this section is to evaluate the effect on cellulose on polyamide 6-10, in this case both the fiber and the polymer are renewable. Theses sample were not molded at the University of Waterloo laboratory, they were molded at Ford Motors Company as a part of research collaboration. The samples tested here were molded using ISO standards.

4.4.1 Specimen Color

Figure 4- 38 is a picture of a series dumbbell bars, starting from the right side they are PA610 (pure polyamide 6-10, no cellulose), and composites with 3% , 10% , 20% and 30% cellulose (Suzano).. The pure PA610 present some yellowish color while all the other four samples showed a dark brown to black color. This indicates the significant degradation of the composite resulting from cellulose thermal degradation.

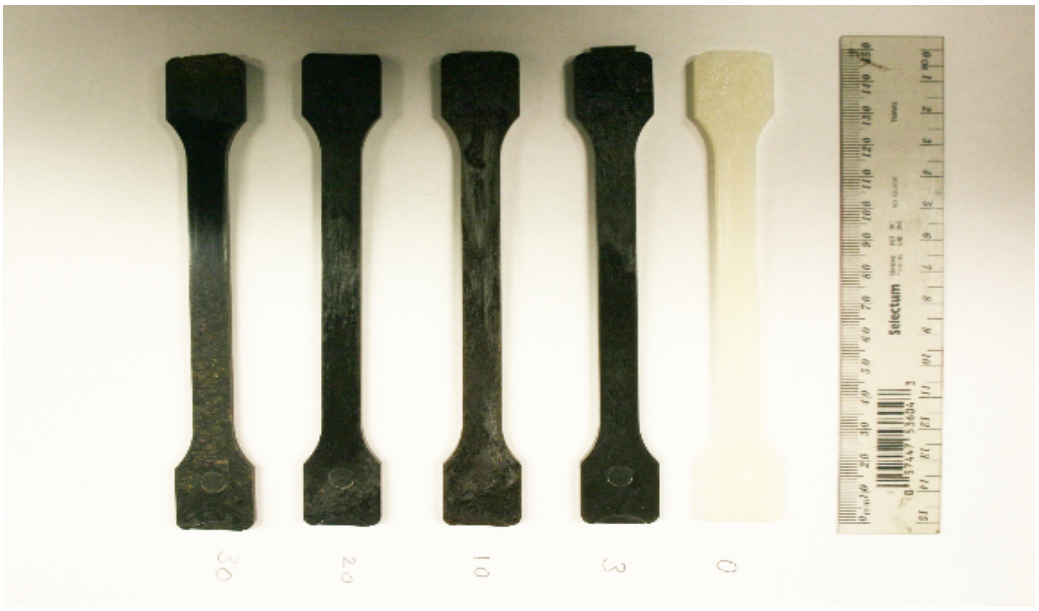

Figure 4- 38 Picture of polyamide / cellulose (from left to right, 30%, 20%, 10%, 3% and 0% of cellulose)

4.4.2 Mechanical Properties

4.4.2.1 IZOD Impact Test

Figure 4- 39 shows the results of impact strength of samples prepared using ISO molds, therefore the units are reported in kJ/m^2. The pure polyamide 6-10 showed the highest value of impact strength, whereas addition of cellulose decreased the impact strength. The decrease in impact strength is attributed to usual reasons as observed in composites investigated in previous sections. Addition of short fibers to polymer matrix increased crack initiation, meaning the material is more brittle[1]. Note that adding low levels of cellulose did not decrease the impact strength significantly, that is, addition of 3% or 10% of cellulose had approximately the same level of impact strength. Adding 30% wood fiber results in a 64% decrease in impact strength compared with the pure PA6-10 which is also the lowest value tested from this series of composites.

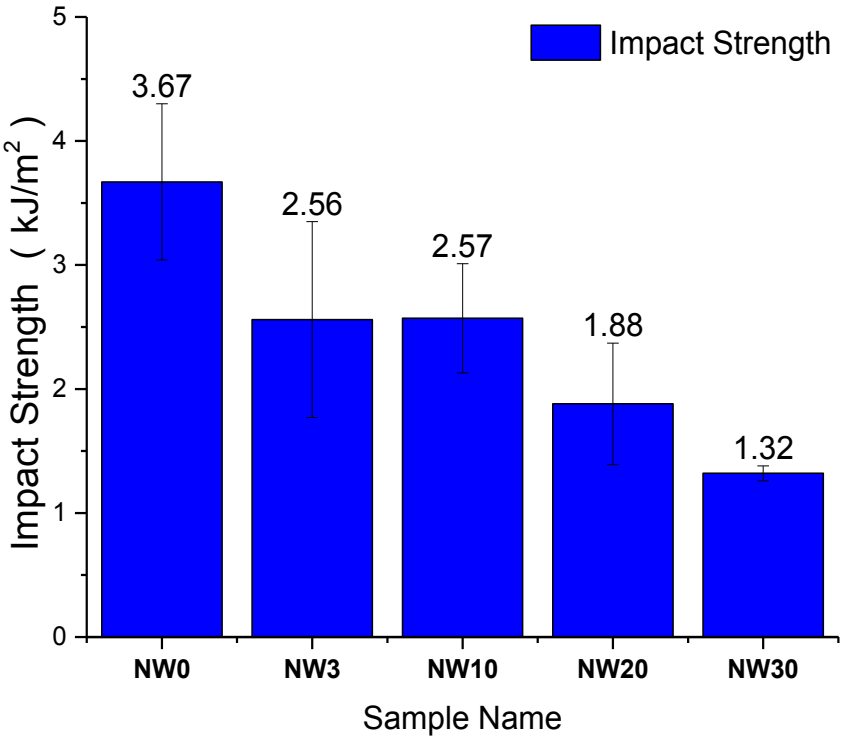

Figure 4- 39 Impact strength of PA6-10/ 3%, 10%, 20% and 30% cellulose composite

4.4.2.2 Tensile Test

Figure 4- 40 and **Figure 4-** 41 shows the results of tensile modulus and tensile strength respectively. The most attractive part of adding cellulose fiber to the polymer matrix is the high tensile modulus inherited from the fiber.

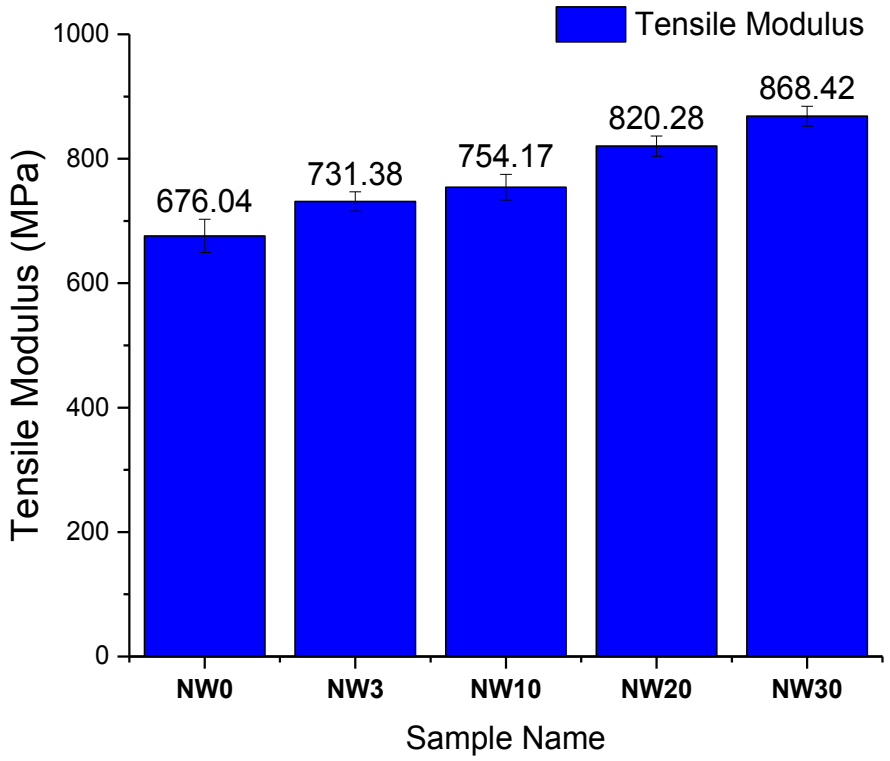

Figure 4- 40 Tensile modulus of PA6-10/ 3%, 10%, 20% and 30% cellulose composite

Figure 4- 40 shows an obvious increase of the tensile modulus as the cellulose content is increased. Generally, higher fiber content mixed in the composite aims at achieving higher modulus and strength, so that it is necessary to investigate the fiber content's effect on the mechanical performance.

Other authors reported the effect of hemp fiber content on polypropylene investigating the addition of 30%, 40%, 50% and 70% fiber loading. The tensile modulus showed an increase from 30%, with maximum modulus obtained at 50%, followed by decrease in modulus with higher fiber loading. The tensile modulus at 50% loading was almost 2.5 times higher than pure polypropylene [33]. Also, the tensile strength of flax reinforced high-density polyethylene (HDPE) was reported

for several fiber loadings ranging from 5% to 40%, the tensile strength increased with the increase of fiber loading until reaching a maximum with 20% of fiber [3]. The results obtained here have a different behavior. The tensile strength decreased 31.2% by adding 3% of cellulose. It is important to note that the processing temperature of polyamide is well above the processing temperatures for polypropylene or polyethylene. The decrease in tensile strength is attribute to thermal degradation of the cellulose, which may have resulted in poor interfacial bonding between polyamide matrix and the cellulose fiber. The interfacial adhesion comes mostly from week intermolecular connection such as hydrogen bonds, which may have been compromised by the thermal degradation of cellulose [68].

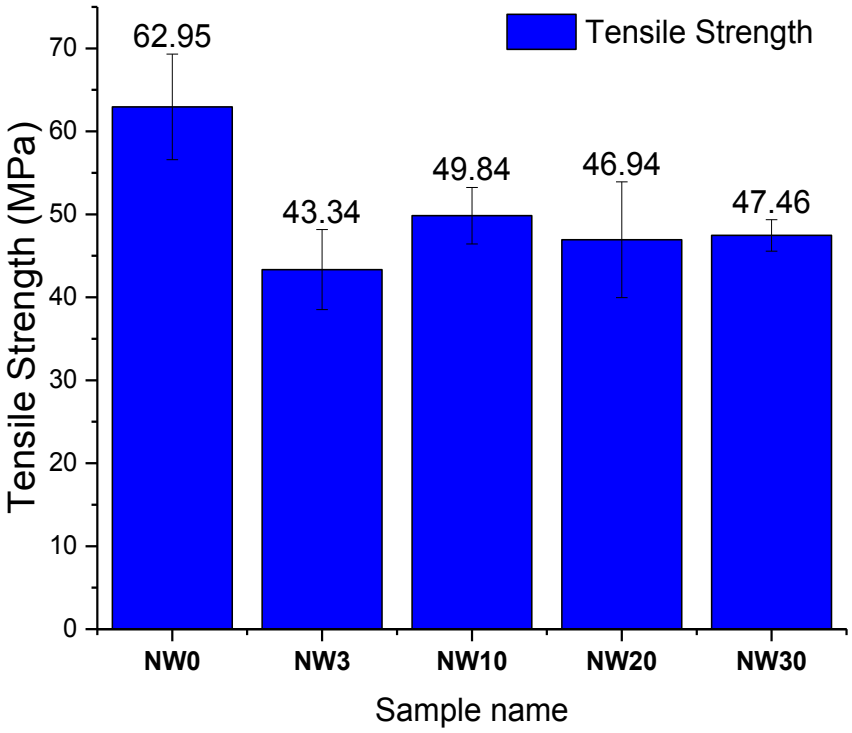

Figure 4- 41 Tensile strength of PA6-10/ 3%, 10%, 20% and 30% cellulose composite

4.4.2.3 Flexural Test

The effect of different levels of cellulose on the flexural properties of PA6-10 and cellulose composites is shown in **Figure 4-** 42 and Figure 4- **43**. As shown in **Figure 4-** 42, this property increased for composites when compared with pure PA6-10. The best performance was observed with 10% of cellulose loading, which was a 17% improvement. Aydemir found that with the increase of the cellulose loading, the flexural modulus increased linearly which also means an increase in stiffness. This agrees with other research results which find that adding wood fiber, a mix of natural fiber, MCC and alpha cellulose fiber all improve the flexural performance of the composite [2].

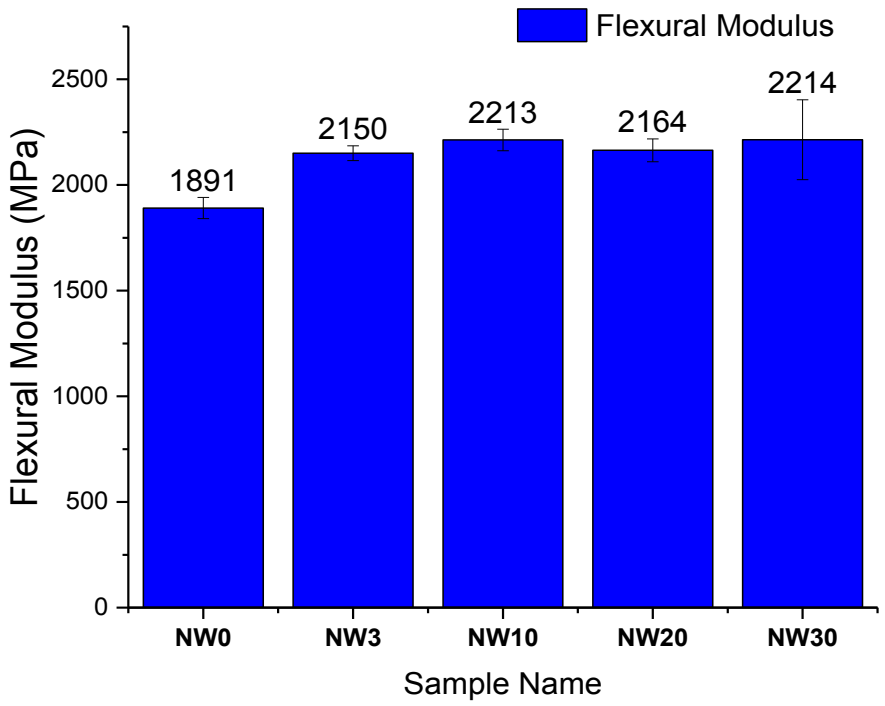

Figure 4- 42 Flexural modulus of PA6-10/ 3%, 10%, 20% and 30% cellulose composite

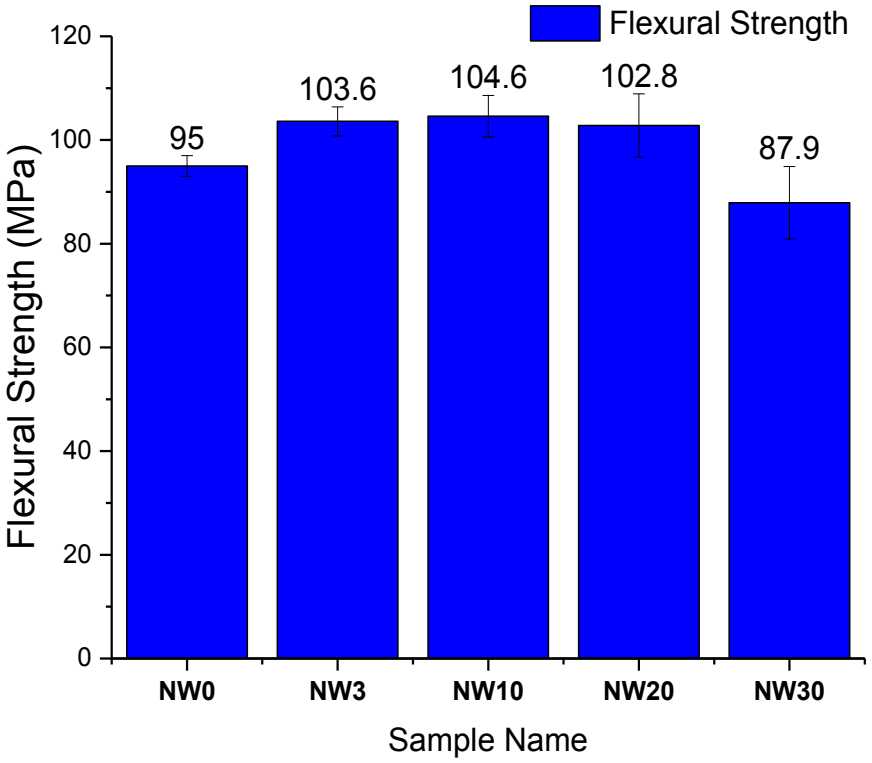

Figure 4- 43 **Flexural strength of PA6-10/ 3%, 10%, 20% and 30% cellulose composite**

4.4.2.4 Gardner Impact Test

Table 4- 7 to Table 4- 11 show the failure table of Gardner test for PA6-10, NW3, NW10, NW20 and NW30 respectively. Note: X means failure and O mean non-failure.

Table 4- 7 Failure table of Gardner test for PA6-10

Drop height (in) X=O	1	2	3	4	5	6	7	8	9	10	11	12	13	14	15	16	n_x	n_0	i	n_i	in_i	i^2n_i
8.75						X											1	0	2	1	2	4
8.50	X		X		O		X		X		X		X				6	1	1	6	6	6
8.25		O		O				O		O		O		X		O	1	6	0	1	0	0
8															O		0	1		0	0	
Total																	8	8		8	8	10

Table 4- 8 Failure table of Gardner test for NW3

Drop height (in) O min	1	2	3	4	5	6	7	8	9	n_x	n_0	i	n_i	in_i	i^2n_i
3	X								X	2	0				
2.75		X				X		O		2	1	2	1	2	4
2.5			X		O		O			1	2	1	2	2	2
2.25				O						0	1	0	1	0	0
Total										5	4		4	4	6

Table 4- 9 Failure table of Gardner test for NW10

Drop height (in) X min	1	2	3	4	5	6	7	8	9	10	11	12	n_x	n_0	i	n_i	in_i	i^2n_i
2.5			X						X		X		3	0	1	3	3	3
2.25		O		X		X		O		O		O	2	4	0	2	0	0
2	O				O		O						0	3		0		
Total													5	7		5	3	3

Table 4- 10 Failure table of Gardner test for NW20

Drop height (in) X=O	1	2	3	4	5	6	7	8	9	10	11	12	13	14	15	16	n_x	n_0	i	n_i	in_i	i^2n_i
2.5			X		X												2	0	2	2	4	8
2.25		O		O		X		X		X		X		X			5	2	1	5	5	5
2	O						O		O		O		O		X		1	5	0	1	0	0
1.75																O	0	1				
Total																	8	8				13

Table 4- 11 Failure table of Gardner test for NW30

Drop height (in) X=O	1	2	3	4	5	6	7	8	9	10	n_x	n_0	i	n_i	in_i	i^2n_i
2.25		X									1	0	2	1	2	4

2	O		X		X				X		3	1	1	3	3	3
1.75				O		X		O		O	1	3	0	1	0	0
1.5							O				0	1				
Total											5	5		5	5	5

Table 4- 12 Summary of failure type

Failure type\ Number	PA610	NW3	NW10	NW20	NW30
N	8	4	7	8	5
C	2	0	0	0	0
E	0	0	0	0	0
I	3	5	5	8	5
H	3	0	0	0	0
B	0	0	0	0	0

- No crack (N)
- Complete shattering (C)
- Crack radiating towards edge of the plate (E)
- Radical crack within impact area (I)
- Hole in plaque (H)
- Brittle splitting (B)

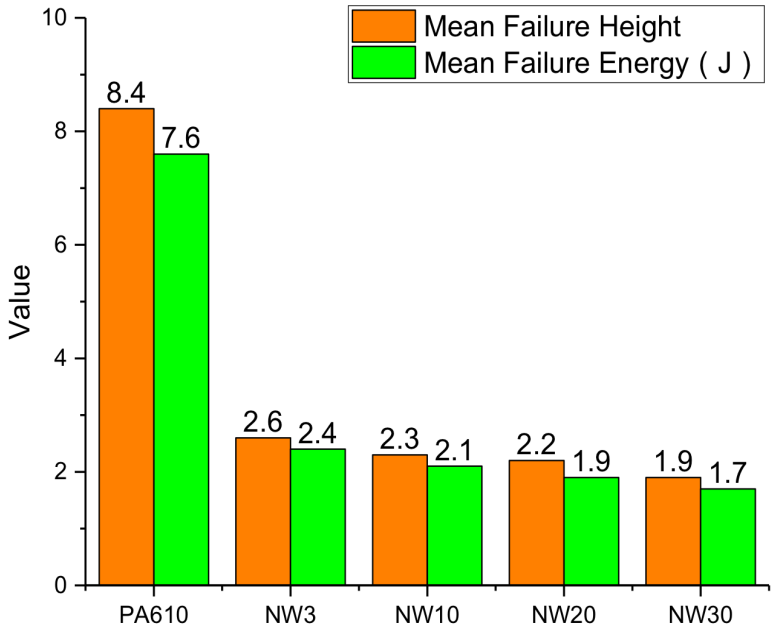

Figure 4- 44 Summary of mean failure height and energy

Table 4- 12 shows the summary of failure type and Figure 4- 44 is the summary of mean failure height and mean failure energy. PA6-10 exhibited three types of failure and the images of failure of PA6-10 are shown in Figure 4- 45. The mean failure height and mean failure energy have a similar trend: with the increase of fiber loading, both mean failure height and mean failure decreased. Compared with pure PA6-10, the composite with 3% of cellulose lead to the mean failure energy decreasing from 7.570 J to 2.373 J. The trends of impact strength measured with the Gardner impact tester agreed well with the impact strength measured by notched Izod impact tester discussed in previous sections.

Figure 4- 45 PA610 failure forms from left to right: I, C and H

4.4.2.5 The Summary Of Mechanical Properties For PA6-10 Reinforced By Wood Fiber

Different mechanical properties of PA6-10 reinforced by wood fiber are shown in Figure 4- 46. The results show that the value of flexural modulus, flexural strength and tensile strength are similar among different samples. The impact strength decreased as the increase of cellulose content, while the tensile modulus increased as the increase of the cellulose content.

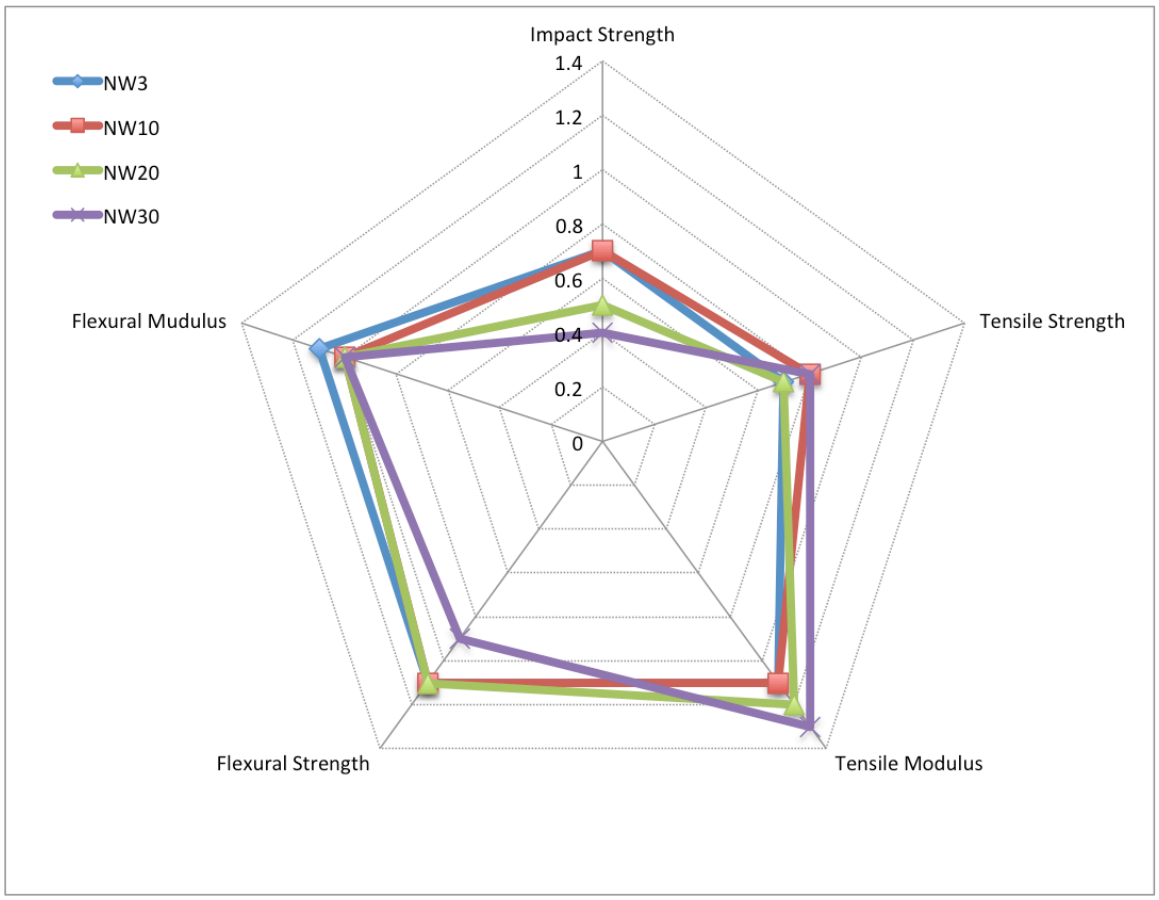

Figure 4- 46 Summary of mechanical properties of PA610 reinforced by wood fiber

4.4.3 Degradation (Thermal Gravimetric Analysis)

The summary of temperatures (°C) for 1%, 5% and 10% weight loss and the temperatures (°C) for the maximum rate (DTGA, derivative) are shown in **Table 4-** 13. The curves for TGA and DTGA are shown in **Figure 4-** 47 and **Figure 4-** 48 respectively.

Table 4- 13 TGA and DTGA analysis summary of polyamide 610/ cellulose composites

Run#	T1% (℃)	T5% (℃)	T10% (℃)	Tmax1 (℃)	Tmax2 (℃)	Tmax3 (℃)	T onset (℃)
PA 610	385.5	438.6	449.0	-	-	476.7	391.2
NW3	344.6	414.8	446.8	-	-	479.9	337.2
NW10	305.9	364.3	388.9	-	-	476.6	300.2
NW20	274.9	351.6	377.9	392.8	409.2	476.0	281.7
NW30	250.1	329.3	362.4	387.1	-	475.4	242.2

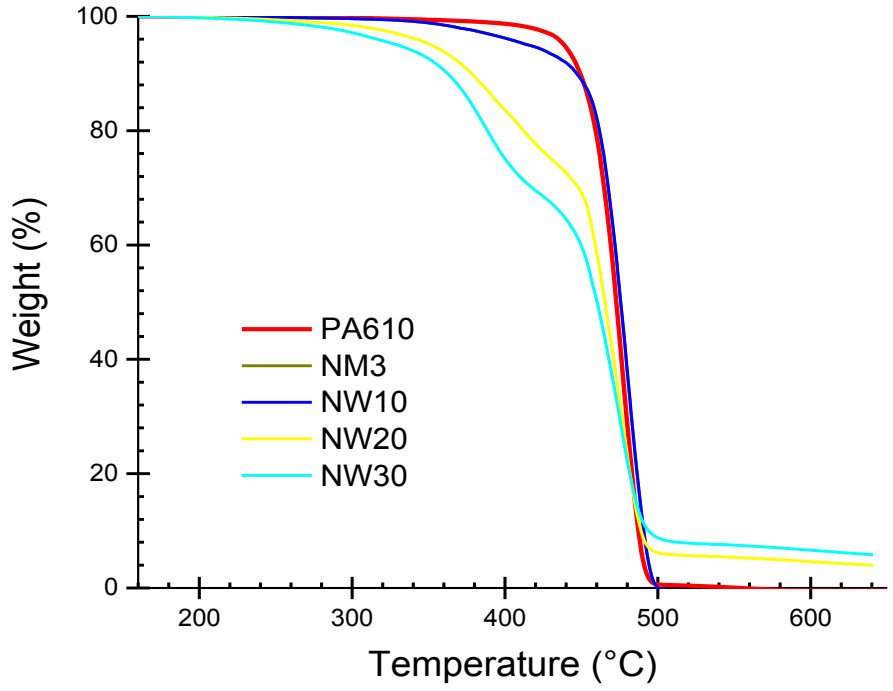

Figure 4- 47 TGA curves of PA6-10/ 3%, 10%, 20% and 30% cellulose composite

From **Figure 4-** 47, the TGA graph of these series of samples can be divided into two groups: Low wood fiber content (PA6-10, NW3, NW10) and high wood fiber content (NW20, NW30). The low fiber content group has reasonable thermal stability until 440℃ while the thermal stability of high wood fiber content group is limited to 330℃. On the other hand, there is almost no residue left at 650℃ for the low wood fiber content group while the high fiber content group still has 8% residue at the same temperature.

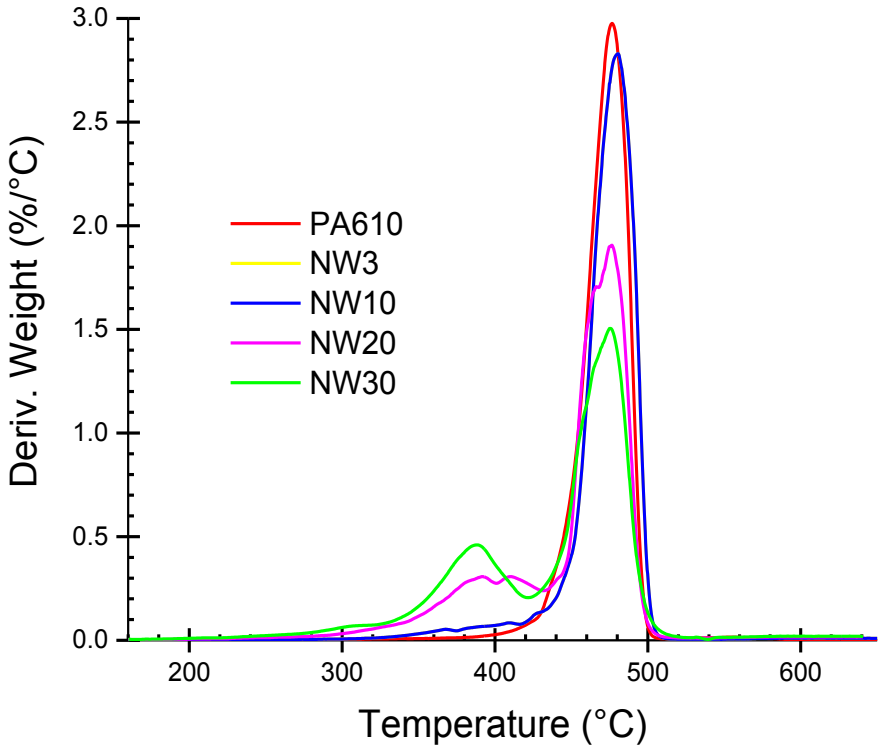

Figure 4- 48 DTGA curves of PA6-10/ 3%, 10%, 20% and 30% cellulose composite

Figure 4- 48 shows only one peak for the low cellulose fiber content group, this means mostly one step for the thermal degradation mechanism while the high cellulose content group has two major degradation steps.

4.4.4 FTIR Results

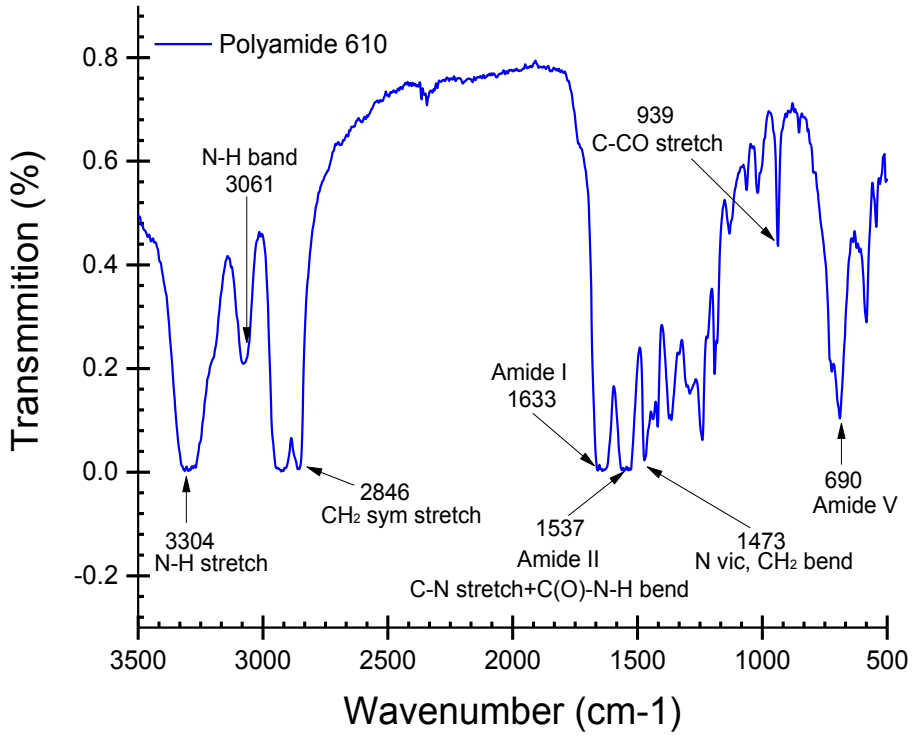

Figure 4- 49 FTIR graph for PA6-10

Figure 4- 49 shows the FTIR curves for PA6-10, N-H stretch and N-H band appears at the wave number 3304 cm^{-1} and 3061 com^{-1} respectively. Amide I stays at 1633cm^{-1}, Amide II (C-N stretch and C(O)-NH bend) stays at 1537 cm^{-1} and Amide V occupied 690 cm^{-1}. And CH_2 (symmetric stretching) showing in 2846 cm^{-1}, C-CO stretch represent at 939 cm^{-1} and CH_2 bend at 1473 cm^{-1}. This set of characteristic wavenumbers coincides with the "fingerprint" of PA610.

4.4.5 XRD Results

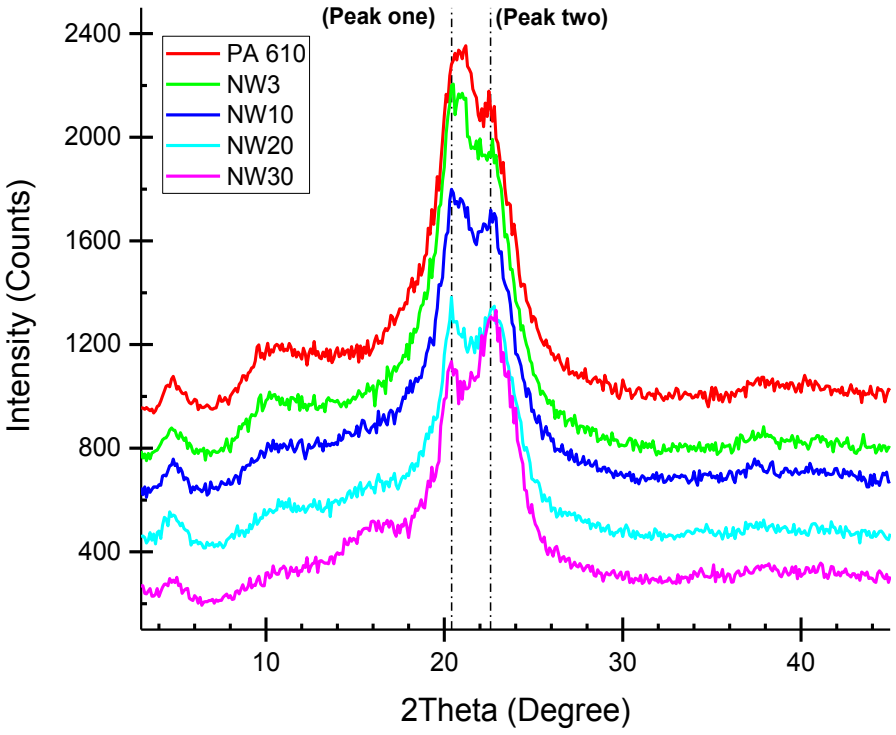

Figure 4- 50 XRD curves for PA6-10/ 3%, 10%, 20% and 30% cellulose composite

Figure 4- 50 shows the offset XRD curves of PA6-10 and four different fiber loading composite. The XRD curve could not be convoluted, since the crystalline form and peak fitting for PA6-10 is still not well established and no published literature can be found.

4.5 Oxidation Induction Time (OIT) Results

There are three sets of tests, part one is performing the OIT test in three temperatures (185 ℃, 190 ℃, and 195 ℃) for RPA6/cellulose composite, part two is performing the OIT test under the same temperature (190 ℃) for RPA6/cellulose and RPA6/cellulose with 5000 ppm Irganox 1010 and part three is performing OIT test in three temperatures (180 ℃, 190 ℃, and 200 ℃) for pure PA6 films. The results are shown in Figure 4- 51, Figure 4- 52 and Figure 4- 53. Note that the OIT curve begins from the point when it is switched to pure oxygen, in other words, this curve does not show the inert gas step.

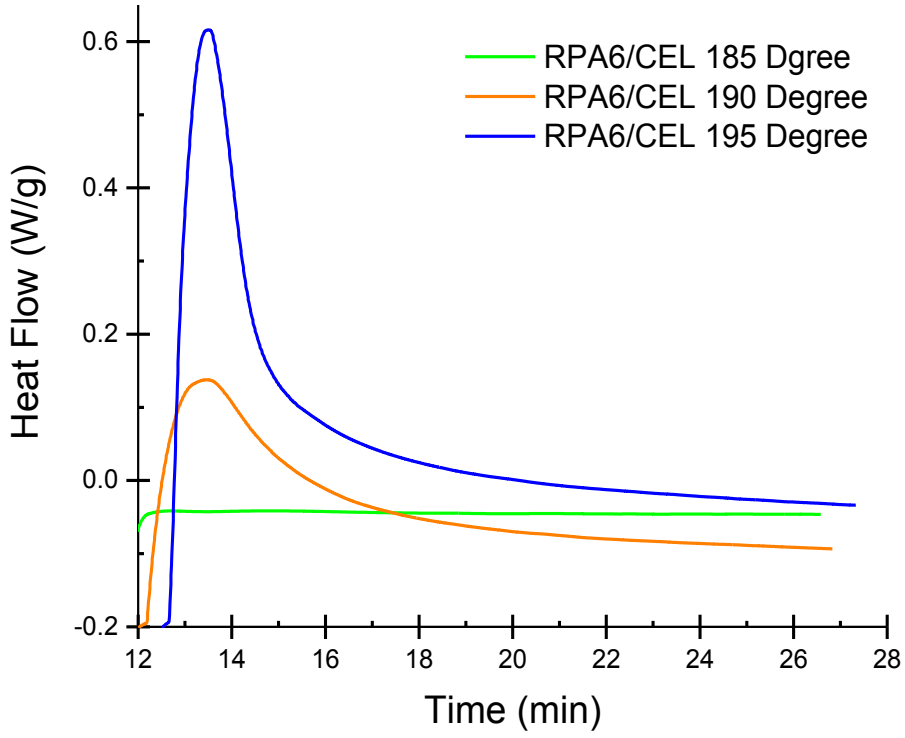

Figure 4- 51 OIT test results for RPA6/CEL composite (without antioxidant) in three temperatures

From Figure 4- 51 we can see that at 185 ℃ the composite did not show any exothermic in the pure oxygen environment, while at 190 ℃ it rapidly oxidized as it

switched to oxygen, which means almost no OIT. Comparing the exothermic peak of 190 ℃ and 195 ℃, the peak of 190 ℃ is lower and broad, which indicates slower and longer oxidation time than the higher and sharp peak at 195 ℃.

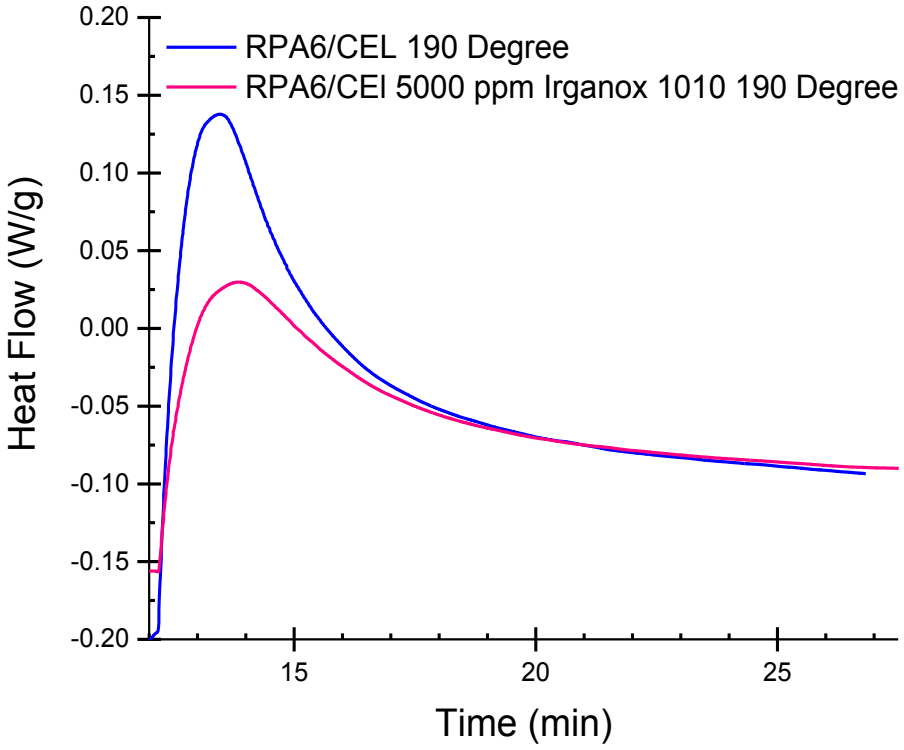

Figure 4- 52 OIT test for RPA6/CEL with and without antioxidant

Figure 4- 52 indicates that the composite directly oxidized after the switch to oxygen atmosphere regardless of whether it contained antioxidants, so it is impossible to procure OIT information for different antioxidant formulas at this temperature. The test was also run for one sample under the oxygen atmosphere from the ramp step and isothermal at 160 ℃ for 300 minutes, but there was no activity until the end. It may be due to the temperature being too low. In order to check the possibility of applying OIT for polyamides, one sample for pure polyamide was evaluated and the results are shown in Figure 4- 53. It shows the same trend as part one and part two: with the increase of temperature, the exothermic peak becomes sharp and narrow meaning a faster and shorter oxidation time.

The attempt to explore use of OIT to evaluate the thermal stability and effect of additives (antioxidants) on polyamide and cellulose composites is novel. To the best of my knowledge, there are no reports in the literature. The motivation to use OIT is coming from its well stablished practice to evaluate stability on polyethylene. However, the results obtained here are still preliminary.

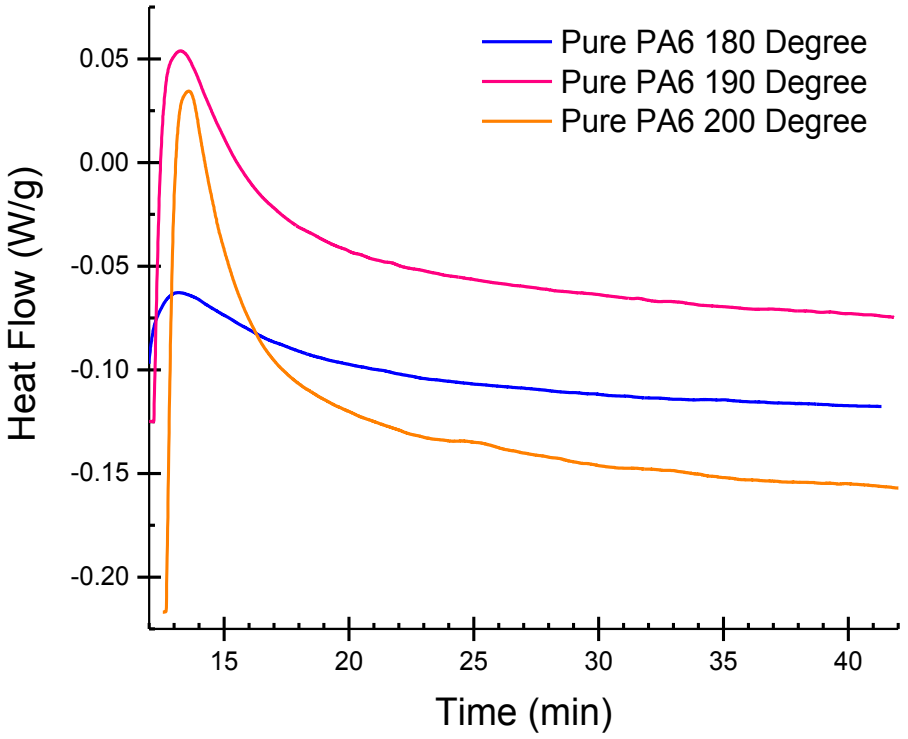

Figure 4- 53 The OIT test results for pure PA6 in different temperature

OIT is often used to evaluate the level of additives (antioxidants and thermal stabilizers) in polyethylene formulation. Figure 4- 54 shows the temperature dependence of oxidation induction time for polyethylene experiment results from TA Instrument. The result demonstrates that with only 5 ℃ increase, the OIT decreased from 30.69 minutes to 17.69 minutes. So one can conclude temperature is a crucial factor in the OIT test [73]. The appropriate OIT should between 5 to 60

minutes and the isothermal temperature should be higher than the melting point for crystalline thermoplastic, since an overly long OIT is not practical based on cost and feasibility [74]. Also, the geometry of the sample is another important factor for OIT, since the oxidation reaction relies heavily on the reaction area or surface-to-volume ratio [74].

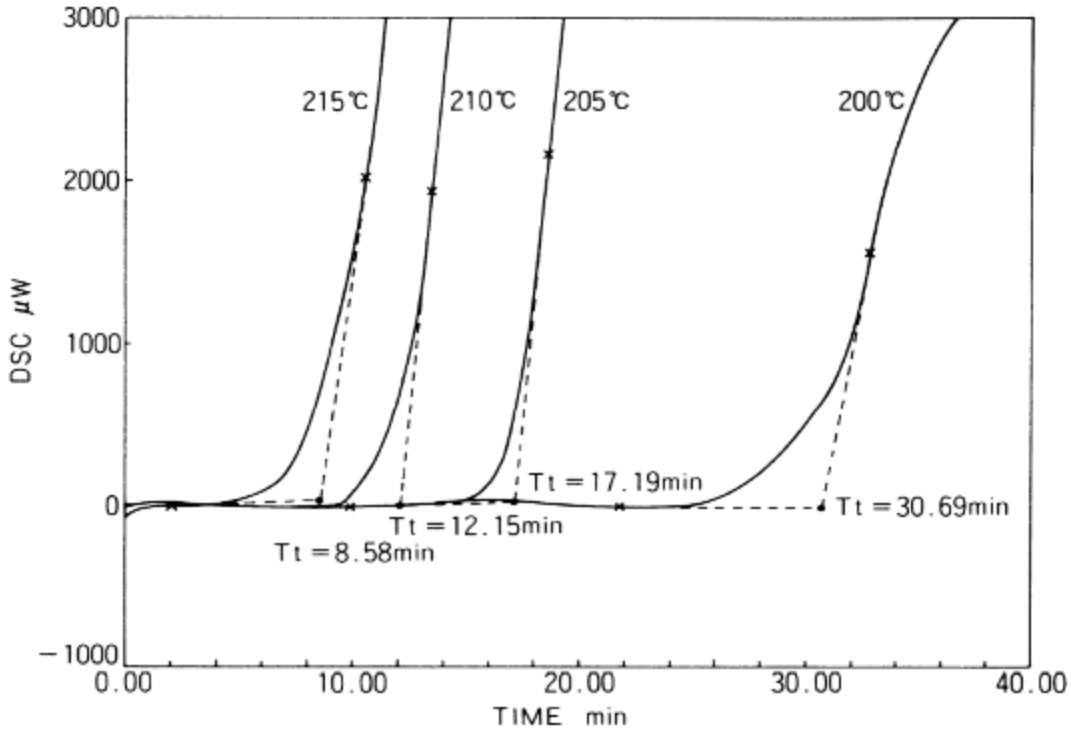

Figure 4- 54 Temperature dependence of oxidation induction time for Polyethylene (PE) [73]

5 Conclusions

1. 20% cellulose decreased impact strength of RPA6 from 58.98 J/m to 25.91 J/M included 13.89 J/m decreased results from an extrusion process.

2. 500 ppm Irganox 1010 increased impact strength by 30.3% from 25.91 J/m to 35.96 J/m. It increased tensile modulus by 21.99% from 488.81MPa to 596.31mPa. It increased tensile strength by 19.46% from 65.37MPa to 78.09MPa. For flexural properties, it also indicates an increase in flexural modulus by 8.75% from 3213MPa to 3494MPa. 500 ppm shows the best performance among 50 ppm, 500 ppm and 5000 ppm Irganox.

3. Irgafox 168 makes almost no difference in composite mechanical properties.

4. Combining Irganox 1010 and Irgafox 168 makes no obvious improvement in composite mechanical properties.

5. The major content in RPA6 is PA6 and still contains another polymer present in SEM image, and it is likely to be polypropylene. The RPA6 includes both alpha and beta crystalline forms. The composite thermal stability decreased after adding 20% cellulose.

6. Among PA6-10, NW3, NW10, NW20 and NW30, NW30 has the best tensile modulus and tensile strength. However there is not much difference in flexural properties among them.

7. PA6-10 shows the highest mean failure height 8.375 inches and highest mean failure energy 7.570 Joule, and both decreased with the increase of fiber loading.

8. 80%RPA6/20%cellulose didn't show OIT at 185℃ while rapidly oxidized at 190℃, which means almost no OIT. For Pure PA6 and composites with or without antioxidants shows no OIT. So the appropriate OIT test procedure for PA6 has not been found.

6 Recommendations

1. Try to find other kinds of antioxidants, which are effective for PA6 and cellulose composites and combine them to improve the mechanical properties.

2. Finding established crystalline forms for PA6-10 and doing peak fitting for PA6/wood fiber composite.

3. Refine OIT procedure for PA6 such as specimen thickness and shape, isothermal temperature, storage before the test and pressure effect.

4. Finding a method to check the dispersion situation of antioxidants.

References

[1] V. Karsli, N. G., Ozkan, C., Aytac, A., & Deniz, "Effects of sizing materials on the properties of carbon fiber‐reinforced polyamide 6, 6 composites.," *Polym. Compos.*, vol. 34, no. 10, pp. 1583–1590, 2013.

[2] D. Aydemir, A. Kiziltas, E. Erbas Kiziltas, D. J. Gardner, and G. Gunduz, "Heat treated wood-nylon 6 composites," *Compos. Part B Eng.*, vol. 68, pp. 414–423, 2015.

[3] H. Ku, H. Wang, N. Pattarachaiyakoop, and M. Trada, "A review on the tensile properties of natural fiber reinforced polymer composites," *Compos. Part B Eng.*, vol. 42, no. 4, pp. 856–873, 2011.

[4] L. C. (2012). Amintowlieh, Y., Sardashti, A., & Simon, "Polyamide 6–wheat straw composites: Effects of additives on physical and mechanical properties of the composite.," *Polym. Compos.*, vol. 33, no. 6, pp. 976–984, 2008.

[5] L. Liu, J. Yu, L. Cheng, and W. Qu, "Mechanical properties of poly(butylene succinate) (PBS) biocomposites reinforced with surface modified jute fibre," *Compos. Part A Appl. Sci. Manuf.*, vol. 40, no. 5, pp. 669–674, 2009.

[6] Y. Yang, T., Ye, L., & Shu, "Thermal stabilization effect of biphenol monoacrylate on polyamide 6.," *J. Appl. Polym. Sci.*, vol. 110, no. 2, pp. 856–863, 2008.

[7] P. Aparecido and J. C. Giriolli, "Natural Fibers Plastic Composites for Automotive Applications," *SABIC Innov. Plast.*, pp. 1–9, 2006.

[8] D. J. Ozen, E., Kiziltas, A., Erbas Kiziltas, E., & Gardner, "Natural fiber blends-filled engineering thermoplastic composites for the automobile industry.," *SPE Automot. Compos. Conf. Exhib.*, pp. 1–12, 2012.

[9] G. Gardiner, "Thermoformable Composite Panels," *Compos. World*, pp. 1–26, 2006.

[10] D. J. (2013). Ozen, E., Kiziltas, A., Kiziltas, E. E., & Gardner, "Natural fiber blend—nylon 6 composites.," *Polym. Compos.*, vol. 34, no. 4, pp. 544–553, 2013.

[11] C. ©. 2016 DuPont., "Vehicle Weight Reduction for Optimal Performance," 2016. [Online]. Available: http://www.dupont.com.au/.

[12] E. E. Kiziltas, H. Yang, A. Kiziltas, and S. Boran, "Thermal Analysis of Polyamide 6 Composites Filled by Natural Fiber Blend," *BioResources*, vol. 11, no. 2, pp. 4758–4769, 2016.

[13] E. Carlson and K. Nelson, "Nylon Under the Hood : A History of Innovation," *SAE, Automot. Eng.*, vol. 104, pp. 84–89, 1996.

[14] G. F. Shan, W. Yang, M. bo Yang, B. hu Xie, Z. ming Li, and J. min Feng, "Effect of crystallinity level on the double yielding behavior of polyamide 6," *Polym. Test.*, vol. 25, no. 4, pp. 452–459, 2006.

[15] C. ©. 2013 R. P. Ltd., "Nylon/Polyamide (PA)," 2013. [Online]. Available: http://www.rutlandplastics.co.uk/advice/nylon.html.

[16] C. ©. 2013 A. P. Products, "MANUFACTURING OF AN OBVR FUEL EMISSION TUBE ASSEMBLY FOR THE AUTOMOTIVE INDUSTRY," 2013. [Online]. Available: http://www.akronpolymer.com/custom-molding-tube-assembly-coployester.html.

[17] J. Holbery and D. Houston, "Natural-fibre-reinforced polymer composites in automotive applications," *J. Miner. Met. Mater. Soc.*, vol. 58, no. 11, pp. 80 – 86, 2006.

[18] SABIC, "The curauá challenge: optimizing natural fibres," *Plast. Addit. Compd.*, vol. 11, no. December, pp. 12–17, 2009.

[19] A. W. Van Vuure, J. A. Ivens, and I. Verpoest, "Mechanical properties of composite panels based on woven sandwich-fabric preforms," *Compos. Part A Appl. Sci. Manuf.*, vol. 31, no. 7, pp. 671–680, 2000.

[20] M. Karimian, H. Hasani, and S. Ajeli, "Analyzing the effect of fiber, yarn and fabric variables on bagging behavior of single jersey weft knitted fabrics," *J. Eng. Fiber. Fabr.*, vol. 8, no. 3, pp. 1–9, 2013.

[21] ©. 2013 F. Technologies., "Where are natural fiber composites used in

automobiles?" 2013.

[22] I. © 2016 UFP Technologies, "FABRICS," 2016. [Online]. Available: http://www.ufpt.com/markets/automotive/materials/fabrics.html.

[23] C. ©. 2015 A. Milberg, Evan, "Researchers Make World's First Model Car with Lignin Carbon Fiber," 2015. [Online]. Available: http://compositesmanufacturingmagazine.com/2016/02/researchers-make-worlds-first-model-car-with-lignin-carbon-fiber/.

[24] ©. 2015 O. L. Dylan Rivera, The Oregonian LLC., "OSU researchers say wood fiber can make car tires more energy efficient," 2009. [Online]. Available: http://www.oregonlive.com/environment/index.ssf/2009/07/osu_researchers_say_wood_fiber.html.

[25] S. (Ed.). Dumitriu, *Polysaccharides: structural diversity and functional versatility.* 2004.

[26] P. Zugenmaier, *Crystalline Cellulose and Cellulose Derivatives Characterization and Structures*. 2008.

[27] A. O'sullivan, "Cellulose: the structure slowly unravels," *Cellulose*, vol. 4, no. 3, pp. 173–207, 1997.

[28] "Burning of wood," *Combustion*, 2011. [Online]. Available: http://virtual.vtt.fi/virtual/innofirewood/stateoftheart/database/burning/burning.html.

[29] S. (Eds.). Bhattacharyya, D., & Fakirov, "Synthetic polymer-polymer composites," *Carl Hanser Verlag GmbH Co KG.*, pp. 1–23, 2012.

[30] ©2016Baidu, "Polyamide 6 monomer preparation," 2014. [Online]. Available: http://baike.baidu.com/view/1252172.htm.

[31] Y. Amintowlieh, "Nylon-6 / Agricultural Filler Composites," University of Waterloo, 2010.

[32] C. Millot, L. A. Fillot, O. Lame, P. Sotta, and R. Seguela, "Assessment of polyamide-6 crystallinity by DSC: Temperature dependence of the melting enthalpy," *J. Therm. Anal. Calorim.*, vol. 122, no. 1, pp. 307–314, 2015.

[33] H. Chen and P. Cebe, "Investigation of the rigid amorphous fraction in Nylon-6," *J. Therm. Anal. Calorim.*, vol. 89, no. 2, pp. 417–425, 2007.

[34] Y. Amintowlieh, “Nylon-6 / Agricultural Filler Composites,” 2010.

[35] C. ©. S. 2016, “Antioxidants Working Mechanism,” 2016. [Online]. Available: http://adhesives.specialchem.com/selection-guide/antioxidants-for adhesives/primary-antioxidants#mechanism.

[36] T. Shu, Y., Ye, L., & Yang, “Study on the long‐term thermal‐oxidative aging behavior of polyamide 6.Effects of expandable graphite and modified ammonium polyphosphate on the flame-retardant and mechanical properties of wood flour-polypropylene composites,” *Shu, Y., Ye, L., Yang, T.*, vol. 110, no. 2, pp. 945–957, 2008.

[37] T. Seguchi, K. Tamura, A. Shimada, M. Sugimoto, and H. Kudoh, “Mechanism of antioxidant interaction on polymer oxidation by thermal and radiation ageing,” *Radiat. Phys. Chem.*, vol. 81, no. 11, pp. 1747–1751, 2012.

[38] J. T. Kim and A. N. Netravali, “Mercerization of sisal fibers: Effect of tension on mechanical properties of sisal fiber and fiber-reinforced composites,” *Compos. Part A Appl. Sci. Manuf.*, vol. 41, no. 9, pp. 1245–1252, 2010.

[39] K. M. Praveen, S. Thomas, Y. Grohens, M. Mozetič, I. Junkar, G. Primc, and M. Gorjanc, “Investigations of plasma induced effects on the surface properties of lignocellulosic natural coir fibres,” *Appl. Surf. Sci.*, vol. 368, pp. 146–156, 2016.

[40] L. He, W. Li, D. Chen, D. Zhou, G. Lu, and J. Yuan, “Effects of amino silicone oil modification on properties of ramie fiber and ramie fiber/polypropylene composites,” *Mater. Des.*, vol. 77, pp. 142–148, 2015.

[41] L. T. Ng, J. L. Garnett, and S. Mohajerani, “Role of additives in wood-polymer composites. Relationship to analogous radiation grafting and curing processes,” *Radiat. Phys. Chem.*, vol. 55, no. 5–6, pp. 633–637, 1999.

[42] M. I. Gutierrez, M. C., De Paoli, M. A., & Felisberti, “Biocomposites based on cellulose acetate and short curauá fibers: Effect of plasticizers and chemical treatments of the fibers.,” *Compos. Part A Appl. Sci. Manuf.*, vol. 43, no. 8, pp. 1338–1346, 2012.

[43] R. Jacobson, D. Caulfield, K. Sears, and J. Underwood, “Low Temperature Processing of Ultra-Pure Cellulose Fibers into Nylon 6 and Other

Thermoplastics," *Sixth Int. Conf. Woodfiber-Plastic Compos.*, pp. 127–133, 2001.

[44] M. Feldmann and A. K. Bledzki, "Bio-based polyamides reinforced with cellulosic fibres - Processing and properties," *Compos. Sci. Technol.*, vol. 100, pp. 113–120, 2014.

[45] K. Shi, L. Ye, and G. Li, "Structure and hydrothermal stability of highly oriented polyamide 6 produced by solid hot stretching," *RSC Adv.*, vol. 5, no. 38, pp. 30160–30169, 2015.

[46] G. W. Beckermann and K. L. Pickering, "Engineering and evaluation of hemp fibre reinforced polypropylene composites: Fibre treatment and matrix modification," *Compos. Part A Appl. Sci. Manuf.*, vol. 39, no. 6, pp. 979–988, 2008.

[47] A. Arbelaiz, B. Fernández, J. A. Ramos, A. Retegi, R. Llano-Ponte, and I. Mondragon, "Mechanical properties of short flax fibre bundle/polypropylene composites: Influence of matrix/fibre modification, fibre content, water uptake and recycling," *Compos. Sci. Technol.*, vol. 65, no. 10, pp. 1582–1592, 2005.

[48] M. Kumar, R. K. Singh, H. Shekhar, and P. Poomalai, "Studies on banana fiber reinforced high density polyethylene (HDPE)/ polyamide (PA) -66 blend composites," *Wudpecker Journals*, vol. 1, no. July, pp. 62–73, 2013.

[49] T. Information and P. Additives, "Irganox ® 1010," 2010.

[50] H. Stable and P. Processing, "Ciba ® IRGAFOS ® 168," 2009.

[51] B. H. Stuart, *Polymer analysis*, vol. 30. 2008.

[52] P. Specimens and E. I. Materials, "Standard Test Methods for Flexural Properties of Unreinforced and Reinforced Plastics and Electrical Insulating Materials 1," *Annu. B. ASTM Stand.*, no. C, pp. 1–11, 2011.

[53] P. Code, "International Standard," *Test*, vol. 2000, 2006.

[54] ASTM, "Standard Test Method for Tensile Properties of Plastics by Use of Microtensile Specimens," *Am. Soc. Test. Mater.*, vol. 08, no. October, pp. 5–9, 2014.

[55] T. English-language, "International Standard ISO 527-1," vol. 2005, 2006.

[56] ASTM International, “ASTM D256 - Standard Test Methods for Determining the Izod Pendulum Impact Resistance of Plastics,” *Annu. B. ASTM Stand.*, pp. 1–20, 2010.

[57] T. English-language, “International Standard ISO 180,” vol. 2005, 2006.

[58] “Izod Impact Testing (notched Izod)ISO 180.PDF.” [Online]. Available: http://wxphp.com/wxd_6iuj75ovlb3pebe0ildt_1.html.

[59] ASTM standard, “Standard Test Method for Impact Resistance of Flat, Rigid Plastic Specimen by Means of a Striker Impacted by a Falling Weight (Gardner Impact).,” *ASTM Int.*, vol. i, no. Reapproved, pp. 1–8, 1996.

[60] F. C. Fernandes, M. De Paoli, and F. C. Fernandes, “Properties of polyamide-6 / cellulose composites enhanced by lignin-containing fibers,” no. September, pp. 6–9, 2015.

[61] J. R. Connolly, “Introduction to X-ray Powder Diffraction X-Ray Analytical Methods Uses of X-Ray Powder Diffraction Introduction to X-ray Powder Diffraction XRD for Dummies : From Specimen to analyzed sample with minimal math,” pp. 1–9, 2007.

[62] M. A. Ganzoury, N. K. Allam, T. Nicolet, and C. All, “Introduction to Fourier Transform Infrared Spectrometry,” *Renew. Sustain. Energy Rev.*, vol. 50, pp. 1–8, 2015.

[63] ASTM International, “ASTM D3895 - Test Method for Oxidative-Induction Time of Polyolefins by Differential Scanning Calorimetry,” *Annu. B. ASTM Stand.*, pp. 1–8, 2014.

[64] B. Lánská, “Stabilization of polyamides—I. The efficiency of antioxidants in polyamide 6.,” *Polym. Degrad. Stab.*, vol. 53, no. 1, pp. 89–98, 1996.

[65] A. Buchenauer, “Wood Fiber Polyamide Composites for Automotive Applications,” University of Waterloo, 2016.

[66] D. Yousefian, H., & Rodrigue, “Effect of nanocrystalline cellulose on morphological, thermal, and mechanical properties of nylon 6 composites.,” *Polym. Compos.*, pp. 1473–1479, 2016.

[67] M. C. Khoathane, O. C. Vorster, and E. R. Sadiku, “Hemp Fiber-Reinforced 1-Pentene/Polypropylene Copolymer: The Effect of Fiber Loading on the

Mechanical and Thermal Characteristics of the Composites," *J. Reinf. Plast. Compos.*, vol. 27, no. 14, pp. 1533–1544, 2008.

[68] B. Guo, Q. Zou, Y. Lei, M. Du, M. Liu, and D. Jia, "Crystallization behavior of polyamide 6/halloysite nanotubes nanocomposites," *Thermochim. Acta*, vol. 484, no. 1–2, pp. 48–56, 2009.

[69] A. Thygesen, J. Oddershede, H. Lilholt, A. B. Thomsen, and K. St??hl, "On the determination of crystallinity and cellulose content in plant fibres," *Cellulose*, vol. 12, no. 6, pp. 563–576, 2005.

[70] Y. Peng, Y. Chi, W. Dong, D. Sun, and W. Mi, "The reinforcing effect of carbon fibers and pa6 on the mechanical properties of a PU composites," *Mech. Compos. Mater.*, vol. 49, no. 3, pp. 245–250, 2013.

[71] K. Zarshenas, A. Raisi, and A. Aroujalian, "Surface modification of polyamide composite membranes by corona air plasma for gas separation applications," *RSC Adv.*, vol. 5, no. 25, pp. 19760–19772, 2015.

[72] C. Barbeş, L., Rădulescu, C., & Stihi, "ATR-FTIR spectrometry characterisation of polymeric materials," *Rom. Reports Phys.*, vol. 66, no. 3, pp. 765–777, 2014.

[73] H. H.-T. S. Corporation, "Oxidation Induction Time Measurements by DSC," 1988.

[74] P. Y. B.-C. Tan, C. U. PerkinElmer, Inc. Shelton, and How, "How to Optimize OIT Tests ?," *PerkinElmer, Inc*, 2012.

Appendix

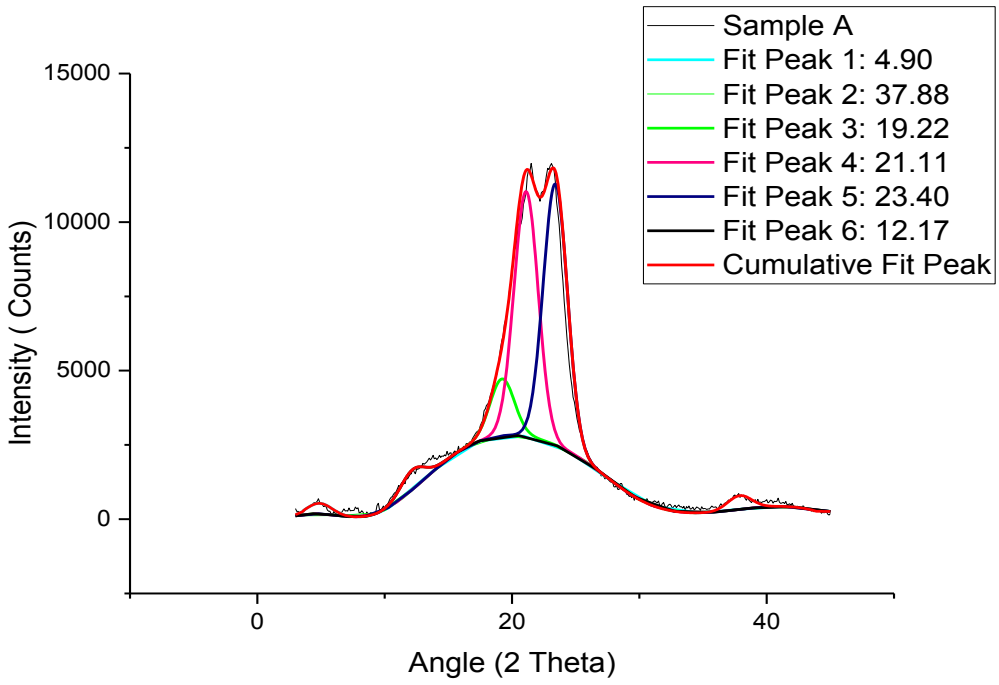

Appendix 4- 1 Convolution of sample A XRD curve

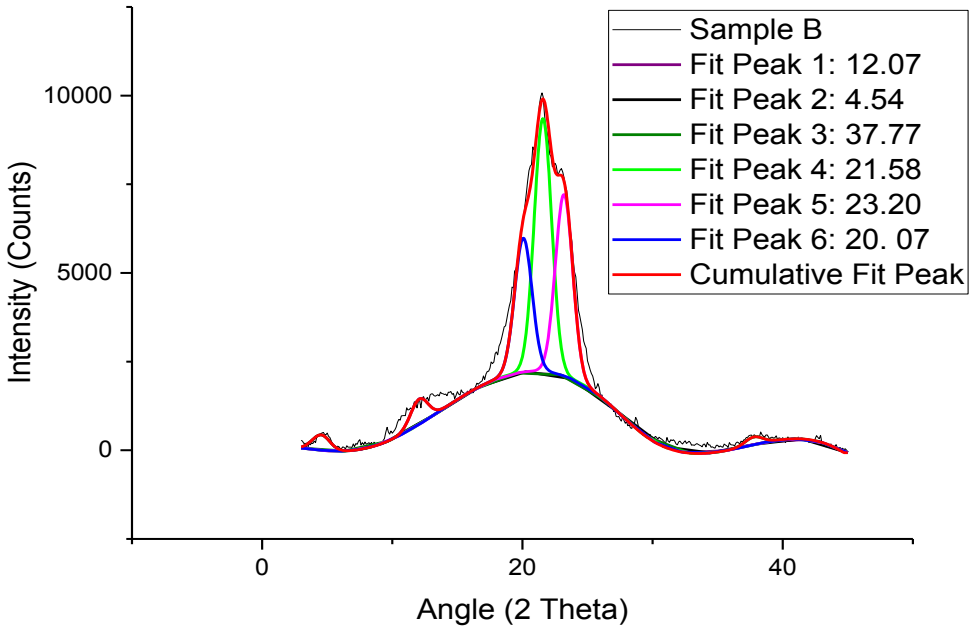

Appendix 4- 2 Convolution of sample B XRD curve

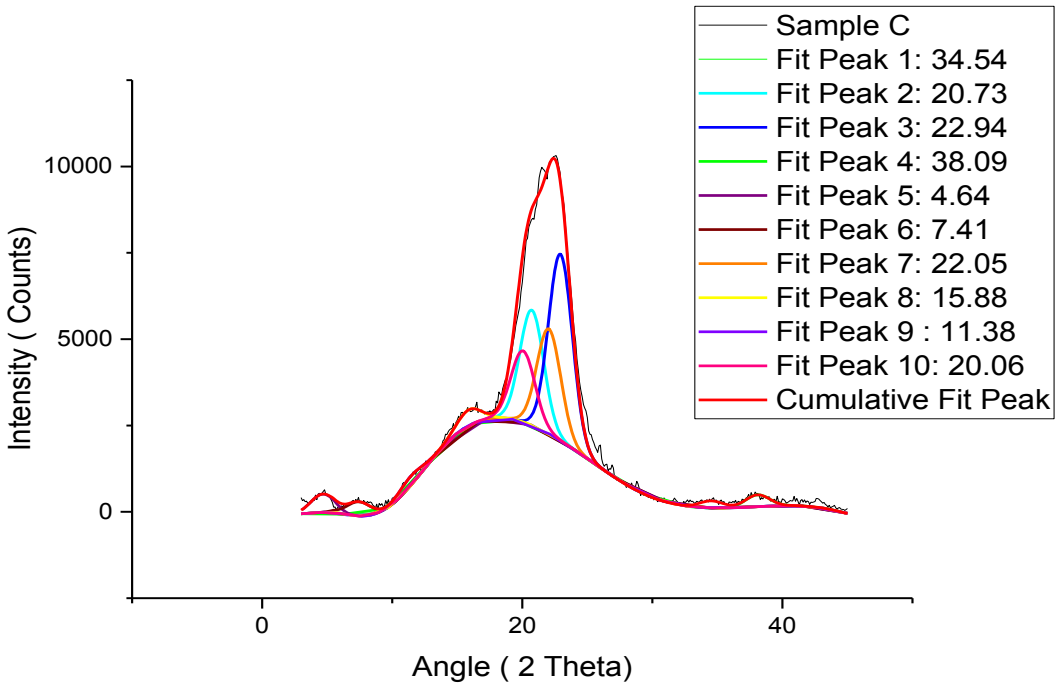

Appendix 4- 3 Convolution of sample C XRD curve

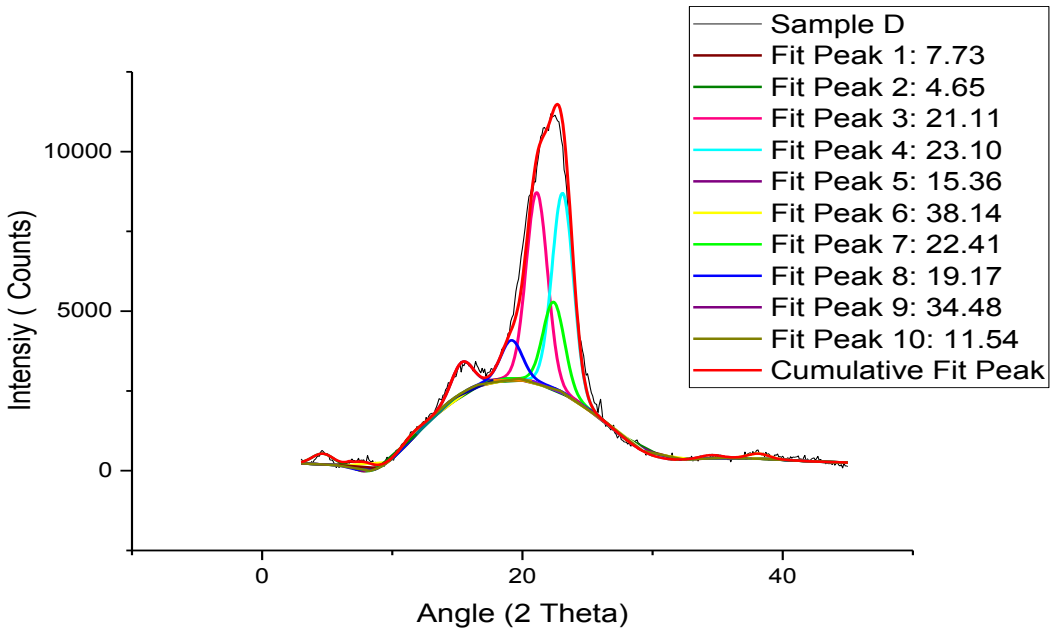

Appendix 4- 4 Convolution of sample D XRD curve

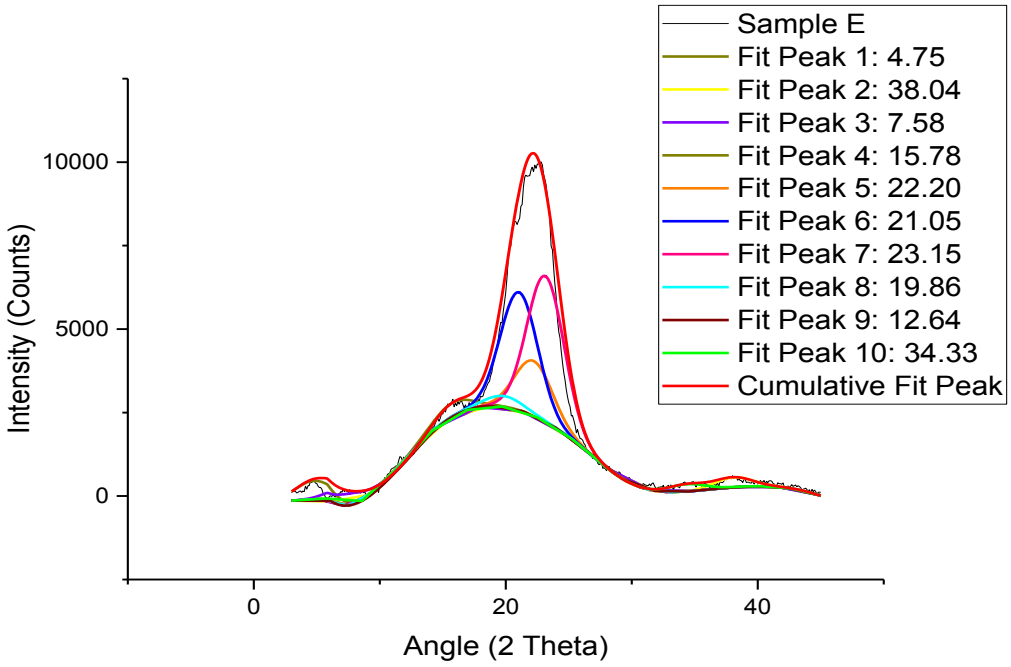

Appendix 4- 5 Convolution of sample E XRD curve

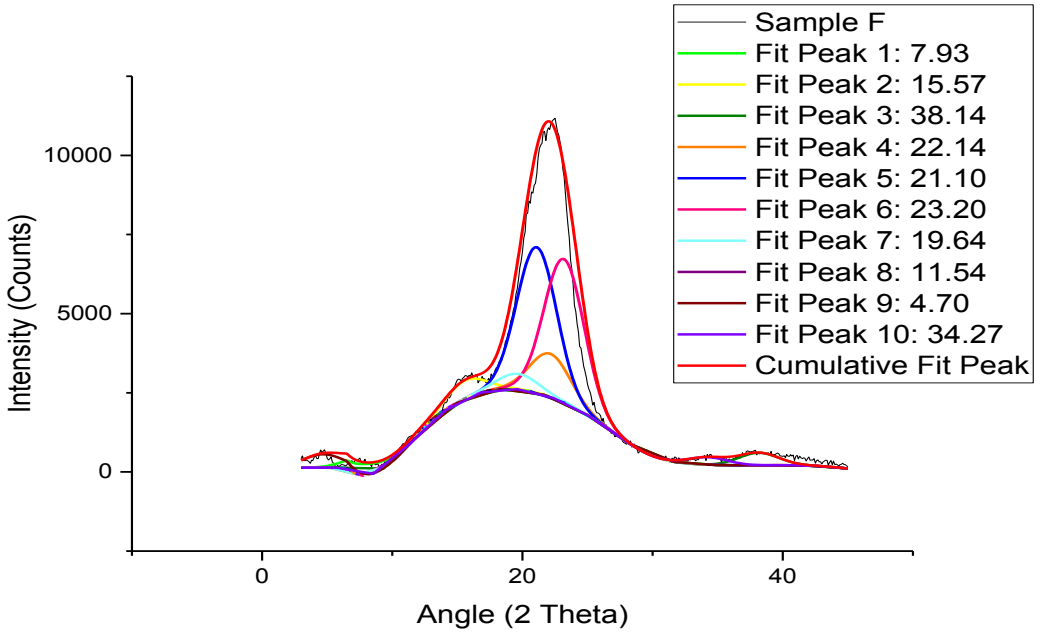

Appendix 4- 6 Convolution of sample F XRD curve

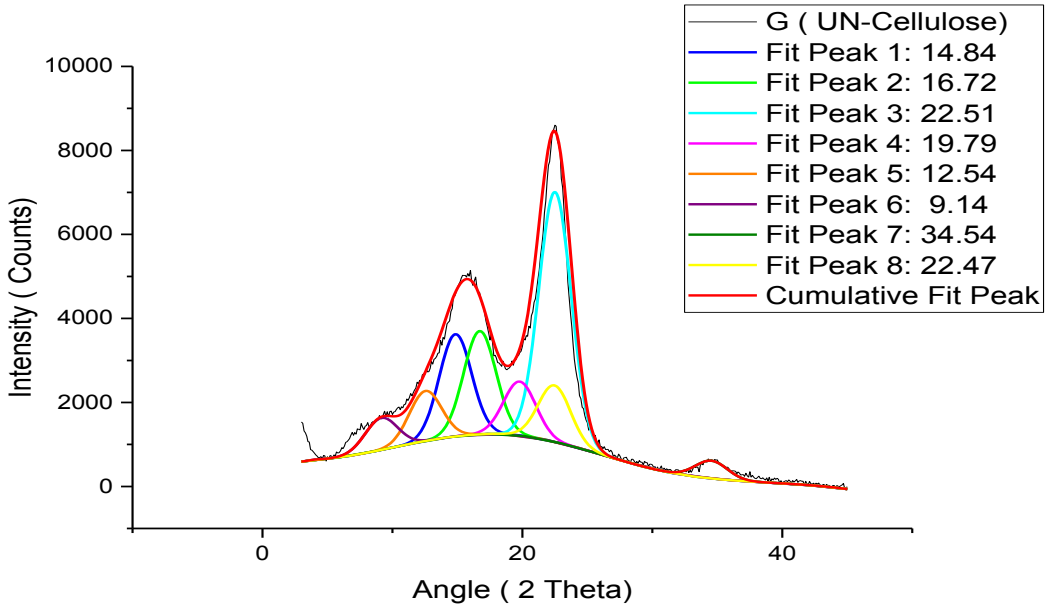

Appendix 4- 7 Convolution of sample undried XRD curve

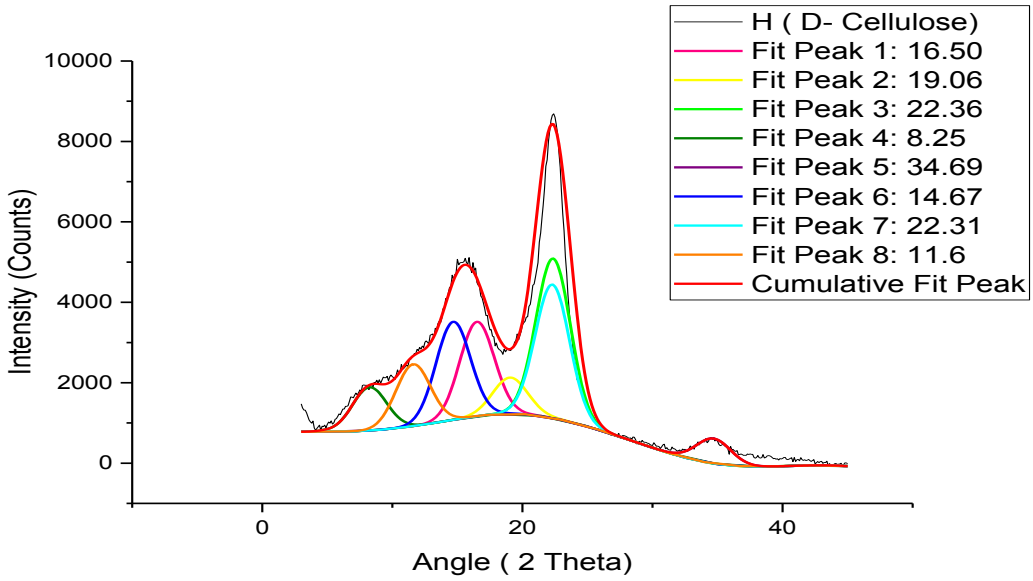

Appendix 4- 8 Convolution of dried cellulose XRD curve

Calculation For Cellulose Crystallinity

For un-dried cellulose according to the convolution in Appendix 4- 7:

Segal Method

$I_{200}(2\theta)$ = 22.515° $I_{AM}(2\theta)$ =18.720°

Intensity= 9594.75 Intensity= 3854.04

$$X_{CR}= \frac{I200-IAM}{I200} \times 100\%$$

= 59.83%

For dried cellulose according to the convolution in Appendix 4- 8:

Segal Method

$I_{200}(2\theta)$ = 22.40° $I_{AM}(2\theta)$ =18.614°

Intensity= 9688.30 Intensity= 3787.54

$$X_{CR}= \frac{I200-IAM}{I200} \times 100\%$$

= 60.91%

Cellulose I: I_{AM} $18° \leq 2\theta \leq 19°$

I_{200} $22° \leq 2\theta \leq 23°$

Appendix 4- 9 Calculation of cellulose crystallinity